



Electrokinetics at liquid-liquid interfaces: Physical models and transport mechanisms

Yunfan Huang, Moran Wang^{*}

Department of Engineering Mechanics and Laboratory of APS, Tsinghua University, Beijing 100084, China

ARTICLE INFO

Keywords:

Liquid-liquid interface
Electrical double layer
Electrokinetics
Multiphase flow
ITIES

ABSTRACT

The electrification effects and electrokinetic flow phenomena at immiscible liquid-liquid interfaces have been a subject of scientific inquiry for over a century. Unlike solid-liquid interfaces, liquid-liquid interfaces exhibit not only multiphysical and cross-scale characteristics but also diffuse soft properties, including finite thickness, fluidity, ion adsorbability, and permeability, which introduces diverse interfacial charging mechanisms and conductive dielectric properties, imparting unique characteristics to electrokinetic multiphase flow systems. Electrokinetic multiphase hydrodynamics (EKmHD), grounded in electrochemistry and colloid and interface science, has experienced renewed interest in recent years. This is particularly evident in systems such as the interface between two immiscible electrolyte solutions (ITIES) in electrochemistry, self-propelling droplets in physicochemical hydrodynamics, and digital microfluidics in electromechanics. The multiphase diffuse soft nature of charged liquid-liquid interfaces introduces novel physical scales and theoretical dimensions, positioning EKmHD as a potential foundation for a new interdisciplinary field rather than merely a cross-disciplinary area. This review highlights the need for an integrated research approach that combines interfacial charging mechanisms with electrokinetic flows, alongside a cross-scale modeling framework for interfacial multiphysical transport. It systematically organizes the characteristics of liquid-liquid interfaces from the perspectives of charging mechanisms and electrokinetic behaviors, with particular emphasis on spontaneous partition- and adsorption-induced charging at the interface, and the strong coupling between multiphase diffuse soft interface flow and ion transport. Furthermore, the paper comprehensively summarizes the transport mechanisms of electrokinetic multiphase flows concerning interfacial ion transport and fluid flow, while refining the corresponding dominant dimensionless parameters. Additionally, it systematically consolidates current understanding of typical electrokinetic multiphase flow scenarios, with special focus on potential future research directions. These include the electrokinetic double-sided coupling effects in ITIES systems, solidification and nonlinear effects in droplet/bubble electrophoresis, the validity of the leaky dielectric model, electrokinetic instabilities of jets and ion-selective soft interfaces, and the active and passive control of two-phase electrokinetic wetting dynamics and displacement.

1. Introduction

Electrokinetics focuses on the coupled transport of solute ions and solvent molecular fluid backgrounds near charged surfaces in electrolyte solutions [1–3]. The so-called *interface charging* or *interface electrification* refers to the formation of two layers of equal amounts of opposite charges at around interfaces (i.e., the *electric double layer* in the broad sense) and forming an interphase potential difference, where the separation of positive and negative charge centers is caused by the redistribution of charged components due to spontaneous chemical potential

differences or induced by external electric fields [1,4,5]. Consequently, for charged interfaces in electrolyte solutions, there arises the possibility of non-equilibrium potential fields driving the migration of solute ions in the net charge layer near the interface, thereby dragging the motion of the solvent molecular fluid background; this is the most fundamental picture of *electrokinetic flow and transport* behavior. Therefore, why the equilibrium interface in the solution is charged, how ions are distributed within the net charge layer at the interface, and how the non-equilibrium transport of ions near the net charge layer at the interface is coupled with interfacial flow, are the core issues of concern in electrokinetics [6–8].

^{*} Corresponding author.

E-mail address: mrwang@tsinghua.edu.cn (M. Wang).

<https://doi.org/10.1016/j.cis.2025.103518>

Received in revised form 30 March 2025;

Available online 17 April 2025

0001-8686/© 2025 Elsevier B.V. All rights are reserved, including those for text and data mining, AI training, and similar technologies.

Nomenclature

ITIES	interface between two immiscible electrolyte solutions
EKmHD	electrokinetic multiphase hydrodynamics
EDL	electrical double layer
EChem	electrochemistry
PDS	pure dielectric solvent
LQM	liquid metal
RTIL	room-temperature ionic liquid
SES	strong electrolyte solution
WES	weak electrolyte solution
PFD	perfect dielectric
PFC	perfect conductor
HCD	highly conductive dielectrics
WCD	weakly conductive dielectrics
EHD	electrohydrodynamics
iPC	interfacial physicochemical charging
iIT	interfacial ion transport
iFF	interfacial fluid flow

This review will focus on spontaneously charged immiscible oil-water interface system and review the research on its electrokinetic transport mechanisms. Here, the aqueous phase refers to a strong electrolyte solution, while the oil phase denotes an immiscible organic phase that may contain electrolytes. The latter is categorized into *nonpolar oils* and *polar oils*, primarily distinguished by the relative magnitudes of their dielectric constants and electrical conductivities [9,10]. Nonpolar oils are commonly found in naturally occurring hydrophobic biomolecules or artificially constructed pure small-molecule oil systems in laboratories. Their molecules typically exhibit weak polarity, surface-inert hydrophobicity, and a dielectric constant much smaller than water (approximately 1/15 of water's), with negligible conductivity, behaving as near-perfect dielectrics. Research on such systems is prevalent in life sciences or colloid and interface science. Polar oils, on the other hand, often appear in naturally occurring impurity-containing oils or artificially constructed systems in laboratories such as the *interface between two immiscible electrolyte solutions* (ITIES). Their molecular structures contain polar groups, and their dielectric constants, while smaller than water's, remain non-negligible (up to 1/2 of water's). Their conductivity depends on the nature of solute ions (if organic ions are present, conductivity is relatively high; hereafter, polar oil systems are assumed to contain organic ions unless specified). These systems typically behave as *conductive dielectrics*, and their study is more common in geosciences or electrochemistry. For conciseness, this review refers to the study of spontaneous charging and electrokinetic multiphase flow phenomena at liquid-liquid immiscible interfaces as *electrokinetic multiphase hydrodynamics* [11–13].

1.1. Brief historical overview

The charging effect at immiscible liquid-liquid interfaces is widely present and has a long history of research spanning over a century [1,2]. Lippmann began experimental measurements of the electrocapillary effect at the mercury interface in electrolyte solutions in 1875 [14], which is also the earliest known research on charged liquid-liquid interface systems containing electrolyte solutions under the field of *interface science*. Shortly after that, Chapman published his theoretical study on the electrocapillary effect at the mercury interface in electrolyte solutions in 1913 [15], who almost simultaneously and separately established the diffuse double layer model with Gouy, the latter of which proposed a purely theoretical model for solid-liquid interfaces [16]. The mercury interface system and Chapman's theoretical model greatly inspired the subsequent development of theories on the structure of the

double layer near general charged interfaces, such as Grahame's in-depth research on the electrocapillary effect in 1947 [17]. Unlike the mercury interface, the discovery of spontaneous charging at oil-water interfaces mainly came from experimental studies on the stability of emulsion systems influenced by electrolytes in the field of *colloid science* around 1911 [18,19], which also promoted the extension of the concept of colloids from solid particles to emulsions composed of liquid droplet particles [20,21], and related research later also expanded to bubble systems [22,23]. However, the theory of the double-sided diffuse layer with possible partitioned charging on both sides of oil droplets was not proposed until around 1940 by Verwey and Niessen [24,25].

Although the mechanism of partition-induced charging at oil-water interfaces was proposed long ago, in traditional emulsion systems, which typically involve electrolyte solutions composed of simple inorganic ions, and where the non-aqueous phase usually has poor conductivity, the effect of partition-induced charging on the charging of oil droplets is insignificant. Therefore, the partition-induced charging effect in traditional oil-water interface systems has never received enough attention in the field of colloid and interface science. On the other hand, the selective permeability of biological membranes (such as cell membranes) to ions or other components is considered an important feature for maintaining normal physiological functions. This has triggered research in the colloid science community on the mechanism of transmembrane transport of ion-selective membranes, dating back to 1890 [26,27]. The ITIES system, due to its many similarities to ion-selective membranes, has gradually attracted the attention in this field since 1909 [27,28]. However, although research in colloid and interface science at that time had focused on the effect of electrolytes on the equilibrium interfacial potential difference of the ITIES system, it was not until around 1956 that the *electrochemistry* community began to pay attention to the interphase ionic current of this system, and it took another 20 years for the electrochemistry field to conduct comprehensive research on the non-equilibrium ionic transport across the ITIES interface and the structure of interfacial ion distribution [27,29,30]. In 1976, in an experimental article using a dropping mercury electrode setup to study the electrochemical behavior of ITIES, Koryta, Vanysek, and Brezina formally proposed the concept of ITIES [31], a term that has been in use ever since [12]. Since then, with the development of micro-nano fabrication techniques, technologies such as microelectrodes, micropipettes, and micromanipulators have emerged successively, and research on the ITIES system in the field of electrochemistry has gradually shifted towards related fields such as micro-nano technology, precision measurement, and cell detection [32–34].

Since electrokinetic flow originates from the net charge layer near the interface, its description largely depends on an accurate understanding of the interface charging mechanisms and the characteristics of charge distribution. Looking back, the phenomenon of electrokinetic flow at liquid-liquid interfaces had already been noted by at least 1914 [35]. For instance, McTaggart experimentally discovered in 1914 that bubbles in electrolyte solutions would migrate directionally under the influence of an external electric field [22]. This phenomenon was later also observed by Mooney in 1924 in oil droplet systems within electrolyte solutions [36]. Bull and Gortner successfully measured the streaming potential at gas-liquid and oil-water interfaces using a specially designed apparatus in 1931 [23]. However, it was not until around 1950, when Grahame proposed the theory of the electrocapillary effect and the structure of the electric double layer at the mercury interface, that Frumkin and Levich established the effective theory of electrocapillarity for typical electrokinetic flow phenomena such as the directional migration of mercury droplets under an external electric field [37]. This also contributed to Levich's seminal work, *Physicochemical Hydrodynamics*, marking the birth of this new interdisciplinary field [11]. Shortly after Verwey et al. proposed the theory of double-sided diffuse layers at oil droplet interfaces in 1939, Booth, Jordan, Taylor, and Fedosov also successively conducted preliminary theoretical studies on the directional migration of emulsion droplets under an

external electric field in the 1950s [11,38–40]. Although Booth's and Jordan's theories still inherited the shortcomings of the particle electrophoresis theories at solid-liquid interfaces at that time [41], Fedosov's theory, which inherited Frumkin and Levich's electrocapillary analysis, also had issues of applicability [37]. Additionally, Millikan's famous oil drop experiment in 1911, which measured the trajectory of charged oil droplets formed by a spray in an electric field, first provided evidence for the existence of the elementary charge [42,43]. Despite the data processing of this study being considered not rigorous, it brought the method of controlling the deformation and motion of dielectric droplets with an external electric field into view and, in the 1960s, led to the formation of the field of *electrohydrodynamics* under the impetus of Taylor and Melcher [44–47].

Over the past 60 years, progressing alongside electrokinetics at solid-liquid interfaces, the study of electrokinetic transport mechanisms at liquid-liquid interfaces has achieved significant developments [47–50]. However, disciplinary barriers have also gradually emerged. From the historical review of the development of electrokinetic multiphase hydrodynamics, it can be seen that due to the broad range of disciplines involved and the very different perspectives of different disciplines on similar research objects, the literature on electrokinetic multiphase flows is extremely scattered in different subfields, which poses certain difficulties for systematic mechanism studies and urgently requires sorting out and integrating the existing literature. Originating in electrochemistry and colloid science, electrokinetic transport at liquid-liquid interfaces has been rediscovered in recent years due to advancements in micro/nanofabrication and measurement technologies, as well as the emergence of new material systems and practical demands. Examples include self-propelling reactive droplets in active control [51–54], digital microfluidics with dielectric liquids [55–59], liquid metals in advanced manufacturing [60–63], ionic liquids in new energy applications [64–66], and aqueous two-phase electrolyte systems in biochemical engineering [67–71]. Among these, the interfacial charging and electrokinetic transport behaviors of systems such as inert hydrophobic interfaces and ITIES exhibit fundamental differences compared to traditional solid-liquid interfaces and liquid metal interfaces, which has gradually attracted scholarly attention in recent years [12,72–75], and will be the main focus of this review.

1.2. Scope and perspective

This review will approach from the perspective of electrokinetics, extract model systems from typical application backgrounds of electrokinetic multiphase flow, and meticulously analyze the physical picture and transport mechanisms of interfacial charging and electrokinetic flow at liquid-liquid interfaces from the perspective of interdisciplinary characteristics. In particular, the physical picture of microscopic interfacial charging with macroscopic electrokinetic flow are combined, and a combination of quantitative descriptions of diffuse and sharp interfaces is adopted.

Basically, the sharp interface model treats the interface as a zero-thickness geometrical surface, with the provision of interfacial conditions for various physical fields. It is often used for theoretical analysis to obtain formalized theories and intuitive physical pictures. However, macroscopic equations often only yield theoretical approximate solutions under specific limiting conditions, and their applicability typically relies on validation through numerical simulations or physical experiments. The diffuse interface model, on the other hand, allows the interface to diffuse into a thin solvent mixing layer of finite thickness, with the implementation of phase separation and interfacial tension. It has a solid thermodynamic physical foundation and is easily coupled with complex interfacial kinetic behaviors, which is suitable for numerical simulations studying the mechanisms of multiphase complex interfacial mass transfer. For simplicity, we refer to the former as macroscopic models and the latter as mesoscopic models. Considering the existence of nanometer-thick diffuse layer which may reduce to an

effective interface condition in the coarse-grained model, the physical modeling of electrokinetic multiphase flow has three perspectives that need to be particularly distinguished: the diffuse interface description, the sharp interface description, and the matched asymptotic expansion, as shown in Fig. 1.

It should be noted that in recent years, there have been reviews focusing on the spontaneous charging at oil-water interfaces and electrokinetic multiphase flow at both theoretical and application levels [5,76–79]. Compared with previous studies, this review has the following characteristics.

On the one hand, with regard to research subjects, this review extends the research system of electrokinetic multiphase flow from traditional systems with pure dielectric liquid on the oil side (such as a non-polar oil) to ITIES systems with a conductive dielectric on the oil side (with a polar oil solvent) [38,49,50]. The latter have properties similar to biological membranes and artificial semipermeable membrane systems, with more possibilities of ion *permeability* and *adsorbability* depending on the characteristics of different solvents and solutes. This will result in a strong coupling feature of electrokinetic transport behavior on both sides of the interface, making the electrokinetic characteristics of ITIES, in a sense, possess properties between perfect conductors represented by liquid metals and perfect dielectrics represented by pure dielectric liquids [12,13,80–82]. The ITIES system has been an important intersection of various scientific and engineering fields including colloid science, electrochemistry, electromechanics, neuroscience, membrane science, brain-inspired computing, and chemical engineering over the past decade. Therefore, a systematic collation of the transport mechanisms of this system will potentially and widely impact numerous fields, such as constructing artificial systems to simulate the characteristic behaviors of biological membrane systems (e. g., chemotaxis of cells) based on physicochemical hydrodynamics [83–85].

On the other hand, in terms of research paradigms, this review combines the perspectives of electromechanics and physicochemical hydrodynamics [1,6,47,86]. Both will respectively provide the fundamental physical picture and the main research methods for cross-scale modeling of electrokinetic multiphase flow, a typical multi-physical multiphase soft interface system. In this review, we will fully incorporate the cross-scale modeling research perspective, with typical examples such as the introduction of macroscopic and mesoscopic theoretical models of interfacial charging and electrokinetic flow, and the analysis of transport mechanisms based on mesoscopic models and matched asymptotic expansion theory. Besides, this review will select model systems in combination with application backgrounds and make comparisons and analogies with other interfacial systems to explore the uniqueness of the electrokinetic behavior of ITIES systems [12,13,47,73,87,88].

In particular, we appreciate the reviewers' valuable suggestions and acknowledge that emulsions represent a major class of liquid-liquid interfaces, with surfactants commonly acting as stabilizers [89]. Besides, the surfactants may also play important role in ions partitioning between aqueous phase and non-polar liquids [9,90–92] and thus serves as a quite different mechanism from the organic ions solved in the polar liquids [76]. It is noteworthy that there have been several monographs or reviews on the interfacial thermodynamics [89] and kinetic transport behaviors [93,94] of the non-ionic surfactants as well as their impact on interface fluid dynamics [95]. However, as for the complex dynamic behaviors of ionic surfactant (including kinetic transport and hydrodynamics) around the surface of electrolyte solutions [96–98], as well as the facilitated ion transport through the liquid-liquid interface with surfactants, the related quantitative description is still a challenging problem, which is far beyond the scope of this review. In this review, we will focus on the charged liquid-liquid interfaces without surfactants.

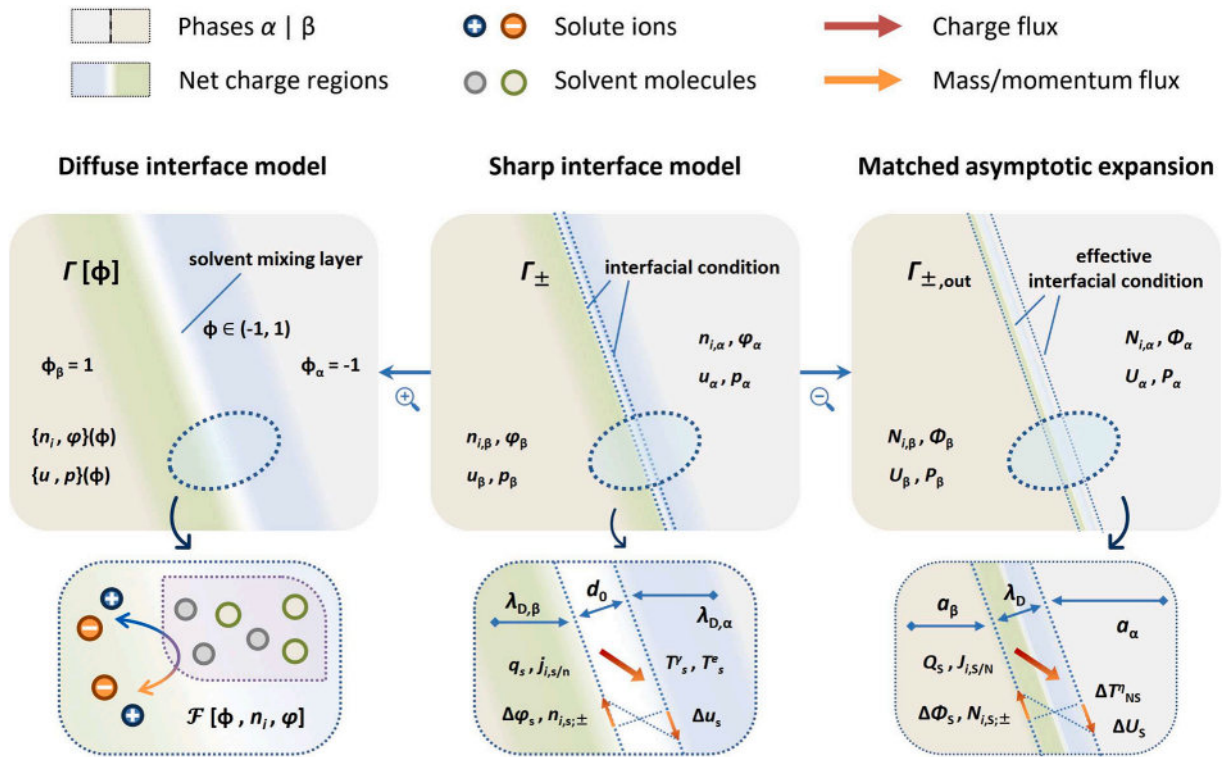


Fig. 1. Three typical perspectives of cross-scale physics and modeling of EKMD. In particular, the finite-thickness solvent mixing layer (left) is mainly used for the continuous distribution of physical quantities across the interface in the diffuse interface models. The interfacial condition (middle) is primarily for the matching of physical quantities on both sides of the liquid-liquid geometric interface in the sharp interface models. The asymptotic-matching-based effective interfacial condition (right) is mainly for the matching of physical quantities at the outer edges of the double-sided diffuse layers during the matched asymptotic expansion solution. The detailed meanings of the symbols in the figure can be found in the subsequent sections. In terms of spatial scales, the characteristic thickness of the solvent mixing layer at the oil-water interface is generally 0.1 – 1 nm, the characteristic thickness of the aqueous phase diffuse layer is typically in the range of 1 – 100 nm, and the geometric dimensions of the liquid-liquid two-phase flow system are generally on the order of 1 – 100 μm. It should be noted that the solvation effects of ions are not shown in the schematics for simplicity.

1.3. Article organization

The review is organized as follows. First, we will review the fundamental mechanisms and physical models of interfacial charging from the perspective of two-liquid interface electrochemistry and interfacial electrokinetic transport from the perspectives of two-phase physico-chemical hydrodynamics and electro-mechanical hydrodynamics, which can be found in Sections 2 and 3, respectively. Then, in Section 4, we will systematically construct the core physical picture of electrokinetic multiphase hydrodynamics and attempt to define corresponding dimensionless control parameters through the organization of transport mechanisms, demonstrating the possibility of new phenomena and mechanisms. Last but not at least, in Section 5, the main model systems involved in the typical application backgrounds will be covered, such as droplet electrophoresis, two-liquid electroosmotic flow, two-liquid streaming potential, two-liquid electroconvective instability, electrokinetic flows on slippery surfaces, ion-tuned interfacial property coupling with two-phase displacement and electric field-driven electrokinetic two-phase displacement, with the key transport mechanisms analyzed and future research directions outlined.

2. Physical model I: Interface charging of two-liquid interface

This section will meticulously discuss the ion partition and adsorption behavior of charged liquid-liquid interface systems and provide a corresponding effective thermodynamic description. It will also elucidate the prominent features and typical characteristics of the charging mechanisms at liquid-liquid interfaces, thereby providing a theoretical foundation for the subsequent cross-scale modeling that connects the

microscopic interfacial charging mechanisms with the macroscopic characteristics of electrokinetic viscous flow.

The ion partition and adsorption behavior at liquid-liquid interfaces is an inherent property of charged liquid-liquid interface systems, with the possible ion partition effects on both sides of the liquid-liquid interface offering more possibilities in the interfacial charging mechanisms compared with solid-liquid interfaces. Regarding the partition and adsorption of solute ions at charged liquid-liquid interfaces, Section 2.1 will briefly introduce the physical pictures and thermodynamic descriptions of both phenomena. It should be noted that, due to the solute ions in electrolyte solutions carrying net charges, various complex polarization effects will be triggered by electrostatic fields near the interface. Therefore, the classification into partition and adsorption behaviors here is merely a simplification and abstraction of their more general behaviors [99]. However, this simplification is sufficient to grasp their main characteristics and can be conveniently extended to the description of non-equilibrium transport behaviors, which is also very important for the mechanism study of upscaling coarse-grained transport behaviors at charged liquid-liquid interfaces [82]. For a unified quantitative description of partition and adsorption behaviors and the limitations of the aforementioned classification method, refer to the discussions in Section 2.2.

2.1. Fundamentals of typical charging mechanisms

The equilibrium distribution of solute ions near liquid-liquid interfaces is an important subject of study in the fields of interfacial electrochemistry as well as colloid and interface science, and it also serves as a crucial basis for the analogy of biological membrane ion

channels through the properties of ion *selective permeability* and *specific adsorbability* of liquid-liquid interfaces. Generally, the characteristics of solute distribution near liquid-liquid interfaces can be clearly divided as shown in Fig. 2.

To provide a quantitative description of the equilibrium interfacial charging characteristics, one can introduce the concepts of the single-particle transfer free energy and adsorption free energy of a specific ion near a particular liquid-liquid interface. This reflects the free energy changes and potential field distribution associated with the interaction between solute ions and the solvent molecular background. Specifically, the *free energy of transfer* $\Delta_{\alpha,\beta}^{\beta,g,i}$ represents the system free energy change for a single ion i transferring from one bulk liquid phase α to another bulk liquid phase β , characterizing the potential barrier height across the two bulk phases and reflecting the interface's *permeability* to ion i . Meanwhile, the *free energy of adsorption* $\Delta_{\alpha,s}^{\alpha,g,i}$ represents the system free energy change for a single ion i adsorbing from bulk phase α to the interfacial phase s (i.e., the finite-thickness solvent mixing layer), characterizing the average depth of the potential well near the interface and reflecting the interface's *adsorbability* for ion i . It is noteworthy that the physical intuition behind the effective interfacial potential field treatment for solute-solvent interactions is strikingly similar to the representative approaches in analyzing *colloid transport* [86] and interfacial transport mechanisms of *osmosis* [72].

2.1.1. Ion partition and interface polarizability

The concept of *polarizability* (also known as the ability to be polarized) can naturally be analogized from metal or dielectric systems in electrodynamics to charged interface systems in electrolyte solutions. This concept is used to describe the ability of charged components around an interface to establish a new thermodynamic equilibrium on both sides under an external field, thereby weakening the external

electric field [4,29,76]. Generally, the stronger the ability of charged components to form a interphase electrical current through the interface, the lower the polarizability of the charged interface system. In a broad sense, polarization features describe the response of a specific charged component and a specific multiphase interface composition under an external electric field. This is often used to characterize the polarization features of a single ion at a given interface (here referred to as the *charged interface subsystem*). However, in practical applications, the same concept is also widely used to describe the overall ion partition behavior of a given liquid-liquid interface system. It makes demands on the polarization behavior of different ions, thereby classifying the given liquid-liquid interface and the *charged interface system* composed of all solute ions therein, as shown in Table 1 [100].

In Table 1, the behaviors shown in the first and last rows are generally considered to exist only in ideal cases. When a certain ion can freely pass through the phase interface without causing any other effects, the subsystem is referred to as *completely non-polarizable*, and sometimes it is also called *irreversible*. On the contrary, when a certain ion not only cannot freely pass through the phase interface but also cannot cross the Gibbs dividing surface, it may exhibit adsorption behavior or inert behavior depending on the strength of the specific adsorption of ions on the interface. Such a subsystem is called *ideally polarizable* (as shown in Fig. 3). Due to the inevitable mixing of components near the interface in practical situations, the ideally polarizable interface can (relatively) accurately hold true only in interfacial systems composed of liquid metals or air and electrolyte solutions. In fact, this is also the simplest feature among many interfacial polarization features, and thus it has been used in the early studies of electrocapillarity [14,16,17].

In actual systems, the situation that is more commonly encountered lies between completely non-polarizable and ideally polarizable, as

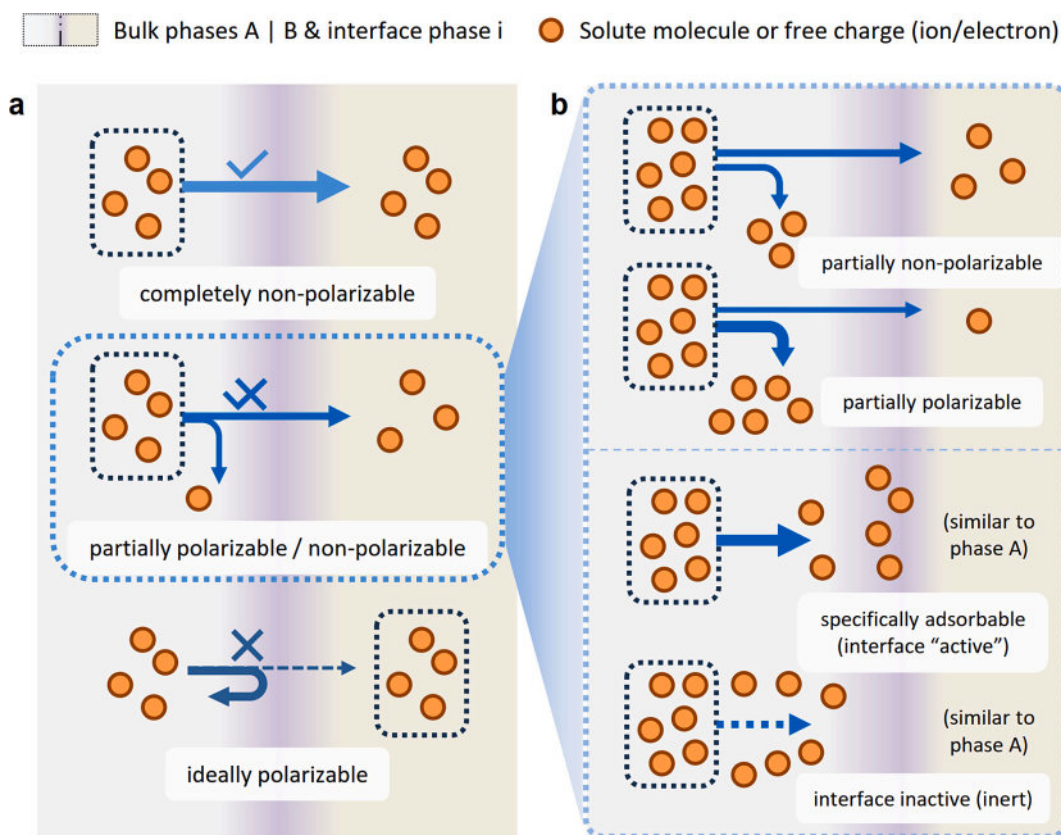


Fig. 2. Classification of interface solute partition and adsorption. (a) Comparisons between completely non-polarizable, partially polarizable / non-polarizable, and ideally polarizable. (b) Comparisons between partially non-polarizable and partially polarizable, specifically adsorbable and interface inactive. It should be noted that the solvation effects of ions are not shown in the schematics for simplicity.

Table 1
Polarization features of charged interface system.

Concepts	Description	Example
Completely non-polarizable	charged components can freely cross interface with no interphase chemical potential difference	$R^+X^-(w) R^+X^-(o)$ with $P_{R^+X^-}^{w/o} \approx 1$
Partially non-polarizable	at least one common charged component that is relatively easy to cross the interface	$R^+X^-(w) S^+X^-(o)$ with $P_{X^-}^{w/o} \geq 1$ (or slow interfacial reaction)
Partially polarizable	at least one charged component that is relatively hard to cross the interface	$R^+X^-(w) S^+X^-(o)$ with $P_{X^-}^{w/o} \gg 1$ (or fast interfacial reaction)
Completely polarizable	fast evolution into thermodynamic equilibrium under external normal voltage, common charged component may exist	$R^+X^-(w) R^+X^-(o)$ with $P_{R^+X^-}^{w/o} \geq 1$
Ideally polarizable	charged components on both phases are precisely separated by a zero-thickness geometric plane	liquid metal or air with aqueous solution, $R^+X^-(w) S^+Y^-(o)$ with $P_{R^+X^-}^{w/o} \gg 1$, $P_{S^+Y^-}^{w/o} \ll 1$

shown in the middle three rows of Table 1. At this time, ions can partially pass through the phase interface and exhibit *partition* behavior on both sides of the interface. Such a subsystem is referred to as *partially polarizable* (which is also *partially non-polarizable*). For partially polarizable interfaces, the concept of partition coefficient P_i for component i can be introduced to describe its tendency to partition on both sides of the interface. From the perspective of particle statistics, it is related to the single-particle transfer free energy of that component $\Delta_{\alpha\beta}^{\beta}g_{t,i}^0 \equiv -k_B T \ln P_i^{\beta/\alpha}$ [29]. The transfer free energy of solute ion i is defined as $\Delta_{\alpha\beta}^{\beta}g_{t,i}^0 := \mu_{\beta,i}^0 - \mu_{\alpha,i}^0$, which reflects the potential difference of interaction between the particle and the solvents on both sides. Its theoretical models include linear local theory and nonlinear nonlocal theory. The former uses Born potential theory to establish the correlation with the

ion size, ion charge, and solvent dielectric constant, while the latter further analyzes the solvation effect and its nonlocal polarization characteristics [10,82].

It is important to note that the polarizability of a charged interface system is not only related to the free energy of ion transfer, but also depends on the magnitude of the applied normal voltage. In fact, even if the ion transfer free energy is relatively high, as long as the applied normal voltage is sufficiently strong, ions will always cross the free energy barrier and transfer through the interface due to the strong electromigration effect. Consequently, for some polarizable systems, a special state can be defined within a specific applied normal voltage window, referred to as *completely/perfectly polarizable* or *thermodynamically polarizable*. This concept implies that under the action of the applied normal voltage, the system can still rapidly evolve to a new thermodynamic equilibrium state, which is the most common scenario in practical research. At this point, the subsystem is also termed as *reversible*, and the corresponding applied normal voltage window is called the *electrochemical window* [101].

For charged liquid-liquid interface systems, the partition coefficient of ion activity P_i across the interface (or equivalently, the transfer free energy $\Delta g_{t,i}^0$) to some extent determines the width of the electrochemical window, thereby determining the propensity of the interface towards being polarizable or non-polarizable [102,103]. Specifically, when P_i is close to 1, the charged liquid-liquid interface subsystem is referred to as *tending to be non-polarizable*; conversely, it is called *tending to be polarizable*. In particular, a reactive interface that can rapidly reach a kinetic equilibrium under the action of an applied normal voltage is also considered a special case of a thermodynamically polarizable interface system. Thus, it can be summarized that the main scenarios in which the interface exhibits partially non-polarizable behavior include: low ion transfer free energy resulting in a narrow electrochemical window, strong applied normal voltage exceeding the electrochemical window, and the existence of double-sided chemical reactions or dynamic adsorption at the reactive interface [103,104].

For immiscible electrolyte solution interfaces, they can exhibit various polarization features depending on the strength of the solute

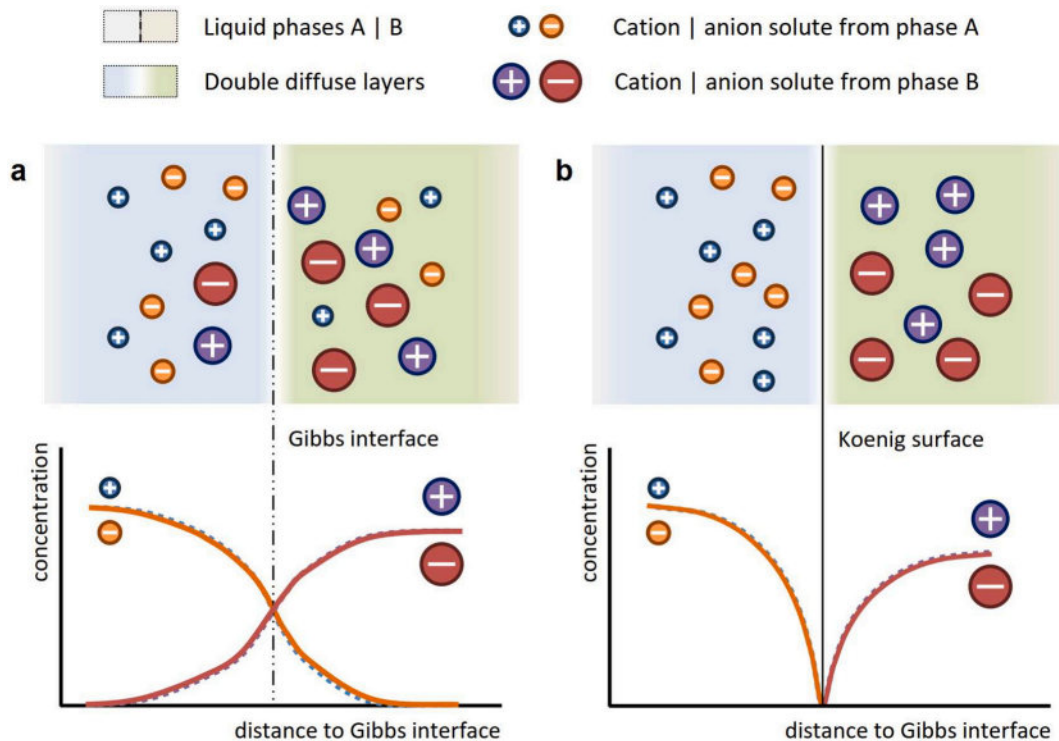


Fig. 3. Comparison between (a) completely polarizable interface and (b) ideally polarizable interface. Adapted from previous literature [29].

ions' ability to pass through the interface. The oil phase is usually a polar oil with a relatively high dielectric constant. For example, inorganic ions (such as inorganic anions or metal cations) typically reside mainly in the aqueous phase and tend to be polarizable, while some organic ions (such as tetraphenylarsonium Ph_4As^+ and tetraphenylborate Ph_4B^-) usually reside mainly in the oil phase and tend to be non-polarizable (as shown in Fig. 4) [29]. The latter two ions, due to their excellent interface non-polarizable behavior, are often used for the measurement of interfacial distribution potential and as standard solute ions for defining the free energy of ion transfer, that is, an additional assumption beyond thermodynamics is adopted: $\Delta_{\alpha\text{St},\text{Ph}_4\text{As}^+}^{\beta}g_{\alpha}^0 = \Delta_{\alpha\text{St},\text{Ph}_4\text{B}^-}^{\beta}g_{\alpha}^0$ [29].

2.1.2. Ion adsorption and interface activity

The specific adsorption behavior of charged components near the two-liquid interface is a rather intuitive mechanism for interface charging. For immiscible liquid-liquid interfaces, due to the existence of interfacial excess energy, i.e., surface tension, solute molecules or ions all have a certain tendency to be adsorbed from the bulk phase to the interface phase or to be repelled from the interface phase to the bulk phase. This can lead to the formation of interfacial ion adsorption/depletion layers. Considering that ions carry net charges, they are not only subject to specific interfacial physicochemical interactions but also to Coulombic electrostatic interactions induced by already adsorbed ions or an applied electric field. The interfacial ion adsorptions induced by these two interactions are respectively referred to as specific adsorption and non-specific adsorption. In fact, whether it is simple metal ions, halide ions, acid radical ions, or organic aromatic ions, surfactant ions, there is a certain degree of specific adsorption caused by interfacial physicochemical interactions. By analogy with the transfer free energy, a specific adsorption free energy can be defined for specific adsorption as $\Delta_{\alpha\delta_{a,i}}^s g_{a,i}^0 = \mu_{s,i}^0 - \mu_{\alpha,i}^0 \equiv -k_B T \ln K_{a,i}^{s/\alpha}$. Here, μ_{α}^0 represents the chemical potential associated with the specific interactions between solute ions and the dielectric solvent background within phase α , while μ_s^0 is the average of the effective interaction potential between solute ions and solvent molecules within the finite-thickness solvent mixing layer (interface phase s). The term $K_{a,i}^{s/\alpha}$ is known as the adsorption constant for component i from the bulk phase α to the interface phase s.

The interfacial excess ion concentration caused by ion adsorption at the interface will reduce the surface tension, which may originate from specific adsorption of ions or from electrostatic adsorption under the action of an applied normal voltage. Considering that the mechanism of specific ion adsorption is ubiquitous, it can be assumed that they all possess a certain degree of interfacial activity similar to surfactants. For inorganic salt ions, Onsager-Samaras theory provides a satisfying predictions of electrical double layer affecting surface tension of dilute electrolyte solutions based on the theory of correlation functions as well as the thermodynamic theory [105], while the effects of external voltage

upon the surface tension of electrolyte solutions can be phenomenologically captured by the thermodynamic analysis [4]. For ITIES systems, due to the possible partial non-polarizability of the interface, the electrocapillary effect becomes more complex, as referred to the previous reviews [106,107].

With regard to the electrification mechanism, specific adsorption can be divided into two major categories: physical adsorption and chemical adsorption. Specifically, physical adsorption corresponds to physical mechanisms without electron transfer, including hydration-dehydration, amphiphilic structures, defect or vacancies, and image forces [108]. Chemical adsorption, on the other hand, corresponds to chemical reactions involving electron transfer among solute ions and solvent molecules, including the ionization of weak electrolytes, ion exchange, precipitation-dissolution, redox reactions, and facilitated ion reactions [109]. Since these processes generally involve multiple charged species, their modes of action and descriptive schemes are more complex. In fact, even in the absence of specific chemical reactions at the interface, purely physical specific adsorption effects will always arise to some extent due to differences in the physical properties of different solute ions, such as charge, size, and polarity [82,110].

2.1.3. Thermodynamic description of charging mechanisms

Combining the previous two subsections, it can be known that the main *electrification mechanisms* of liquid-liquid interfaces can be divided into two categories: specific adsorption and imbalanced partition, as shown in Fig. 5. The former is a natural extension from colloidal solid particle systems to liquid-liquid interface systems, reflecting the interfacial activity characteristics of ions tending to distribute within the solvent mixing layer; it is related to whether components can be enriched near the Gibbs dividing surface and determines the adsorption-induced charging behavior of the interface. The latter is a natural extension from ion-selective membrane systems to liquid-liquid interface systems, reflecting the interfacial polarizability characteristics of ions tending to distribute on one or two sides of the interface; it is related to whether components can pass through the interface and determines the partition-induced charging behavior of the interface.

The concept of transfer free energy is not only used for classifying the polarization feature of charged interface subsystems, but also for quantitatively discussing the equilibrium charging behavior of partially polarizable liquid-liquid interfaces. The single-particle standard interphase potential (standard interphase potential) of ion i is defined as $\Delta_{\alpha}^{\beta} \varphi_i^0 := -\Delta_{\alpha\text{St},i}^{\beta} g_{\alpha}^0 / z_i e$. By combining the electrochemical potential equilibrium of any ion i , the potential difference between the electrically neutral bulk regions on both sides of the equilibrium interface can be derived

$$\Delta_{\alpha}^{\beta} \varphi_{\infty} := \varphi_i^{\beta} - \varphi_i^{\alpha} = \Delta_{\alpha}^{\beta} \varphi_i^0 - \frac{k_B T}{z_i e} \ln \frac{a_i^{\beta}}{a_i^{\alpha}} = \Delta_{\beta}^{\alpha} \varphi_i^{0'} - \frac{k_B T}{z_i e} \ln \frac{c_i^{\beta}}{c_i^{\alpha}} \quad (1)$$

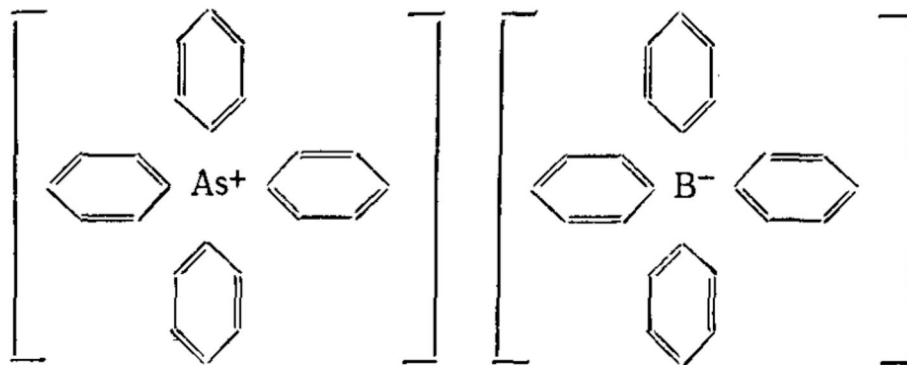


Fig. 4. Molecular structure of tetraphenylarsonium Ph_4As^+ and tetraphenylborate Ph_4B^- . It is seen that, due to the presence of benzene rings around the charged ions, the two ions can exist in both the oil and water phases with certain concentrations, thus exhibiting the interfacial non-polarizable behavior. Reproduced from previous literature [29].

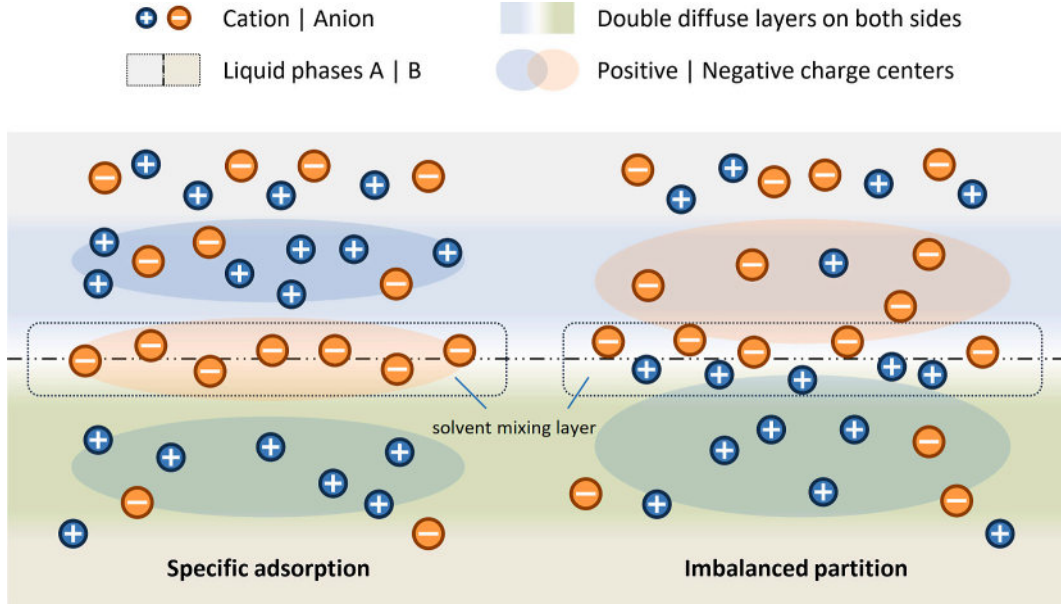


Fig. 5. Comparison between two basic forms of charging mechanisms of two-liquid interface. Specific adsorption (left) and imbalanced partition (right) present different distributions of charge centers and corresponding polarization fields. It should be noted that the solvation effects of ions are not shown in the schematics for simplicity.

Here, a_i^α and c_i^α are the activity and molar concentration of ion i in phase α , respectively. They are related by the activity coefficient γ_i^α as $a_i^\alpha = \gamma_i^\alpha c_i^\alpha$, where the interactions between ions and solvent reflected in the transfer free energy $\Delta_{\alpha}^{\beta} g_{i,t}^0$ and the Coulomb electrostatic interactions experienced by ions reflected in the electric potential energy $z_i e \varphi$ have been excluded. In combination with the definition of the partition coefficient $P_i^{\beta/\alpha}$, we have

$$\frac{a_i^\beta}{a_i^\alpha} = \exp \left[-\frac{z_i e}{k_B T} (\Delta_{\alpha}^{\beta} \varphi_{\infty} - \Delta_{\alpha}^{\beta} \varphi_i^0) \right] = P_i^{\beta/\alpha} \exp \left(-\frac{z_i e}{k_B T} \Delta_{\alpha}^{\beta} \varphi_{\infty} \right). \quad (2)$$

Here, taking the simplest case of an immiscible electrolyte solution interface where the same pair of cations and anions are distributed on both sides of the α and β phases, $B^+ A^- (\alpha) | B^+ A^- (\beta)$, it is easy to derive its interphase equilibrium potential as

$$\Delta_{\alpha}^{\beta} \varphi_{\infty} = \frac{\Delta_{\alpha}^{\beta} \varphi_{+}^0 + \Delta_{\alpha}^{\beta} \varphi_{-}^0}{2} \simeq \frac{k_B T}{2e} \ln \frac{P_{+}^{\beta/\alpha}}{P_{-}^{\beta/\alpha}} = -\frac{\Delta_{\alpha}^{\beta} g_{+} - \Delta_{\alpha}^{\beta} g_{-}}{2e}. \quad (3)$$

This potential is referred to as the *distribution potential*, from which the equilibrium concentration partition ratio can be obtained as

$$\frac{c_i^\beta}{c_i^\alpha} \simeq \frac{a_i^\beta}{a_i^\alpha} = P_i^{\beta/\alpha} \exp \left(-\frac{z_i e}{k_B T} \Delta_{\alpha}^{\beta} \varphi_{\infty} \right) = \exp \left(-\frac{\Delta_{\alpha}^{\beta} g_{+} + \Delta_{\alpha}^{\beta} g_{-}}{2k_B T} \right). \quad (4)$$

In the above derivation, the approximate assumption $\gamma_{+}^{\alpha} / \gamma_{+}^{\beta} \simeq \gamma_{-}^{\alpha} / \gamma_{-}^{\beta}$ has been utilized. It can be seen that the difference in partition coefficients of cations and anions (i.e., *selective permeability*) will cause a non-zero distribution potential. This implies that the *imbalanced partition* of cations and anions (i.e., $\Delta_{\alpha}^{\beta} g_{+} \neq \Delta_{\alpha}^{\beta} g_{-}$) will trigger the charging of the liquid-liquid interface, constituting another important electrification mechanism in addition to (similar to the solid-liquid interface) spontaneous specific adsorption.

For specific adsorption, assuming that the specific adsorption free energy of ion i from both bulk phases to the interface phase is the same under the standard reference state, i.e., $\Delta_{\alpha}^s g_{a,i}^0 \equiv \Delta_{\alpha}^s g_{a,i}^0 \equiv \Delta_{\beta}^s g_{a,i}^0$, the total adsorption free energy, which includes both specific and non-specific adsorption, can be expressed as

$$\Delta_{\alpha}^s g_{a,i}^{\text{total}} = \Delta_{\alpha}^s g_{a,i}^0 + \beta_{\alpha,i} k_B T y_i, \quad \Delta_{\beta}^s g_{a,i}^{\text{total}} = \Delta_{\alpha}^s g_{a,i}^0 + \beta_{\beta,i} k_B T y_i, \quad (5)$$

Here, $\beta_{\alpha,i}$, $\beta_{\beta,i}$ are constants independent of $\Delta_{\alpha}^{\beta} \varphi_{\infty}$, and y_i represents the driving force difference for non-specific adsorption behavior. A specific realization form is provided, namely the Butler-Volmer type adsorption of surfactant ions [106]. The standard reference state is set as $\Delta_{\alpha}^{\beta} \varphi_{\infty} = \Delta_{\alpha}^{\beta} \varphi_i^0$, $\beta_{\beta,i} = \beta_{\alpha,i} - 1$, and $y_i = (z_i e / k_B T) (\Delta_{\alpha}^{\beta} \varphi_{\infty} - \Delta_{\alpha}^{\beta} \varphi_i^0)$. Under these conditions, we have $\Delta_{\alpha}^s g_{a,i}^{\text{total}} - \Delta_{\beta}^s g_{a,i}^{\text{total}} = z_i e (\Delta_{\alpha}^{\beta} \varphi_{\infty} - \Delta_{\alpha}^{\beta} \varphi_i^0)$, which implies that the driving force for the asymmetric non-specific adsorption behavior stems from the difference between the equilibrium distribution potential and the single-particle standard interfacial potential. Unless otherwise specified, the adsorption free energy mentioned in the subsequent text refers to the specific adsorption free energy.

Spontaneous partition- and adsorption-induced charging at liquid-liquid interfaces typically coexist in a given charged liquid-liquid interface system [111], but their relative significance may vary across different systems. Based on the presence of the two charging mechanisms—imbalanced partition and specific adsorption—charged liquid-liquid interface systems can be broadly categorized into four types. The ion distribution characteristics and corresponding spontaneous charging mechanisms are summarized and compared in Table 2.

2.2. Unified thermodynamic description of interface charging

2.2.1. Sharp and diffuse interface models

To provide a unified description of spontaneous charging mechanisms such as imbalanced partition and specific adsorption, there are typically two modeling approaches: the sharp interface model and the diffuse interface model. Both can be extended to describe multiphase flow coupled with mass transfer and electromechanical hydrodynamics phenomena, as will be discussed in Section 3.1. It should be noted that the general forms of these models are primarily presented here.

The sharp interface model treats the solvent mixing layer at the liquid-liquid interface as a geometric surface of zero thickness and considers it as a separate phase (denoted as phase s). In this model, Henry's law and adsorption isotherm models are used to describe the interfacial charge density, while generalized EDL models and the Poisson-Boltzmann equation are employed to describe the distribution

Table 2
Classification of charged interface systems including aqueous electrolyte solutions.

Type	Free energy attributes	Ion distribution	Electrification mechanism	Typical exemplar systems
Inert depletion	$\Delta g_{t,i} \rightarrow \infty$, $\Delta g_{a,i} \simeq 0$	one or both bulk phases, no significant excess within interface phase	only induced by external field	inert dielectrics, insoluble gas, some liquid metal
Simple partition	$\Delta g_{t,+} \neq \Delta g_{t,-}$ and $0 < \Delta g_{t,i} < \infty$, $\Delta g_{a,i} \simeq 0$	both bulk phases, no significant excess within interface phase	imbalanced partition	organic electrolyte solution with relatively high permittivity and strong organic electrolyte, soluble gas, charged gel layer
Simple adsorption	$\Delta g_{t,+} = \Delta g_{t,-}$ or $\Delta g_{t,i} \rightarrow \infty$, $0 < \Delta g_{a,i_0} < \infty$	one or both bulk phases, no significant excess within interface phase	specific adsorption	organic electrolyte solution or pure dielectrics with relatively low permittivity, some liquid metal (including amphiphilic ions as solutes)
Partition-Adsorption coupling	$\Delta g_{t,+} \neq \Delta g_{t,-} < \infty$, $0 < \Delta g_{a,i_0} < \infty$	both bulk phases, significant excess within interface phase	imbalanced partition & specific adsorption	organic electrolyte solution with relatively high permittivity and general organic electrolyte (including weak organic electrolyte)

of ion concentrations. Specifically, Henry's law is primarily used to describe the partition behavior of components across the interface, typically taking the form $c_{i,\alpha}^s = H_i c_{i,\beta}^s$. Here, X_α^s represents the value of the quantity X on the α side of the interface, and H_i is the Henry coefficient or partition coefficient for ion i [73,81,112]. The adsorption isotherm model, on the other hand, is used to describe the specific adsorption behavior of a particular component i_s at the interface, usually expressed as $\Gamma_s = \Gamma_\alpha(c_{i_s,\alpha})$. The concentration $c_{i_s,\alpha}$ can be chosen based on the characteristics of the model, either as the local interfacial quantity $c_{i_s,\alpha}^s$ on the α side of the interface or as the bulk quantity $c_{i_s,\alpha}^\infty$ in the electrically neutral region. The form of the adsorption isotherm function $\Gamma_\alpha(c_{i_s})$ depends on the properties of the solute and its interaction with the interface [49,50,80,112,113]. To calculate the concentration of components in the electrically neutral regions of the liquid phases α on both sides of the interface, one can combine the internal electro-neutrality conditions (neglecting the case of overlapping double layers at the micro and nano scales) with the possible weak electrolyte dissociation equilibrium constants K_{ii}^α of components i and \bar{i} , resulting in the following:

$$\sum_i n_{i,\alpha}^\infty = 0, \quad K_{ii}^\alpha = n_{i,\alpha}^\infty n_{\bar{i},\alpha}^\infty, \quad \forall \alpha. \quad (6)$$

Here, $n_{i,\alpha}$ and $n_{i,\alpha}^\infty$ represent the *number density* of component i in phase α and its electrically neutral region, respectively, with units of ion number per unit volume (i.e., m^{-3}). Consequently, the ion concentration distribution within the diffuse layer can be determined by solving the following Poisson-Boltzmann equation in conjunction with the aforementioned boundary conditions [29,82].

$$n_{i,\alpha} = n_{i,\alpha}^\infty \exp\left(-\frac{z_i e \varphi_\alpha}{k_B T}\right), \quad (7)$$

$$-\nabla \cdot (\epsilon_\alpha \nabla \varphi_\alpha) = \rho_{ea} \equiv \sum_i z_i e n_{i,\alpha}. \quad (8)$$

The diffuse interface model characterizes the solvent mixing layer at the liquid-liquid interface as a region of finite thickness (which can roughly correspond to the interface phase in the sharp interface model), and employs a phase parameter ϕ to depict the difference in solvent fraction at different distances d_s from the interface. The commonly used Cahn-Hilliard phase field model can provide an equilibrium distribution of the phase parameter as $\phi = \tanh(d_s/d_0)$, which takes values of ± 1 within the bulk liquid phases and ranges between $(-1, 1)$ within the solvent mixing layer. Note that this equilibrium solution neglects the influence of solute ions on the distribution of the solvent phase parameter. Specifically, we may refer to the region where $d_s \in (-d_0, d_0)$ as the interface phase, with d_0 being the characteristic thickness of the solvent interface layer, typically on the order of nanometers or less. The specific interactions of each solute ion i with solvent molecules near the interface and their concentration distribution can be quantitatively described by

correlating the additional free energy corrections $\Delta g_{t,i}$ and $\Delta g_{a,i}$ with the solvent phase parameter ϕ , which is known as the generalized force correction model. At this point, the Poisson-Boltzmann equation including the additional free energy correction $\Delta g_i(\phi) = \Delta g_{t,i}(\phi) + \Delta g_{a,i}(\phi)$ can be written as [82].

$$n_i = n_{i,w} \exp\left[-\frac{z_i e \varphi}{k_B T} - \frac{\Delta g_i(\phi)}{k_B T}\right], \quad (9)$$

$$-\nabla \cdot (\epsilon(\phi) \nabla \varphi) = \rho_e \equiv \sum_i z_i e n_i. \quad (10)$$

This allows for an approximate description of the equilibrium transverse distribution of solute ions across the interface. It is important to note that the additional free energy considered here not only includes the effects of solvation of solute ions but also takes into account the effective additional potential influences arising from various interactions such as chemical interactions and ion exchange or correlation effects among solute ions.

For charged liquid-liquid interface systems containing only two solute ions, we can provide a schematic of the corresponding transverse free energy, ion concentration, and electric potential distribution based on the diffuse interface model, as shown in Fig. 6. For charged liquid-liquid interface systems containing three or more solute ions, the interfacial charging characteristics become more complex. Here, typical possible systems are classified according to ion partition behavior, and the specific ion concentration and electric potential distributions can be given according to similar theoretical models as mentioned above [29]. For the sake of clarity, in the following text, when mentioning polarizable or non-polarizable interfaces without a prefix, it is assumed to refer to interfaces that tend to be polarizable and non-polarizable, rather than ideally polarizable or completely non-polarizable. If there are also specifically adsorbed ions in the system, the corresponding adsorption free energy can be added on the basis of the aforementioned partition behavior according to the specific situation.

If we denote the number of anion/cation species in the polarizable interface subsystem that tend to enrich in phase α as N_α^\pm , and the number of anion/cation species in the $\alpha - \beta$ non-polarizable interface subsystem as $N_{\alpha-\beta}^\pm$, then we can write the commonly used combinations in practical modeling as follows: polarizable interface with two ions $(N_\alpha^\pm, N_\beta^\pm, N_{\alpha-\beta}^\pm) = (2, 0, 0)$ or $(1, 1, 0)$, polarizable interface with four ions $(N_\alpha^\pm, N_\beta^\pm, N_{\alpha-\beta}^\pm) = (2, 2, 0)$, non-polarizable interface with two ions $(N_\alpha^\pm, N_\beta^\pm, N_{\alpha-\beta}^\pm) = (0, 0, 2)$, partially non-polarizable interface with three ions $(N_\alpha^\pm, N_\beta^\pm, N_{\alpha-\beta}^\pm) = (1, 1, 1)$, and partially non-polarizable interface with five ions $(N_\alpha^\pm, N_\beta^\pm, N_{\alpha-\beta}^\pm) = (2, 1, 2)$, etc. [82]. From this discussion, it is also evident that a prominent difference between charged liquid-liquid interfaces and solid-liquid interfaces is that, for the

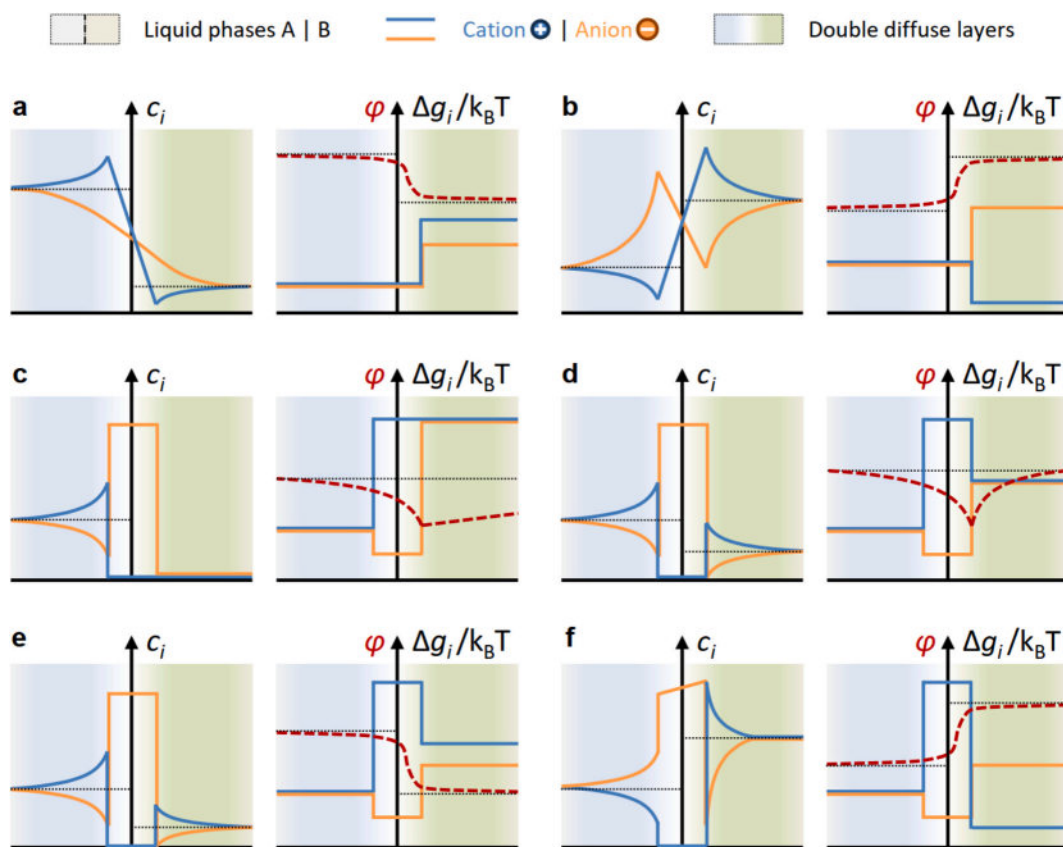


Fig. 6. Interfacial ion-potential distribution around two-liquid interface for different charging mechanisms. (a) Simple partition (cooperative). (b) Simple partition (reversed). (c) Simple adsorption (depleted). (d) Simple adsorption (penetrated). (e) Partition-adsorption coupling (synergistic). (f) Partition-adsorption coupling (antagonistic).

latter, ions can be classified based on whether they participate in the adsorption kinetics controlling interface charging and whether they have additional specific interactions with the solid-liquid interface into *potential determining ions*, *specifically adsorbed ions*, and *indifferent ions*. In contrast, for the former, except scenarios of inert adsorption, almost all ions should be considered as potential determining ions.

2.2.2. Discussions on the model applicability and limitations

Here we will first discuss the prominent features of spontaneous charging at liquid-liquid interfaces from the perspective of ion partition and adsorption behaviors, and provide several comments on the applicability and limitations of the thermodynamic models.

For the ion partitioning behaviors, the dependence of the interface equilibrium potential on different charged interface systems is complex and diverse, leading to various types of interfacial potentials between liquid phases under thermodynamic equilibrium conditions [29]. For instance, the distribution potential at the interface of immiscible electrolyte solutions is related to the degree of electrolyte dissociation and the formation of ion complexes; the Donnan/Nernst potential in semi-permeable/selective ion exchange membranes is associated with the selective permeability of the interface; and the redox potential in interfacial electrochemical reactions is connected to oxidation-reduction reactions. At this point, there will be a significant effective interaction potential gradient between solute ions and solvent molecules near the solvent mixing layer, which is closely related to the ion interfacial adsorption and interphase transport behaviors to be discussed later.

For non-polar oil systems containing simple inorganic ions, although the size difference between cations and anions may also be significant, leading to a transfer free energy difference of up to $2k_B T$, thereby contributing a distribution potential of the order of the thermal potential $V_T \equiv k_B T/e$, the effect of the imbalanced partition-induced charging is

almost negligible. In fact, the small dielectric constant and extremely low ion concentration of the oil phase result in a much larger Debye length (and thus a larger capacitance of the oil-side diffuse layer) compared with the aqueous phase. Since the potential drop across the interface is proportional to the capacitance of the diffuse layer on each side, this leads to the effective interfacial potential on the oil side being tens to hundreds of times that of the aqueous phase. However, the relatively thick diffuse layer on the oil side significantly reduces the interface charge density induced by charging through the electrical double layer (EDL), meaning that the imbalanced partition-induced charging effect is very weak, which is consistent with our usual physical intuition. Nevertheless, for systems with more polar oil phases and the presence of organic ions (i.e., ITIES systems), the imbalanced partition-induced charging effect may not be negligible [82].

Unlike ion partition, which is determined by the difference in solute-solvent interaction potentials within the bulk regions of the two corresponding liquid phases, ion adsorption behavior involves the difference in effective solute-solvent interaction potentials between the interface phase and the bulk phase. Therefore, it is also profoundly influenced by the finite thickness characteristic of the liquid-liquid interface. This implies that specifically adsorbed ions may either be distributed within the solvent mixing layer, partially immersed in it, or closely arranged on both sides to form ion pairs. Considering that the thickness of the solvent mixing layer at the liquid-liquid interface is typically on the same order of magnitude as the size of solute ions and the Bjerrum length, the specifically adsorbed ions within it will exhibit finite excluded-volume and electrostatic correlation effects. The former may lead to volume-associated saturation characteristics in non-dilute solutions, while the latter results in image correlation effects due to changes in the dielectric constant within the Bjerrum length, both of which require certain effective modifications to the adsorption electrification mechanism

modeling based on single-particle free energy. In addition, historically, specific adsorption has been used not only to describe the physicochemical spontaneous adsorption of single ions into the solvent mixing layer but also to refer to the paired adsorption of cations and anions on both sides of the solvent mixing layer due to pairing actions or electrostatic interactions. The latter case can also be referred to as a kind of *correlation-induced imbalanced partition*, which goes beyond the conceptual scope necessary for the discussion in this article. Unless otherwise specified, all references to specific adsorption in the following text refer to the former case that can be described by single-particle free energy.

It should be noted that while the transfer free energy can provide the interfacial equilibrium potential difference and ion partition, the adsorption free energy can yield a formal linear specific adsorption, and the thermodynamic differential relationships can give the general relationship between the interfacial excess ions and the change in surface tension, all of the above phenomenological thermodynamic descriptions fail to reflect the specific mechanisms of charging induced by the interactions between solute ions and solvent in the vicinity of the solvent mixing layer at the liquid-liquid interface. In fact, although the intuitive meanings of transfer or adsorption free energy were given earlier, and a unified description of the two typical charging mechanisms (i.e., imbalanced partition and specific adsorption) was provided through the modification of free energy, such phenomenological classification only offers an effective description of the equilibrium distribution of ions and potential near the charged liquid-liquid interface [82].

In terms of model formulation, the aforementioned thermodynamic descriptions feature *mean-field correction approximations* and *simplifications of interfacial interaction potentials*. The transfer or adsorption free energy merely represents a rough categorization of the various interactions between solute ions and solvent molecules in different charged interfacial systems. Specifically, it simplifies these interactions into the ion selectivity corresponding to the difference in interactions between the solute ions and the uniform liquid phases on both sides of the interface, as well as the specific adsorptivity of ions corresponding to the difference in interactions between the solute ions and the uniform liquid phase versus the solvent mixing layer at the interface. To align the free energy descriptions suitable for upscaling coarse-grained modeling with real physics, a bottom-up analysis of the complex interaction mechanisms and specific potential distributions within the nanoscale range near the interface is required. From this perspective, there are two significant limitations to the current practice of using single-particle free energy corrections for the equilibrium distribution of solute ions at the interface.

On one hand, the description of single-particle free energy is essentially a mean-field approximation of the complex many-body behavior of interfacial ions. Therefore, it can only employ effective corrections dependent on the characteristic parameters of the system for correlated behaviors. These correlated behaviors include electrostatic attraction or repulsion between double diffuse layers, volume exclusion due to ion penetration or near-saturation adsorption in the solvent mixing layer, image forces, and non-local electrostatic interactions within the solvent mixing layer with inhomogeneous dielectric constants [114,115]. To analyze the specific interfacial charging mechanisms of particular systems and to consider the actual distribution characteristics of ions with various correlation effects, an interfacial equilibrium charging model determined jointly by interfacial physicochemical kinetics and electrostatics is introduced. This model serves as an equilibrium constitutive relationship to effectively describe the details of particle interactions within the nanoscale range near the interface [4].

On the other hand, the interaction between solute ions and the solvent molecular fluid background not only affects the distribution of solute ions but also influences the equilibrium distribution of interfacial phase parameters within the solvent mixing layer. This can be regarded as the effects of concentration diffusio-osmosis and electromechanical hydrodynamics, thus necessitating an effective correction of the solvent chemical potential from the perspective of system free energy [116].

Therefore, for charged liquid-liquid interfaces that are near equilibrium, in order to provide an effective free energy distribution within the solvent mixing layer for upscaling coarse-grained modeling, it is necessary to simultaneously provide a quantitative description of the equilibrium distribution structure of phase parameters and ions near the interface. For such multiphysical and multicomponent systems including charged liquid-liquid interfaces, we will briefly introduce their general phase field models in Section 3.2.

In terms of applicable processes, the aforementioned thermodynamic descriptions require that the charged interfacial system be in a *thermodynamic near-equilibrium state*. For ion non-equilibrium transport kinetics, the interfacial normal component of the applied electric field will induce ions to redistribute across the interface and can even induce interphase currents in cases where the interface is non-polarizable. At this point, it is required to determine the controlling steps of interfacial ion transport. If the process is controlled by interfacial mass transfer, it is necessary to analyze the process of ion relaxation to a new quasi-equilibrium state, during which the thermodynamic description near the interface can still be approximately applied; if it is controlled by interfacial physical or chemical kinetics, the interfacial transport of ions is relatively slow, and thus the thermodynamic language is difficult to apply and needs to be replaced by non-equilibrium kinetics descriptions of interfacial physicochemistry. For a quantitative description of multiphase flow-coupled mass transfer behavior, see Section 3.1.

3. Physical model II: Electrokinetic flow of two-liquid interface

Following the general approach in the interfacial electrokinetics, after determining the distribution of ions and potentials at the charged interface under equilibrium conditions, it is necessary to consider the coupled non-equilibrium transport behavior of interfacial ions and fluids. On one hand, based on the ion partition and adsorption characteristics of the charged interfacial system and in conjunction with appropriate interfacial physicochemical non-equilibrium kinetic mechanisms, an appropriate description of the transport kinetic behavior of solute ions near the interface should be provided. On the other hand, based on the conductive and dielectric characteristics of the charged interface and the surrounding liquids, and in combination with the fundamental knowledge of non-uniform continuum electrostatics under the electrostatic limit, the interfacial conditions near the interface should be given, and further upscaled to the asymptotic matching coarse-grained relationships of various physical fields outside the double-sided diffuse layers, represented by interfacial stress. This provides the core physical picture for understanding interfacial electrokinetic flow and transport. This implies that the interfacial physicochemical transport of solute ions and the electromechanical interfacial fluid flow coupled with the electric field are the two foundations for the quantitative description of electrokinetic multiphase flow behavior.

Reviewing the historical development of electrokinetic multiphase hydrodynamics, the aforementioned studies correspond to the two disciplinary fields of physicochemical two-phase hydrodynamics and electromechanical two-phase hydrodynamics. This section will first highlight the basic physical modeling picture of electrokinetic multiphase flow systems through discussions in Sections 3.1 on these two disciplinary fields. The former focuses on the interfacial mass transfer transport processes coupled with multiphase flow, while the latter focuses on the interfacial electromechanical fluid dynamic behavior coupled with ion transport. Subsequently, in Section 3.2, the theoretical development of electrokinetic multiphase hydrodynamics will be reviewed and quantitative descriptions of macroscopic and mesoscopic theoretical models will be provided. This will lay the foundation for the discussions in Section 4, where we will further summarize the characteristic dimensionless numbers and semi-quantitatively discuss the transport mechanisms of electrokinetic multiphase flow.

3.1. Interdisciplinary foundation of electrokinetic multiphase flow

3.1.1. Physico-chemical hydrodynamics and flow-coupled mass transfer

Electrokinetic multiphase flow is a typical multiphase interfacial flow and mass transfer system. Since electrokinetics focuses not only on the interfacial adsorption and transport behavior of ions but also on the interfacial flow phenomena coupled with ion transport, it is generally considered a branch of *physico-chemical hydrodynamics* [11,86,117,118]. The renowned scholar Levich is commonly regarded as one of the founders and promoters of this field, which primarily concerns the characteristics of flow behavior mediated by interfacial transport of multi-component systems, taking into account phenomena such as interfacial adsorption, solute transport, and fluid flow. The core of physico-chemical hydrodynamics lies in the characterization of interfacial mass transfer, with the challenge in liquid-liquid multiphase conditions being the coupling of interfacial mass transfer with the description of multiphase interfaces [119]. This section will discuss the characteristics and applicability of multiphase flow-coupled interfacial mass transfer models, which typically involves the kinetic characteristics of interfacial physicochemical processes.

Considering the discussion on the concept of interfacial polarizability from the previous section, the specific interaction characteristics of solutes with the solvents on both sides near the interface, together with the strength of the non-equilibrium potential difference across the interface, jointly determine whether the solute can achieve transport across the interface. Consequently, the description of multiphase interfacial mass transfer can be divided into two categories: quasi-equilibrium partition and/or adsorption of interfacial components and non-equilibrium interfacial transport models. The former usually corresponds to thermodynamically polarizable or ideally polarizable interfaces, where the distribution of components at the interface is entirely determined by the quasi-equilibrium interfacial physicochemical interactions, typically controlled by mass transfer diffusion near the interface. The latter usually corresponds to partially non-polarizable interfaces, involving non-equilibrium interfacial physicochemical kinetic descriptions of interfacial component transport, typically controlled by strong non-equilibrium transport or chemical reactions at the interface. The interfacial mass transfer models introduced here can provide the interfacial component conditions for the macroscopic theory of electrokinetic multiphase flow in the following section.

For an ideally or thermodynamically polarizable interface with the interphase mass transfer dominated by mass migration, such as when the interface is in adsorption/partition quasi-equilibrium and involves simple interphase physical ion transfer, different effective mass transfer kinetic models can be employed to describe the interfacial transport based on the degree of non-equilibrium. The quasi-equilibrium adsorption/partition model for interfacial components typically takes the form of sharp interface models, including Henry's law and adsorption isotherms, which have been discussed in Section 2.2. The diffusion dynamics model is a typical weak non-equilibrium model, usually taking the form of a diffuse interface model. Specifically, its typical form is the flux term of the Maxwell-Stefan equations or phase field equations $\mathbf{j}_\alpha = -M_\alpha \nabla \mu_\alpha$. Here, μ_α is the chemical potential of component (of phase) α , which is usually related to the detailed distribution of interaction potentials of components within the nanoscale range near the interface, and M_α is its Maxwell-Stefan diffusion coefficient or phase diffusion coefficient [120,121]. In the limiting case of an ideally polarizable interface, the aforementioned diffusion dynamics model reduces to a sharp interface model form with $j_n = 0$ in the steady state.

For a partially non-polarizable interface with the interphase mass transfer controlled by interfacial kinetic source, such as in cases with strong phase change boundaries, complex adsorption kinetics, electron transfer in redox reactions, or facilitated ion transfer, it is necessary to add the interfacial component flux determined by the kinetics of interfacial adsorption or chemical reactions. This is more common in the fields of phase change heat transfer or electrochemistry and typically has

the characteristics of sharp interface models. Among them, the molecular kinetic theory model is mainly used for strong non-equilibrium interfacial mass transfer transport where phase change occurs at the boundary [122,123], and its typical form is $w = w_{s+} \sigma_{\text{scatter}} \left[1 - \left(\frac{\gamma_0}{\gamma_s} \right) \left(\frac{T_0}{T_s} \right)^{1/2} \Gamma \right] \simeq \sigma_{\text{scatter}} \sqrt{\frac{M}{2\pi RT}} (P_s^* - P_0)$, where w is the mass transfer rate, and the physical quantities T, γ, P are distinguished as bulk phase state quantities denoted by the subscript 0 and other local interfacial quantities denoted by the subscript s. The typical form of the adsorption kinetics model is Langmuir kinetics [94], that is, $\frac{d\Gamma}{dt} = k_a c_s (\Gamma_\infty - \Gamma) - k_d \Gamma$, where Γ_∞ represents the saturated adsorption density at the interface, and k_a and k_d are kinetic constants related to the adsorption and desorption free energies. The interfacial chemical reaction kinetics are usually described based on transition state theory, here referred to as chemical dynamics [124,125].

When solute components carry a net charge, for specific charged liquid-liquid interface systems, the characteristic specific physico-chemical interactions between solute ions and the solvents on both sides, together with the strength of the applied electric field, jointly determine whether ions can achieve transport across the interface under specific applied voltage conditions. In other words, these interfacial physicochemical kinetic effects define the electrochemical window of the interface. When both sides of the interface are well conductive and the charged components at the interface tend to be non-polarizable, such as when both sides of the interface are immiscible strong electrolyte solutions or one side is a strong electrolyte aqueous solution and the other side is a liquid metal, this corresponds to the fields of *electrochemistry* (EChem) and *membrane science*. *Electrochemistry* focuses on the interfacial charge transport behavior across electrode interfaces, which includes mechanisms such as electromigration, diffusion, and chemical kinetics, and the interfacial flux typically takes the form of a Butler-Volmer type equation [27,28,109,126]. *Membrane science* focuses on the interfacial mass transfer characteristics of porous medium films with component-selective permeability. It commonly employs *lumped* effective models, which can be divided into steady-state models in the double-film theory or unsteady-state models such as solute osmosis theory and surface renewal theory [127].

This paper will primarily focus on oil-water interface systems that tend to be polarizable. In this case, the liquid-liquid interface is partially polarizable and the applied voltage is within the electrochemical window, hence the ion transport across the interface typically does not involve interfacial chemical reactions. In fact, in the theoretical research of electrokinetic multiphase flow, certain assumptions are often made about the polarizability of charged liquid-liquid interface systems. The most common assumptions are ideally polarizable interfaces and thermodynamically polarizable interfaces. The former assumes that solute ions on both sides of the interface cannot cross the Gibbs interface to the other side, that is, the interphase ion transport flux is zero, while its interfacial charging characteristics are given by the spontaneously adsorbed charge density or possible external field-induced charging [12,87,88]. The latter assumes that solute ions on both sides of the interface can cross the Gibbs interface to the other side, that is, the interphase ion transport flux can be non-zero, but under given external electric field conditions, ions around the solvent mixing layer still maintain an electrochemical quasi-equilibrium distribution state. Its interfacial charging characteristics are determined by the given specific adsorption isotherms or the interphase partition coefficients of various ions [49,50,80,81]. In the fields of electrochemistry and membrane science, the net charge layer at the interface is often abstracted into a geometric surface in a lumped form description, and the flow within the net charge layer near the interface is usually neglected. For electrokinetic multiphase flow, it is necessary to further couple the convection and diffusion behaviors of ions within the net charge layer near the interface in order to apply it to the description of thermodynamically polarizable interfaces [80–82].

3.1.2. Electromechanical hydrodynamics and electrokinetic flow

Since it focuses on the mechanical deformation and motion behaviors of electrolyte solutions containing charged ions coupled with electric fields, electrokinetics also belongs to the branch of *electromechanics*, which was jointly pioneered by electrical engineer Melcher and the renowned fluid dynamicist Taylor, primarily concerning the motion and deformation behaviors of continua under the action of electric fields [128–131]. For immiscible liquid-liquid interface systems with an electrolyte aqueous solution on one side, based on the bulk dielectric and conductive characteristics and the interfacial charging mechanisms, the other liquid phase in contact with the electrolyte aqueous solution can be classified into five categories: *pure dielectric solvent* (PDS), *liquid metal* (LQM), *room-temperature ionic liquid* (RTIL), *strong electrolyte solution* (SES), and *weak electrolyte solution* (WES), as shown in Table 3 [13,47,132], where \mathcal{K} and ϵ represent conductivity and permittivity, respectively. Depending on the liquid phase property and the interfacial transport mechanisms, studies related to electromechanical two-phase hydrodynamics can roughly correspond to three different fields, i.e., SES-SES or SES-LQM in EChem, SES-X in EKmHD, and others in classical EHD (in a narrow sense). Since the electrochemistry of liquid-liquid interfaces has been discussed earlier, the focus here is on the general physical mechanism comparison of the other two fields, while the analysis of key mechanisms in typical specific scenarios of electrokinetic multiphase flow systems is left to Section 4 for elaboration.

As shown in Fig. 7, the deformation and motion behavior of liquid-liquid two-phase interface systems with different conductive and dielectric characteristics under the action of an electric field exhibit significant differences. Traditional continuum electrostatics typically focuses on interfaces of perfect conductors or perfect dielectrics, where the electric field force is perpendicular to the interface, and thus can only achieve force balance in the normal direction through the generation of interface tension via interface normal deformation [47]. Pure dielectric solvents usually have a finite dielectric constant and almost do not dissociate ions, resulting in a nearly zero conductivity, and therefore can be characterized using the *perfect dielectric* (PFD) model. In contrast, liquid metals have extremely high electron mobility and high conductivity, and their dielectric properties can typically be neglected under quasi-electrostatic field approximations, thus they can be characterized using the *perfect conductor* (PFC) model. Compared with these, the electromechanical fluid dynamics of ionic systems typically focuses on *conductive dielectrics*, which possess both the dielectric properties of the background solvent and the conductive properties of solute ions, such as electrolyte solutions and room-temperature ionic liquids.

For electrolyte solutions, the background solvent possesses a finite zero-frequency dielectric constant, capable of accommodating electrostatic fields; meanwhile, the solute ions can move freely under an external electric field, thus exhibiting a certain degree of conductivity. Consequently, they can typically form net free charges (*conductive*) at the interface through induced or spontaneous charging and accommodate a finite tangential electric field (*dielectrics*), thereby generating shear stress under the tangential electric field and driving tangential fluid flow, which is the fundamental mechanism of electrokinetic flow.

Among them, strong electrolyte solutions have relatively high conductivity if not too dilute, thus exhibiting a strong screening effect, and can therefore be referred to as *highly conductive dielectrics* (HCD); in contrast, weak electrolyte solutions and extremely dilute strong electrolyte solutions have low ionic strength, hence their conductivity is poor and the screening effect is weak, and they can be collectively referred to as *poorly/weakly conductive dielectrics* (WCD). For the sake of simplicity, this paper will subsequently not distinguish between highly conductive dielectrics and (by default, not too dilute) strong electrolyte solutions. For weakly conductive dielectrics, unless it causes ambiguity, it is assumed to refer to extremely dilute strong electrolyte solutions, although the latter is different from weak electrolyte solutions where the ionization equilibrium exists and the ionization equilibrium constant is dependent on the electric field strength [47,81].

When at least one side of the interface has a high bulk conductivity and the spontaneous charging of the interface cannot be ignored, this typically corresponds to a scenario where one side is a highly conductive dielectric. In this case, the diffusion of bulk ions cannot be ignored, and the spontaneously charged interfacial net charge layer can be driven by an external electric field, corresponding to *electrokinetic multiphase hydrodynamics* (EKmHD). The historical development of this field has been detailed in Section 1, and will not be reiterated here. It should be noted that when the electric field strength caused by external polarization exceeds the double layer electric field of the spontaneously charged interface, the interface of a strong electrolyte aqueous solution may also induce a non-negligible additional charge due to the difference in electrical properties on both sides, and may even trigger flow instability, which is referred to as induced-charge electrokinetic flow [133]. This paper will focus primarily on the two-phase electrokinetic flow phenomena at oil-water interfaces dominated by spontaneous charging under weak or moderately strong external fields, where the applied electric field is typically on the order of V/mm.

When at least one side of the interface has a low bulk conductivity and the interface charging is mainly induced by external electric field, this typically corresponds to a scenario where both sides of the interface are weakly conductive dielectrics. In this case, the diffusion of bulk ions is much smaller than their electromigration effects, and the free charges accumulated by the action of a strong external field are considered to exist only at the interface, thus allowing the interfacial fluid to be driven by an external electric field, corresponding to *electrohydrodynamics* (EHD) in the narrow sense. This field was jointly pioneered by Melcher and Taylor in the 1960s to 1970s [46], and Saville established a solid theoretical foundation for its *leaky dielectrics* model based on order-of-magnitude analysis at the end of the 20th century [47]. In recent years, Zhakin and Vlahovska have successively made reviews on this topic [58,134]. Here, the applied electric field is usually strong (on the order of V/ μm), the net interfacial charge is usually dominated by external field-induced polarization, and due to the poor conductivity of the leaky dielectric liquid, the effect of ion diffusion is negligible. We refer to the leaky dielectrics model based on this as the *classical theory* of electrohydrodynamics.

It should be noted that, despite the conceptual terminology

Table 3
Classification of liquid phases according to interfacial electromechanical properties.

Type	Abbr.	Bulk property	Charging mechanism	Example	Related areas
Pure dielectric solvent	PDS	$\mathcal{K} \approx 0, \epsilon < \infty$, (generally non-polarizable)	still unclear, could be ion specific adsorption	non-polar oil, air	EK, EHD
Liquid metal	LQM	high $\mathcal{K}, \epsilon \equiv \epsilon_0$ (electronic conductivity)	induced by external field	Hg, Ga, Bi	EChem, EK, EHD
Room-temperature ionic liquids	RTIL	high $\mathcal{K}, \epsilon < \infty$ (ionic conductivity)	still unclear, could be induced by external field	$\text{AlCl}_3\text{-[N-EtPy]Cl}$	Synthetic chemistry, power and chemical engineering
Strong electrolyte solution	SES	generally high $\mathcal{K}, \epsilon < \infty$ (ionic conductivity)	ion imbalanced partition or specific adsorption	TPATPB ($\text{C}_2\text{H}_4\text{Cl}_2$)	EChem, membrane science
Weak electrolyte solution	WES	low $\mathcal{K}, \epsilon < \infty$ (ionic conductivity)	still unclear, could be ion imbalanced partition	ionogenic polar oil, water	EK, EHD

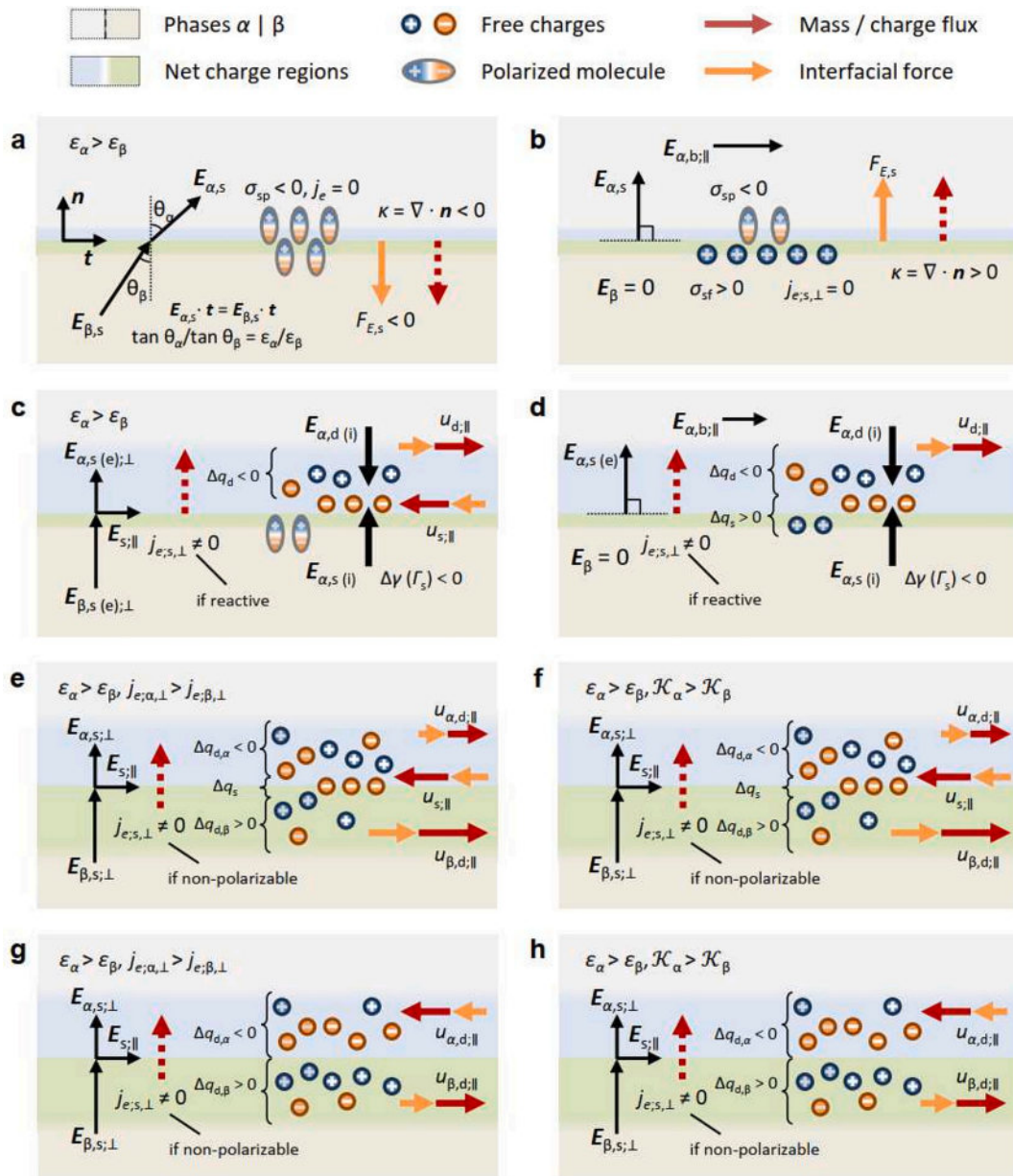


Fig. 7. Interfacial electromechanics around two-liquid interface under steady electric field. (a) PFD - PFD. (b) PFD [α] - PFC [β]. (c) HCD [α] - PFD [β]. (d) HCD [α] - PFC [β]. (e) HCD - HCD, adsorption-based. (f) WCD - WCD, adsorption-based. (g) HCD - HCD, partition-based. (h) WCD - WCD, partition-based. Here, PFD: perfect dielectrics, PFC: perfect conductor, HCD: highly conductive dielectrics, WCD: poorly/weakly conductive dielectrics.

suggesting that electrohydrodynamics should already encompass the research subjects of electrokinetic multiphase hydrodynamics [13,80,81], there are still significant differences between the narrow sense of electrohydrodynamics and electrokinetic multiphase hydrodynamics in terms of research subjects and approaches, as shown in Table 4. The main differences are twofold: first, whether the interfacial charging is dominated by spontaneous interfacial physicochemical factors, and second, whether the interface motion is mediated by the net charge in the diffuse layer [13,47]. Electrokinetic multiphase hydrodynamics needs to consider the spontaneous charging mechanisms at the oil-water interface as well as the convective diffusion and electromigration of ions within the nearby diffuse layer, while classical electrohydrodynamics mainly considers external field-induced polarization charging and only accounts for the electromigration behavior of bulk ions. Therefore, the latter often employs a more direct leaky dielectric model for simplified approximate descriptions, whereas the former must adopt a complete description that takes into account both spontaneous

interfacial charging and double-layer ion transport. However, it is gratifying to note that in recent years, there have been successive studies on weakly conductive dielectrics that consider ion diffusion and convection, attempting to re-examine the electrohydrodynamics model from the perspective of electrokinetic multiphase hydrodynamics. This indicates a trend of integrated development between the two, as described in the following subsection.

3.2. Macroscopic and mesoscopic transport models of EKmHD

This section will introduce the general forms of macroscopic models of electrokinetic multiphase flow from the aspects of bulk governing equations and interfacial conditions. Then, we will compare different interfacial transport models, providing a basic reference for the subsequent discussion on transport mechanisms and the extraction of dimensionless numbers, and then discuss the differences between macroscopic and mesoscopic models of electrokinetic multiphase flow.

Table 4

Comparison between classical electrohydrodynamics (EHD) and electrokinetic multiphase hydrodynamics (EKmHD).

	EHD	EKmHD
Typical systems	Taylor pump [46], Taylor cone [135]	droplet electrophoresis [48,50] or diffusiophoresis [48,49]
Representatives	Taylor-Melcher [45,46]; Saville [6,47]	Frumkin-Levich [11,37]; Baygents-Saville [49,50]
Components	WES on both sides	SES on at least one side
Electric properties	WCD	HCD
Charge transport	Ohmic conduction	diffusion, electro-migration and convection
Formulation	leaky current approximation, few charges and strong electric field	charge relaxation, surface conduction may be important
Charging mechanism	induced charging by strong external electric field	physico-chemically spontaneous charging with weak external electric field
Formulation	interface electrical matching condition	interface physico-chemical kinetic condition
Driving forces	shear stress originated from induced charge under tangential electric field	spontaneously formed net charge layer under tangential electric field
Electro-magnetic field	quasi-electrostatic field approximation	
Two-phase flow	Navier-Stokes equations in bulk, stress balance at interface	
Ion transport	conductive flux conservation	Nernst-Planck equation

3.2.1. General formulation of macroscopic models

3.2.1.1. Governing equations. Regarding the bulk governing equations, they mainly consist of three parts: electrostatics, fluid flow, and ion transport [49,50,136,137]. Since the transport properties of each equation are related to the specific bulk phase α , they are all initially denoted with the subscript α for emphasis, while all physical field quantities and transport properties without subscripts can be understood according to the material properties indicating the phase α . For various conservative physical fields such as mass, charge, and component and their fluxes involved in the transport processes, they are basically denoted according to the notations in Bird's monograph [127] and electrokinetic multiphase flow literature [80,87,88]. Specifically, the *mass density* (or simply density) and *charge density* of the solution are denoted as ρ and ρ_e , respectively. The *mole fraction*, *molar concentration*, and *number density* of component i are denoted as x_i , c_i , and n_i , respectively. The *mass density flux*, *molar concentration flux*, *number density flux*, and *electric current* (i.e., charge density flux) of component i are denoted as \mathbf{j}_i , \mathbf{j}_i^* , \mathbf{j}_i^{**} , and \mathbf{i} , respectively.

For *electrodynamics*, in typical electrokinetic systems in EKmHD, the following scaling relationships generally hold which is similar to electrohydrodynamics [47,136].

$$\tau_p \gg \tau_E \gg \tau_B. \quad (11)$$

Here, τ_p represents the time scale of the physical problem (such as viscosity, diffusion, vibration, boundary motion, etc.), $\tau_E = \epsilon/\mathcal{K}$ is the time scale for the variation of the electric field, and $\tau_B = \mathcal{M}/\mathcal{K}a^2$ is the time scale for the variation of the magnetic field; where \mathcal{K} and \mathcal{M} are the electrical conductivity and magneto-permeability, respectively, and a is the characteristic length scale of the system. The aforementioned scaling relationships imply that the quasi-electrostatic field approximation is valid, thus the evolution of the electromagnetic fields in this system can be decoupled from each other according to Maxwell's equations. Thus, the electrostatics can be simplified to the electrostatic Poisson equation that describes the distribution of the electric potential (for each phase α)

$$-\nabla \cdot (\epsilon_\alpha \nabla \varphi) = \rho_e = \sum_i z_i e n_i. \quad (12)$$

Here, φ denotes the electric potential, and ϵ_α represents the dielectric constant of phase α . The influence of electrostatics on fluid flow and ion transport is reflected through the electrostatic Maxwell stress in the momentum equation and the electro-migration (electrophoresis in essence) term in the conservation equation of charged components, as well as the modification of the ion diffusion coefficient by electrostatic interactions.

For *fluid flow*, under the condition of incompressible flow, the continuity equation and momentum equation (for each phase α) are [49,50,127].

$$\nabla \cdot \mathbf{u} = 0, \quad (13)$$

$$\rho \left(\frac{\partial \mathbf{u}}{\partial t} + \mathbf{u} \cdot \nabla \mathbf{u} \right) = \nabla \cdot (-p\mathbf{I} + \mathbf{T}^n + \mathbf{T}^e). \quad (14)$$

Here, \mathbf{u} is the velocity field, p the pressure, \mathbf{I} the identity tensor, and \mathbf{T}^n is the Newtonian viscous stress tensor

$$\mathbf{T}^n = \eta_\alpha [\nabla \mathbf{u} + (\nabla \mathbf{u})^T], \quad (15)$$

which contributes to the volume force $\mathbf{F}_N \equiv -\nabla p + \nabla \cdot \mathbf{T}^n = -\nabla p + \eta_\alpha \nabla^2 \mathbf{u}$ along with the pressure gradient. Here, η_α is the dynamic viscosity of phase α . \mathbf{T}^e is the electric Maxwell stress tensor [136,137].

$$\mathbf{T}^e = \epsilon_\alpha \left[\mathbf{E}\mathbf{E} - \frac{1}{2}E^2\mathbf{I} \right]. \quad (16)$$

The corresponding electric field force is given by $\mathbf{F}_e \equiv \nabla \cdot \mathbf{T}^e = \rho_e \mathbf{E} - \frac{1}{2}E^2 \nabla \epsilon_\alpha + \nabla p_{es}$, whose physical meanings include the Coulomb force $\rho_e \mathbf{E}$ due to net charge, the dielectric gradient force $-\frac{1}{2}E^2 \nabla \epsilon_\alpha$ due to inhomogeneous dielectric constant, and the electrostriction gradient force ∇p_{es} in a conservative form related to the local strain within fluid element induced by the electric field. The induced electrostrictive pressure p_{es} is expressed as

$$p_{es} = \frac{1}{2} \epsilon_\alpha a E^2, \quad \beta_e = \left(\frac{\rho}{\epsilon_\alpha} \right) \frac{\partial \epsilon_\alpha}{\partial \rho}. \quad (17)$$

Here, β_e^{-1} is the electrostriction coefficient, which is typically negligible. Then, the momentum equation can be explicitly written as

$$\rho \left(\frac{\partial \mathbf{u}}{\partial t} + \mathbf{u} \cdot \nabla \mathbf{u} \right) = -\nabla p + \eta_\alpha \nabla^2 \mathbf{u} + \rho_e \mathbf{E} - \frac{1}{2}E^2 \nabla \epsilon_\alpha. \quad (18)$$

In this formulation, p_{es} has already been incorporated into the dynamic pressure p . Specifically, in the macroscopic models used for describing bulk transport with zero-thickness sharp interfaces, if there is no significant heterogeneity in bulk density and dielectric constant (such as due to significant temperature gradients), then these will reduce to uniform material property parameters ρ_α and ϵ_α , and the electric field force need only retain the Coulomb force term $\rho_e \mathbf{E}$. For mesoscopic numerical models with diffuse interfaces, there will always be variations in the phase parameter ϕ within the solvent mixing layer, and the density $\rho(\phi)$ and dielectric constant $\epsilon(\phi)$ will also vary in the direction of $\nabla \phi$. At this point, it is necessary to retain the dielectric gradient force term $-\frac{1}{2}E^2 \nabla \epsilon(\phi)$ in the electric field force, and generally, it is also necessary to add the stress tensor \mathbf{T}^∇ contributed by the gradient of the interfacial phase parameter $\nabla \phi$ (see the following subsection).

For *ion transport*, different models are employed based on the differences in the dielectric and conductive behavior of the liquid phase, where the differences in various studies usually lie. They can be classified into pure dielectric solvents, liquid metals, strong electrolyte solutions, and weak electrolyte solutions.

Among them, the perfect dielectric model that describes pure

dielectric solvents is the simplest case, as there are no free charges within it, hence $\rho_e = 0$ [138,139]. For liquid metals as perfect conductors, their dielectric constants can be neglected under quasi-electrostatic field conditions, and the electron mobility within them is high and much greater than the ion mobility. Therefore, the relaxation time for the system that is required to evolve to a steady state under the action of a quasi-electrostatic field is usually negligible, and only the following electron number conservation equation is required

$$\nabla \cdot \mathbf{i} = 0. \quad (19)$$

Considering that the mobility of electrons is much greater than that of ions, and the convective velocity of the fluid is much smaller than the directional motion velocity of metal electrons under the influence of electromigration, the constitutive model of electric current can be given by Ohm's law $\mathbf{i} = \sigma_e \mathbf{E}$, which in turn yields $\rho_e = 0$ and $\varphi = \text{const}$ [48,140].

For strong electrolyte solutions as highly conductive dielectrics, not only do solute ions exist as free charges which make the solution conductive, but there is also a dielectric solvent background that can accommodate a finite electric field within it. Moreover, the viscous interactions between solute ions and the solvent molecular fluid background during their motion are typically not negligible to determine the finite mobility of ions. Generally, the transport of solute ions can be described using the Nernst-Planck equation or the Maxwell-Stefan equations [38,50]. Among them, the Maxwell-Stefan equations [82,120] have the broadest applicability and can be used to describe non-equilibrium transport in non-dilute solutions

$$\frac{\partial n_i}{\partial t} + \nabla \cdot (n_i \mathbf{u} + \mathbf{j}_i^{**}) = 0, \quad (20)$$

where the specific form of ion i 's flux \mathbf{j}_i^{**}

$$\mathbf{j}_i^{**} \equiv -\widehat{D}_{i,\alpha} n_i \frac{\nabla \mu_i}{k_B T} = -\widehat{D}_{i,\alpha} (\nabla n_i + n_i \nabla \ln \gamma_i^\alpha). \quad (21)$$

Here, $\mu_i = \mu_{i,\alpha}^0 + k_B T \ln(a_i/n^\ominus)$ represents the chemical potential of ion i , where $\mu_{i,\alpha}^0$ denotes the chemical potential of the solute ion interacting with the solvent in phase α , and $a_i \equiv \gamma_i^\alpha \gamma_i^x n_i$ is the activity of ion i , with n^\ominus being the molar concentration of the solution under standard conditions. The transport coefficients in \mathbf{j}_i^{**} are dependent on the phase α in which ion i resides; $\widehat{D}_{i,\alpha}$ is the Maxwell-Stefan diffusion coefficient of ion i in phase α . γ_i^α is the effective activity coefficient of ion i that depends on the local electric potential φ , defined as $\gamma_i^\alpha := \exp(z_i e \varphi / k_B T)$, and γ_i^x is the activity coefficient of ion i that depends on the interactions between solution components other than Coulombic electrostatic effects.

In particular, under the condition of dilute solutions and weak electric field (induced polarization) where steric and electrostatic correlations between solute components can be neglected, we have $\gamma_i^x \equiv 1$. At this point, the chemical potential can be simplified to $\mu_{i,\alpha} = \mu_{i,\alpha}^0 + k_B T \ln(\gamma_i^\alpha n_i / n^\ominus)$. The aforementioned Maxwell-Stefan equation can then be reduced to the following Nernst-Planck equation

$$\frac{\partial n_i}{\partial t} + \nabla \cdot (n_i \mathbf{u} - D_{i,\alpha} \nabla n_i - z_i e \omega_{i,\alpha} n_i \nabla \varphi) = 0. \quad (22)$$

Here, $D_{i,\alpha} \equiv \widehat{D}_{i,\alpha}$ is the Fickian diffusion coefficient of ion i in phase α neglecting non-ideal solution effects, and $\omega_{i,\alpha} \equiv D_{i,\alpha} / k_B T$ is the electromigration (electrophoresis in essence) mobility of ion i within phase α . Under conditions close to thermodynamic equilibrium, where $\partial_t = 0$ and $\mathbf{u} = 0$, the above equation further reduces to the Poisson-Boltzmann equation. In some literature, it is also extended to weak non-equilibrium conditions under the influence of an external field and is referred to as the Poisson-Smoluchowski formula [141].

For weak electrolyte solutions as weakly conductive dielectrics, the

modeling approaches are the most diverse, but they are typically based on the aforementioned ion transport models with appropriate approximations. Due to the ionization process of weak electrolytes in the solvent and possible spontaneous charging mechanisms at the interface, it is necessary to consider the production or consumption terms brought about by chemical reactions in the ion transport equations, as well as spontaneous partition- or adsorption-induced charging behavior at the interface, which is referred to as the modified Saville model [81]. In addition to the direct application of the aforementioned ion transport models, under different approximation conditions, various schemes such as charge transport models and charge injection models can be derived, leading to different treatments of solid boundaries and fluid-fluid interfaces [47,81]. When the dissociation coefficient of solute molecules is small or the differences in diffusion coefficients of different ions are negligible, the ion transport models can be reduced to corresponding charge diffusion models or charge injection models. The latter is mainly applicable to special cases where a certain type of ion dominates during unipolar injection.

3.2.1.2. Interfacial conditions. The complex behavior of electrokinetic multiphase flow originates from the ion-fluid coupled transport within the interfacial net charge layer; therefore, the formulation and treatment of interfacial conditions are crucial. For the sake of simplicity and clarity, the perspective of sharp interface macroscopic models is adopted here, which neglects the effects induced by the finite thickness of the solvent mixing layer at the liquid-liquid interface, such as capacitive charging, shear strain rate, and concentration diffusio-osmosis. The resolution of these effects depends on the quantitative solution of diffuse interface models (see the following subsection), which are then incorporated into the sharp interface macroscopic theory through the reduced forms of interfacial conditions such as jumps in electric potential, velocity, and shear stress [82]. Specifically, the interfacial conditions consist of three parts: mechanical matching, electrical matching, and component conservation at the interface, where the interfacial component condition is the core. The key to its description lies in the correlated depiction of local quasi-equilibrium of interfacial ion concentrations and local balance of interfacial ion transport fluxes. Compared with neutral components, the charging mechanisms and ion transport kinetics of charged components require extra coupling with the electric field.

Interfacial mechanical matching condition includes continuity condition and stress balance condition [142].

$$\|\mathbf{u}\| = 0, \quad \|(\mathbf{T}^v + \mathbf{T}^e)\| \cdot \mathbf{n} = \|p\| \mathbf{n} + \gamma \kappa_c \mathbf{n} - \nabla_s \gamma. \quad (23)$$

Here, $\|(\cdot)\| \equiv \|(\cdot)\|_\beta^\alpha := (\cdot)_\alpha - (\cdot)_\beta$ denotes the jump of the physical quantity (\cdot) across the interface from phase α to phase β , and $\mathbf{n} \equiv \mathbf{n}_{\beta/\alpha}$ is the unit normal vector pointing from phase β outward towards phase α . $\nabla_s = (\mathbf{I} - \mathbf{nn}) \cdot \nabla$ represents the tangential gradient operator at the interface, and thus $\kappa_c \equiv \nabla_s \cdot \mathbf{n}$ is the sum of the local principal curvatures of the interface. The viscous stress tensor \mathbf{T}^v and the Maxwell stress tensor \mathbf{T}^e have been previously described, while the interfacial tension coefficient is defined as $\gamma = \int_{-\infty}^{\infty} \mathbf{t} \cdot \mathbf{T}^v \cdot \mathbf{t} dn$. Here, \mathbf{t} is the unit tangential vector along any direction of the interface, and \mathbf{T}^v is the stress tensor related to the pressure and the gradient of the interfacial phase parameter $\nabla \phi$, the specific meaning of which will be explained in the following paragraph. It should be noted that the additional momentum flux contribution caused by interfacial mass transfer has been neglected here, which is usually induced by strong non-equilibrium factors such as phase change and interfacial chemical reactions. To be explicit, the interfacial stress conditions are further elaborated here according to the components in the local interface coordinate system, as follows:

$$\mathbf{n} \cdot \|(\mathbf{T}^v + \mathbf{T}^e)\| \cdot \mathbf{n} = \|p\| + \gamma \kappa_c, \quad (24)$$

$$\mathbf{t} \cdot \|(\mathbf{T}^v + \mathbf{T}^e)\| \cdot \mathbf{n} = -\nabla_s \gamma. \quad (25)$$

Here, the interfacial tension gradient term $\nabla_s \gamma$ on the right-hand side of the tangential stress balance equation is related to the excess adsorption of interfacial ions, and its specific theoretical form can be referred to in the article by Baygents et al. [49]. However, for the majority of non-surfactant ions involved in electrokinetic multiphase flow, this term is usually negligible.

In fact, the pressure tensor $\mathbf{P} \equiv p\mathbf{I} - \mathbf{T}^\nabla \equiv -\mathbf{T}^\nabla$ originates from the momentum flux conservation quantity implied in the general form of the interfacial gradient free energy functional, satisfying $\int_{\partial V} \mathbf{T}^\nabla \cdot d\mathbf{A} = 0$ (for any ∂V). Here, \mathbf{T}^∇ represents the contribution from the gradient of the interfacial phase parameter $\nabla \phi$, and in the case of a binary mixture, this stress can be written as [121].

$$\mathbf{T}^\nabla \equiv \Lambda_p \nabla \rho_\alpha \nabla \rho_\alpha - \frac{1}{2} \Lambda_p |\nabla \rho_\alpha|^2 \mathbf{I}. \quad (26)$$

Here, ρ_α denotes the local mass fraction of solvent α within the solvent mixing layer, and Λ_p represents the interfacial excess energy density. In the sharp interface limit, the divergence of the aforementioned pressure tensor contributes to an equivalent volumetric force $\mathbf{F}, d^2 S_\perp = \int_{d^2 S_\perp} \mathbf{T}^\nabla \cdot d\mathbf{A}$, where $d^2 S_\perp = d\mathbf{n} \otimes d\mathbf{S}$ is the thin cylindrical surface with axis $d\mathbf{n}$, $d\mathbf{S}$ is the interfacial element, and $d\mathbf{n}$ is the element along the direction of \mathbf{n} . The specific form of this volumetric force corresponds to the pressure jump across the interface $\|p\| \mathbf{n}$, as well as the interfacial tension $\delta_s \gamma \kappa \mathbf{n}$ and the interfacial tension gradient force $\delta_s \nabla_s \gamma$, where δ_s is the Dirac function with the distance to the interface as the independent variable. It should be noted that when the thickness of the diffuse layer is comparable to that of the solvent mixing layer, the additional velocity gradients and shear stress gradients (manifested as effective interfacial tension gradients) caused by the shear strain rate and solute ion concentration may not be negligible. In this case, additional tangential velocity jumps $\|u_s\| = \Delta u_s$ and shear stress jump contributions need to be supplemented.

The interfacial electrical matching condition reflects the interaction between the field and charge near the interface, and its general form is $\|\epsilon \mathbf{E}\| \cdot \mathbf{n} = q_s, \quad \|\mathbf{E}\| \cdot \mathbf{t} = 0. \quad (27)$

Here, $q_s = \sum_i z_i e n_{i,s}$ represents the interfacial charge density, and $n_{i,s}$ is the surface density of adsorbed ionic species i at the interface. Using the aforementioned interfacial electrical matching conditions, the specific expression for the Maxwell stress jump can be written as [47].

$$\mathbf{n} \cdot \|\mathbf{T}^\epsilon\| \cdot \mathbf{n} = \|\epsilon(\mathbf{E} \cdot \mathbf{n})^2\| - \left\| \frac{1}{2} \epsilon E^2 \right\|, \quad (28)$$

$$\mathbf{t} \cdot \|\mathbf{T}^\epsilon\| \cdot \mathbf{n} = q_s \mathbf{E} \cdot \mathbf{t}. \quad (29)$$

Thus, the electric field contributes not only to an effective pressure jump but also provides an additional source of interfacial shear stress in the stress matching at the interface. It should be noted that when the thickness of the diffuse layer is comparable to that of the solvent mixing layer, the additional potential jump caused by capacitive charging of the interface phase may not be negligible, and the corresponding potential jump contribution $\|\varphi\| = \Delta \varphi_s$ needs to be supplemented.

The interfacial concentration and flux condition reflects the interfacial charging mechanism and the component conservation at the interface [142]. Here, the most general interfacial component conservation condition that includes interfacial ion adsorption is presented, while the interfacial charging mechanism model is deferred to the following subsection. The interfacial component conservation condition typically treats the interfacial phase s as a separate phase, from which the general form of interfacial component conservation can be written as [11,49,50,80,134].

$$\frac{D_n n_{i,s}}{Dt} + n_{i,s} \kappa_c \mathbf{u} \cdot \mathbf{n} + \nabla_s \cdot (n_{i,s} \mathbf{u}_s + \mathbf{j}_{i,s}^{**}) + \|\mathbf{j}_i^{**}\| \cdot \mathbf{n} = r_{i,s}. \quad (30)$$

Here, $D_n/Dt = \partial_t + \mathbf{u}_n \cdot \nabla$ is the normal material derivative operator, $\mathbf{j}_{i,s}^{**} = -\omega_{i,s} k_B T \nabla_s n_{i,s} - e z_i \omega_{i,s} n_{i,s} \nabla_s \varphi$ is the tangential flux of interfacial ions, $\mathbf{j}_i^{**} = -\omega_i k_B T \nabla n_i - e z_i \omega_i n_i \nabla \varphi$ is the bulk phase ion flux due to the electrochemical potential gradient (i.e., it does not include the convective effect of the solvent background fluid), and $r_{i,s}$ is the interfacial reaction source term. Here, $\omega_{i,s}$ is the mobility of ionic component i at the interface, $\mathbf{u}_n \equiv \mathbf{n} \mathbf{n} \cdot \mathbf{u}$ and $\mathbf{u}_s \equiv (\mathbf{I} - \mathbf{n} \mathbf{n}) \cdot \mathbf{u}$ are the normal and tangential velocities at the interface, respectively. It can be seen that the balance between the tangential transport $\mathbf{j}_{i,s}^{**}$ at the interface and the normal transport $\mathbf{j}_{i,n}^{**} \equiv \mathbf{j}_i^{**} \cdot \mathbf{n}$ near the interface jointly ensures the conservation of the interfacial component concentration; note that the contributions of additional normal momentum flux have been neglected here [46,121,136]. Noting that

$$\nabla_s \cdot \mathbf{u}_s + \kappa_c \mathbf{u} \cdot \mathbf{n} + \mathbf{n} \cdot (\mathbf{n} \cdot \nabla) \mathbf{u} = 0, \quad \mathbf{n} \cdot \nabla_s = 0, \quad (31)$$

the aforementioned equation can be rewritten into [47].

$$\frac{D_n n_{i,s}}{Dt} + \mathbf{u} \cdot \nabla n_{i,s} + \nabla_s \cdot \mathbf{j}_{i,s}^{**} + \|\mathbf{j}_i^{**}\| \cdot \mathbf{n} = n_{i,s} [\mathbf{n} \cdot (\nabla \mathbf{u}) \cdot \mathbf{n}] + r_{i,s}. \quad (32)$$

If the differences in ion diffusion coefficients can be neglected, and the interfacial diffusion is ignored, then the aforementioned ion transport model can be reduced to a charge transport model [47,136,137,143–145].

$$\frac{D_n q_s}{Dt} + \mathbf{u} \cdot \nabla_s q_s + \nabla_s \cdot \mathbf{i}_{s,M} + \|\mathbf{i}' \cdot \mathbf{n}\| = q_s [\mathbf{n} \cdot (\nabla \mathbf{u}) \cdot \mathbf{n}] + q_s^{\text{react}}, \quad (33)$$

Here, $\mathbf{i}_{s,M} = -\mathcal{K}_s \nabla \varphi$ represents the charge density flux contributed by interfacial electromigration, $\mathbf{i}' := \sum_i z_i e \mathbf{j}_i^{**} = -D \nabla q - \mathcal{K} \nabla \varphi$ represents the charge density flux in the bulk phase due to ion diffusion and electromigration, and q_s^{react} is the charge source term due to interfacial chemical reactions, where $D = \omega k_B T$ and $\mathcal{K}_{(s)} = \sum \omega_{(s)} e^2 z_i^2 n_{i,(s)}$ are the ion diffusion coefficient and (interfacial) conductivity, respectively.

In addition, the modulation of interfacial tension and wettability by ions is also an important aspect of electrokinetic multiphase flow [77,79]. For a comprehensive theoretical analysis on ion-tuned interfacial tension, one can refer to the analysis of droplet diffusiophoresis by Baygents and Saville [49]. This study particularly points out that the effect of simple inorganic ions on the oil-water interfacial tension can be neglected, while the specific treatment for surfactants can be found in the reviews or monographs [95,108,142]. Regarding ion-tuned wettability, the models currently used in electrokinetic flow modeling are simple linear or nonlinear monotonic models [146–148]. Here, the mathematical forms of existing models for ion-tuned wettability are presented. Among them, the linear model [146] is obtained by linearly interpolating experimental measurements of contact angles at two different ion concentrations

$$\theta = \theta_H + \frac{\alpha_3 - \alpha_H}{\alpha_L - \alpha_{HS}} (\theta_L - \theta_H). \quad (34)$$

The nonlinear model assumes that the change in wettability by ions follows a pattern similar to the Langmuir adsorption isotherm [147,148].

$$\theta_{(i,t)} = \theta_0 - (\theta_0 - \theta_{\min}) \frac{(c_H - c_{(i,t)}) (1 + K_{\text{eq}} c_L)}{(c_H - c_L) (1 + K_{\text{eq}} c_{(i,t)})}. \quad (35)$$

The definitions of the physical quantities can be found in the reference [147]. It should be noted that the aforementioned models typically fail to effectively capture the common non-monotonic effects observed in practice [149], and the quantitative patterns and characteristics of ion-tuned wettability remain unclear.

3.2.2. Macroscopic interfacial constitutive relations and mesoscopic models

Due to the possible spontaneous partition-adsorption and other

charging mechanisms at the liquid-liquid interface, as well as the resulting macroscopic discontinuities in physical quantities, the interface exhibits multiphysical and multiphase characteristics with the coupling of electrostatic interactions and physicochemical effects. It is thus necessary to further add appropriate constitutive model constraints into the general form of the aforementioned interfacial component conditions, including interfacial charging mechanisms and interfacial ion transport behaviors, which can be summarized into different macroscopic models (as shown in the first three columns of Table 5). The main features of these models are briefly analyzed below.

On one hand, the interfacial charging mechanism mainly corresponds to the constitutive model of the interfacial charge density q_s . For ideally polarizable interfaces with induced charging, taking liquid metals as an example, the electrical matching condition $\phi_{in} = \text{const}$ and the charge conservation within the metal $Q_{in} = \int_S q_s dS = Q_0$ are typically used as substitutes, where Q_0 is the prescribed charge of the metal [87]. For thermodynamically polarizable interfaces with spontaneous charging, they usually rely on the local quasi-equilibrium assumption of the adsorption-partition equilibrium model, where the surface density of components can be correlated with the adjacent bulk phases on both sides through kinetic equilibrium relationships. For example, the spontaneous adsorption condition based on the local adsorption isotherm $c_{i,s} = \Gamma_i^\alpha \left(\frac{c_{i,s}^\alpha}{c_{i,s}^\beta} \right)$ and the spontaneous partition condition based on the local Henry's law $c_{i,s}^\alpha = H_i c_{i,s}^\beta$, where H_i is the Henry coefficient or partition coefficient for component i . For partially non-polarizable weakly conductive dielectric liquid interfaces, in addition to directly characterizing them using the aforementioned spontaneous charging mechanisms, one can also use the effective interfacial conditions based on the upscaled coarse-grained ion transport models from electrohydrodynamics to capture the leading-order electrokinetic effects, which are typically expressed in the form of the leaky dielectric model [81]. Studies have shown that this model can also be applicable to the electrokinetic multiphase flow of highly conductive dielectric interfaces [80,151].

On the other hand, the interfacial ion transport models mainly correspond to the specific constraints on the tangential and normal ion fluxes j_s and j_n , as well as the interfacial reaction source term r_s , such as whether the interface is non-polarizable, whether convection is neglected, whether diffusion is ignored, and whether chemical reactions occur, reflecting the characteristic behaviors of ion transport at the interface [80,81]. It should be particularly noted that a combination of perspectives is used here: one is the perspective of physical kinetics, which is more physical and commonly used in liquid-liquid extraction or phase change mass transfer, focusing on ion transport across the

interface represented by solvation and adsorption kinetics, using effective descriptions based on quasi-equilibrium models [49,50,80,81,151], simple adsorption kinetics, or interaction free energy within the nanoscale range around the interface [82,116]; the other is the perspective of reaction kinetics, which is more chemical and commonly used in liquid-liquid electrochemistry, focusing on ion transport across the interface represented by interfacial chemical reactions, using effective descriptions such as simple reaction kinetics [11] or the Butler-Volmer type equations [152,153].

It is particularly worth noting that for cases involving spontaneous partition-induced charging, Mori et al. provided the model connection from electrokinetic multiphase hydrodynamics to classical electrohydrodynamics [81,145], with the main results of the connection shown in Table 6. Specifically, when the system satisfies $\nabla \cdot (z_i e \omega_{i,\alpha} n_i \mathbf{E}) \gg \nabla \cdot (D_{i,\alpha} \nabla n_i)$, the diffusion term in the charge diffusion model can be neglected. Consequently, it can be reduced to the Taylor-Melcher model (i.e., the leaky dielectric model) or the upscaled coarse-grained description of the electrophoretic model in the sense of matched asymptotic expansion. The former typically corresponds to the induced charging scenario of partially non-polarizable interfaces, while the latter usually corresponds to the spontaneous charging scenario with a phenomenologically prescribed total charge. The interfacial condition can be written in a form similar to the local charge conservation at the liquid metal interface as mentioned above.

Whether it is the analytical solutions based on matched asymptotic expansions with effective interface condition or numerical simulations using finite volume methods combined with multigrid techniques, the accuracy of macroscopic theoretical results based on sharp interface models strongly depends on the effectiveness of the interfacial conditions. From the perspective of diffuse interfaces, if the thickness of the diffuse layer is comparable to that of the solvent mixing layer, then the additional potential jumps, velocity jumps, and shear stress jumps at the interface due to capacitive charging, shear strain rates, and concentration gradients of the interfacial phase may not be negligible. Therefore, the results of the sharp interface limit cannot be directly applied. In recent years, the significant impact of the finite-thickness solvent mixing effects on ITIES systems has gradually gained attention. By extending the Landau-Ginzburg equilibrium phase field theory [96,98], Rotenberg and colleagues established a general theory for the non-equilibrium transport in ITIES systems [116], and Huang and Wang further expanded it into an effective theory considering complex charging mechanisms [82].

The above research incorporates the complex interactions between solute ions and molecules within the solvent mixing layer into mesoscopic numerical models, which can fully capture the possible effects such as interfacial phase capacitive charging, shear strain rate, and concentration diffusio-osmosis, and is expected to provide a key theoretical bridge for the future quantitative prediction of electrokinetic multiphase flow (as shown in Fig. 1). In fact, it is often necessary to start from the interactions within the nanoscale range of the interface and conduct numerical simulations based on appropriate diffuse interface models to provide reasonable and effective corrections to interfacial conditions for the sharp interface model (as shown in the fourth column of Table 5). Compared with macroscopic models based on sharp interface approaches, mesoscopic numerical models based on diffuse interface theories offer a means to finely depict the interactions between solute ions and the solvent mixing layer at the interface. When the thicknesses of the diffuse layer and the solvent mixing layer are comparable and spontaneous partition-induced charging dominates, the interfacial potential jump in the macroscopic model can be corrected based on the results of the diffuse interface model [82].

Here, taking the phase field model as an example [82,116], which is widely applicable with various solvers, we introduce a typical mesoscopic transport model for electrokinetic multiphase flow. The phase field model employs an *order parameter* (also known as a phase

Table 5
Comparisons of theoretical models for interfacial condition of EKmHD.

	Ideally polarizable	Adsorption & polarizable	Partition & polarizable	Diffuse interface
Representatives	Pascall [12]; Schnitzer [88]; Yang [113]	Saville [47]; Baygents [49,50]; Schnitzer [80]	Schnitzer [80]; Mori [81]; Ma [73]	Rotenberg [116]; Rivas [150]; Huang [82]
Ion transport	Nernst-Planck equation	Nernst-Planck equation	Nernst-Planck equation	modified Maxwell-Stefan equation
Ion distribution	simple adsorption / partition	simple adsorption	simple partition	partition-adsorption coupling
Electrification mechanism	spontaneous / field induced	spontaneous adsorption	spontaneous partition	spontaneous charging
Mechanism description	-	adsorption isotherm	Donnan equilibrium	particle interaction potential

Table 6
Connections between EKmHD and classical EHD models.

	Modified Saville	Charge diffusion	Taylor-Melcher	Electro-migration
Representatives	Baygents [50,151]; Zholkovskij [154]; Schnitzer [80]	Kupersh [155]; Luo [145]; Mori [81]	Sherwood [156]; Feng [157]	Hua [138]; Li [139]
Electrical characteristics	General conductive dielectrics	Poorly conductive dielectrics	Poorly conductive dielectrics	Poorly conductive dielectrics under weak field
Charge transport	ion conservation	charge conservation	charge conservation	charge conservation
Electrification mechanism	field induced or spontaneous partition	field induced or spontaneous partition	field induced	spontaneous partition (prescribed)
Ion distribution	partition	partition	balanced partition	imbalanced partition
EDL resolution	✓	✓	×	×

parameter) to characterize the position relative to a finite-thickness phase interface, denoted here by $\phi \equiv (n_\beta - n_\alpha)/(n_\alpha + n_\beta)$, where n_α represents the local particle number density of solvent molecules in phase α . Consequently, $\phi = -1$ and $\phi = 1$ correspond to the interior regions of phases α and β , respectively. The evolution of the phase parameter is described by a phase field equation, and here the form of the Cahn-Hilliard phase field equation is presented, which is characterized by the conservation of the phase parameter [121].

$$\frac{\partial \phi}{\partial t} + \nabla \cdot (\phi \mathbf{u}) = \nabla \cdot (M(\phi) \nabla \mu_\phi). \quad (36)$$

Here, \mathbf{u} is local velocity, μ_ϕ is the solvent chemical potential, and $M(\phi)$ is the phase mobility parameter which may depend on the local phase parameter. The solvent chemical potential can be expressed as

$$\mu_\phi \equiv \mu_\phi^{\text{mix}} + \mu_\phi^{\text{spec}} + \mu_\phi^{\text{el}}. \quad (37)$$

Here, μ_ϕ is contributed by three parts, i.e., the solvent mixing effect μ_ϕ^{mix} , the effective specific interaction potential μ_ϕ^{spec} (including the solvation effect of solute ions), and the electrostatic interaction μ_ϕ^{el} .

Specifically, the contribution of the solvent mixing effect μ_ϕ^{mix} can be obtained from the Landau-Ginzburg free energy that describes the chemical potential of solvent mixtures [96,98].

$$\begin{aligned} \mathcal{F}^{\text{solv}}[n] &= \int d\mathbf{r} \left[n_{\text{solv}} k_B T (\ln n_{\text{solv}} - 1) + \frac{\Lambda_\phi}{2} \left(\frac{(\phi^2 - 1)^2 + (\nabla \phi)^2}{2\epsilon_{\text{pf}}^2} \right) \right] : \\ &= \mathcal{F}_{\text{solv}}^{\text{ideal}} + \mathcal{F}^{\text{mix}}, \end{aligned} \quad (38)$$

therefore

$$\mu_\phi^{\text{mix}} \equiv \frac{\delta \mathcal{F}^{\text{mix}}}{\delta \phi} \Big/ V = \Lambda_\phi \left[-\nabla^2 \phi + \frac{(\phi^2 - 1)\phi}{\epsilon_{\text{pf}}^2} \right]. \quad (39)$$

Here, $n_{\text{solv}} = n_\alpha + n_\beta$ represents the total local particle number density of solvent molecules in both phases, Λ_ϕ is the density parameter of interfacial excess energy, ϵ_{pf} is the characteristic thickness parameter of the solvent mixing layer (related to the characteristic thickness parameter in Section 2.2 by $d_0 = \sqrt{2}\epsilon_{\text{pf}}$), and the relationship between the latter two parameters and the interfacial tension coefficient is given by $\gamma = (2\sqrt{2}/3)(\Lambda_\phi/\epsilon_{\text{pf}})$ [82]. It has been noted that the aforementioned Landau free energy form is only applicable when the equation of state for both solvent phases is the same [158]. The free energy forms corresponding to the specific interaction potential and electrostatic interactions can be written as [116,159,160].

$$\begin{aligned} \mathcal{F}^{\text{ions}}[\{n_i\}_i] &= \int d\mathbf{r} \sum_i n_i \left[k_B T (\ln n_i - 1) + \mu_i^0(\phi) + \frac{z_i e \varphi}{2} \right] \\ &\equiv \mathcal{F}_i^{\text{ideal}} + \mathcal{F}^{\text{spec}} + \mathcal{F}^{\text{el}}, \end{aligned} \quad (40)$$

therefore

$$\mu_\phi^{\text{spec}} \equiv \frac{\delta \mathcal{F}^{\text{spec}}}{\delta \phi} \Big/ V = \sum_i n_i \left(\frac{\partial \mu_i^0(\phi)}{\partial \phi} \right), \quad \mu_\phi^{\text{el}} \equiv \frac{\delta \mathcal{F}^{\text{el}}}{\delta \phi} = \frac{E^2}{2} \left(\frac{\partial \epsilon(\phi)}{\partial \phi} \right). \quad (41)$$

The aforementioned forms are obtained through equilibrium with the chemical potential of the bulk aqueous solution [160], where the reference chemical potential μ_i^0 can be given by the modification of the free energy reflecting the effective potential of specific interactions at the interface [82]. It can be seen from the above that the distribution of solute ions (equivalent to effective osmotic pressure) and the electric field formed by spontaneous charging at the interface (equivalent to the image potential) will both affect the equivalent thickness and internal pressure distribution of the solvent mixing layer at the charged liquid-liquid interface [116]. In practical calculations, if the precision requirements for the calculation of the internal solute ion distribution and the pressure distribution across the solvent mixing layer are not high and only the lumped result within the solvent mixing layer is needed, the solvent chemical potential may be approximated as μ_ϕ^{mix} with an effective correction to the solvent mixing layer thickness ϵ_{pf} [82].

For the sake of completeness, we also write down other equations involved in electrokinetic multiphase flow, including the electrostatic Poisson equation

$$-\nabla \cdot (\epsilon(\phi) \nabla \phi) = \rho_e \equiv \sum_i z_i e n_i, \quad (42)$$

and the conservation equations for (dilute solute) component, mass and momentum

$$\frac{\partial n_i}{\partial t} + \nabla \cdot (n_i \mathbf{u}) = \nabla \cdot (\omega_i(\phi) \nabla \mu_i) + r_i, \quad (43)$$

$$\nabla \cdot \mathbf{u} = 0, \quad (44)$$

$$\rho(\phi) \left(\frac{\partial \mathbf{u}}{\partial t} + \mathbf{u} \cdot \nabla \mathbf{u} \right) = \nabla \cdot (\mathbf{T}^n + \mathbf{T}^e) + \mathbf{F}^r. \quad (45)$$

Here, the component conservation equation is also known as the Maxwell-Stefan equation (or the modified Nernst-Planck equation), where n_i , μ_i , and r_i represent the number density, chemical potential, and reaction source term of solute ion i , respectively, and

$$\mu_i \equiv \frac{\delta \mathcal{F}^{\text{ions}}}{\delta n_i} = \mu_i^0(\phi) + k_B T \ln n_i + z_i e \varphi. \quad (46)$$

In the momentum conservation equation, the Newtonian viscous stress, Maxwell stress, and the continuous form of interfacial tension are written as

$$\mathbf{T}^n = \eta(\phi) [\nabla \mathbf{u} + (\nabla \mathbf{u})^T], \quad (47)$$

$$\mathbf{T}^e = \epsilon(\phi) \left[\mathbf{E}\mathbf{E} - \frac{1}{2}(\mathbf{E} \cdot \mathbf{E})\mathbf{I} \right], \quad (48)$$

$$\mathbf{F}^r \equiv -\nabla p - \phi \nabla \mu_\phi^{\text{mix}}. \quad (49)$$

Here, $p = p^{\text{ideal}} + p^{\text{mix}} + p^{\text{spec}}$, where $p^{\text{ideal}} = (n_{\text{sol}} + \sum_i n_i)k_B T$, and p^{mix} and p^{spec} represent the contributions from the solvent mixing effect and the specific interaction potential, respectively. Their specific forms do not directly affect the evolution of the velocity field in the momentum equation. It should be noted that the aforementioned equations involve numerous material property parameters, such as the solvent dielectric constant ϵ , the mobility ω_i of solute ion i , the density ρ and the dynamic viscosity η of the fluid. Under the assumption of local thermodynamic near-equilibrium, the corresponding distributions across the interface can be given in the form of interpolation functions associated with the phase parameter ϕ [82,161].

3.2.3. Discussions on the model applicability and limitations

For oil-water interface systems composed of nonpolar oils or containing only common simple inorganic ions, the dielectric constant of the oil phase is approximately 1/10 that of the aqueous phase. Consequently, the free energy barrier for ion transfer from the aqueous phase to the oil phase is typically on the order of $100k_B T$ [10]. In such cases, ion diffusion into the oil phase is weak, resulting in extremely low ion concentrations in the oil phase. The contribution of ion partitioning to interfacial charging is negligible, forming an oil-water interface with a unilateral diffuse layer. Thus, a sharp-interface model can be employed to describe its charging mechanism and electrokinetic transport behavior, where the electrokinetic transport modeling requires the addition of a thermodynamic polarizability condition (intuitively understood as an ion-impenetrability condition) as a constitutive model. Notably, the conclusions drawn in this work for nonpolar oil systems also apply to polar oil systems containing only inorganic solute ions. For such systems, the spatial and temporal scale separation between diffuse layer transport and viscous-scale transport poses significant computational challenges, even when employing numerical methods like finite volume schemes combined with multigrid techniques. When the system's characteristic size is much larger than the diffuse layer's Debye length and interfacial charge is small, the system exhibits linear transport characteristics, making it relatively straightforward to handle. However, for systems on the scale of hundreds of micrometers, additional approximations are still necessary. For cases where nonlinear transport effects cannot be neglected, singular perturbation methods based on matched asymptotic expansions provide an effective upscaling approach, which can also supply efficient boundary conditions for numerical simulations, thereby reducing computational costs.

For oil-water interface systems composed of polar oils containing organic ions, the contribution of ion distribution in the oil phase may become non-negligible, corresponding to typical ITIES systems. From a diffuse-interface perspective, if the electric double layer thickness is comparable to the interfacial solvent mixing layer thickness, additional effects such as capacitive charging of the interfacial phase, potential jumps due to shear strain rate and concentration gradients, velocity jumps, and shear stress jumps may no longer be negligible. Consequently, the sharp-interface limit results cannot be directly applied [121]. In practice, for polar oil systems containing organic ions, the accuracy of both effective boundary conditions derived from matched asymptotic expansions and macroscopic sharp-interface theories strongly depends on the validity of interfacial matching conditions. Therefore, it is often necessary to start from nanoscale interfacial interactions, perform numerical simulations based on an appropriate diffuse-interface model, and derive reasonable effective corrections for the sharp-interface matching conditions. For instance, when the electric double layer and interfacial solvent mixing layer are of comparable thickness and spontaneous partitioning dominates the charging mechanism, the interfacial potential jump in the macroscopic model can be corrected based on diffuse-interface simulation results. Similarly, for concentration polarization behaviors at interfaces with spontaneous adsorption or partitioning-induced charging in complex geometries, quantitative solutions from macroscopic models (whether analytical or

numerical) are generally less universal and direct compared to mesoscopic models.

In the context of non-equilibrium electrokinetic transport, the approach of embedding interaction potentials between particles and the solvent background or solid interfaces into particle transport equations is not uncommon. In recent years, it has been employed in some studies on microscale and nanoscale single-phase flows of neutral components, while its widespread application in transport modeling (such as in colloidal particle systems and electrolyte solutions) has long been established, though typically limited to single-solvent background systems. For liquid-liquid multiphase interfaces, modified interaction potentials have been introduced to describe the interfacial transport behavior of neutral components [162]. Similarly, in the equilibrium-state charge modeling of ITIES systems, complex interaction potentials have been incorporated into the Poisson-Boltzmann equation, but this has been restricted to modeling equilibrium ion distribution structures near the interface [96–98]. Electrokinetic transport systems involving ions at liquid-liquid interfaces still lack a diffuse interface modeling framework from a mesoscopic perspective [116].

In fact, physicochemical two-phase hydrodynamic modeling (including multiphase electrokinetic transport) has practical demands in simulating processes such as surfactant adsorption kinetics coupled with interfacial flows, solid melting/condensation, and reactive dissolution/precipitation [162–164]. From the perspective of capturing realistic interfacial transport processes, a key direction for future development lies in coupling cross-interface chemical kinetics within diffuse interface models. In this regard, the diffuse interface model summarized above not only provides robust diffuse interface modeling support for numerical studies of electrokinetic transport at liquid-liquid interfaces but may also inspire further refinements to lattice Boltzmann models. For instance, the color-gradient model can be readily combined with mean-force corrections to describe various charging mechanisms, such as non-equilibrium partitioning and specific adsorption, making it suitable for characterizing electrokinetic behaviors at both polarizable and non-polarizable liquid-liquid interfaces. In contrast, existing pseudo-potential models are primarily suited for bottom-up descriptions of non-equilibrium partitioning-induced charging and are limited to non-polarizable interfacial systems. Extending them to specific adsorption-induced charging may require redesigning pseudo-potentials by analogy with phase-field models.

More generally, when the characteristic spatiotemporal scales of a system's flow, electric potential, and other properties are comparable to those of ion distribution or transport at multiphase electrokinetic interfaces, quantitative interpretation or prediction must rely on numerical simulations based on diffuse-interface models. In terms of spatial scales, if the system operates at the nanoscale—such as in nanodroplets, nanojets, ultrathin liquid films, electrowetting, or contact line dynamics—its dimensions become comparable to the diffuse layer thickness and solvent mixing layer thickness. In such cases, charge redistribution at liquid-liquid interfaces due to overlapping diffuse layers, as well as the finite-thickness effects of the solvent mixing layer, can no longer be neglected. In terms of temporal scales, if the characteristic timescale of electric field variations matches the ion relaxation timescale during interfacial charging—such as in direct friction- or impact-induced charging between liquid-liquid interfaces, or during the coalescence and breakup of charged droplets—a diffuse-interface description capturing transient ion transport near the solvent mixing layer may be necessary [165–167]. Similarly, if the hydrodynamic timescale of wetting dynamics near solid boundaries aligns with the characteristic timescale of non-equilibrium ion transport, a diffuse-interface approach becomes essential to resolve non-uniform charging states within nanoscale aqueous films [146,148,168,169]. A notable example is the dynamic wettability alteration of oil-water interfaces induced by ions. Experiments have revealed transient relaxation effects caused by non-equilibrium ion transport, yet most current studies either assume instantaneous local wettability responses to concentration changes or

artificially control wettability evolution rates in adsorption kinetics models. These approaches remain qualitative and lack a physically realistic diffuse-interface framework [146–148,169,170]. Thus, developing diffuse-interface descriptions that faithfully represent these complex electrokinetic phenomena remains an important direction for future research.

4. Transport mechanisms and dimensionless parameters in EKmHD

From the theoretical framework presented above, the uniqueness of electrokinetic flow at liquid-liquid interfaces is manifested in two aspects, as illustrated in Fig. 8. First, compared with gas-liquid interfaces, the partial non-polarizability of liquid-liquid interfaces introduces complex charging mechanisms and interphase ion transport, which involves the physicochemical kinetics of the two-liquid interface

(corresponding to Section 3.1) and affects the electric potential distribution and non-equilibrium ion transport behavior within the diffuse layer. Second, compared with solid-liquid interfaces, the high mobility and ion adsorbability of liquid-liquid interfaces lead to interface flow and tangential ion transport along the interface, which involves the physicochemical hydrodynamics and electromechanical hydrodynamics of the two-liquid interface (corresponding to Sections 3.1) and affects the velocity and shear stress matching behavior within the diffuse layer, thereby determining the asymptotic matching effective interfacial conditions for the outer flow regions beyond the double diffuse layers.

To more intuitively present the physical picture and unique mechanisms of electrokinetic multiphase flow at the oil-water interface, this section will first compare the electrokinetic flow at the oil-water interface with other typical charged interfaces, providing fundamental approach for analyzing the transport mechanisms of specific systems. Ultimately, the typical mechanisms of electrokinetic multiphase flow

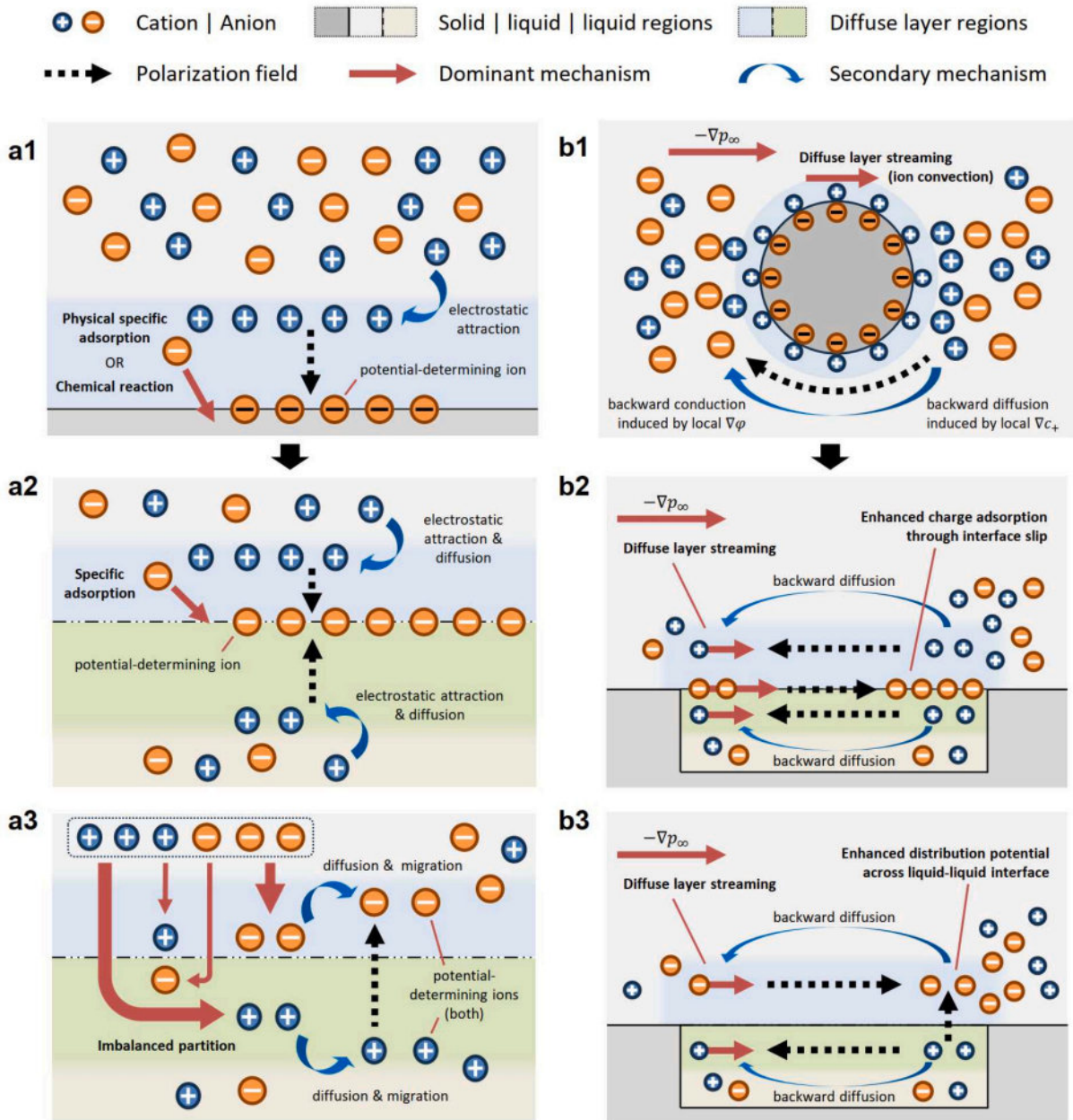


Fig. 8. Electrical double layer polarization in liquid-liquid interface electrokinetics. (a1) Formation of electric double layer. Complex charging mechanisms including specific adsorption (a2) and imbalanced partition (a3). (b1) Pressure gradient upon an enclosure. Slip-induced inhomogeneous charging for specific adsorption (b2) and imbalanced partition (b3) induced interface charging.

will be integrated and summarized in three aspects: interfacial charging mechanisms, interfacial ion transport, and interfacial fluid flow, along with the relevant dimensionless parameters. This lays the groundwork for the subsequent analysis of key mechanisms in typical scenarios of electrokinetic multiphase hydrodynamics.

4.1. Comparison between two-liquid interface electrokinetics and other systems

As an illustrative discussion, this section will take the electrophoresis of colloidal particles in electrolyte solutions as a typical example to compare the differences in electrokinetic mechanisms between dielectric liquids (including conductive dielectric liquids) and solid particles, metal droplets, and bubbles. Considering that the matched asymptotic expansion analysis based on the thin double layer assumption typically provides a key physical picture, some of the analytical approaches in this section refer to relevant theoretical works, including those on solid particles [11,87,171–174], droplets [11,48,73,81,87,140,175], and bubbles [38,88].

4.1.1. Compared with interface electrokinetics at solid surface

Consider the motion of a surface-charged solid particle immersed in a liquid under the influence of an external electric field. If the liquid is a dielectric liquid, the electric force experienced by the particle will ultimately be completely balanced by the viscous drag force provided by the dielectric solvent, a phenomenon known as *viscous retardation*. However, if the liquid is an electrolyte solution, due to the presence of the double layer near the interface, the net charge layer around the particle will, under the drive of the electric field, introduce an additional resistive force in the form of viscous shear, known as *electrophoretic retardation*, which is also referred to as *asymmetric double layer retardation* under non-spherical symmetric double layer conditions [117,176]. It can be seen that the dominant mechanism of electrokinetic phenomena largely depends on how the ion transport within the interfacial double layer leads to the electric force and how this stress is balanced by other stresses near the interface. The former is related to the interfacial charging mechanism and the interfacial polarizability, while the latter is associated with the mechanical constitution and conductive dielectric properties of the colloidal particle. It should be noted that the interfacial charging mechanism and polarizability are usually closely related to the conductive mechanism of the colloidal particle itself, hence the aforementioned two types of factors often exhibit a certain correlation [1,12,87].

For hard solid particles with a high elastic modulus, a slight elastic deformation can provide the balance with the viscous shear stress within the double layer, thereby yielding a no-slip condition at the wall. This allows, at the modeling level, the decoupling of the two-way coupling of the interfacial viscous flow and the interfacial ion transport into a one-way dependency. Consequently, after solving for the electric potential distribution and ion transport within the double layer, the slip velocity boundary at the outer edge of the double layer can be obtained by integrating the interfacial shear stress balance equation and directly used for the flow field solution in the outer region. To obtain the electric potential distribution and ion transport within the double layer, it is necessary to quantitatively solve the perturbed form of the electrostatic field equation and the ion transport equation based on appropriate boundary conditions. This typically depends on factors such as the dominant charging mechanism at the interface, the induced charge/current intensity of the external field, the ion polarizability of the interface, and the symmetry characteristics of the solute ions. Therefore, solid particles with different bulk and interfacial properties, as well as electrolyte solutions with different conductive properties and under different electric field strengths, will exhibit essential differences in electrokinetic flow behavior.

Compared with solid particles, the complexity of conductive dielectric droplets mainly lies in the fact that the liquid-liquid interface

will undergo deformation and shear flow under the action of external stress, that is, inducing a tangential stress jump in effective interfacial conditions. This causes the internal circulation of the droplet to be coupled with the external flow around the droplet, and the driving mechanism of droplet electrophoresis will no longer be the electroosmotic slip velocity but the effective shear stress within the double layer [87,88]. Thus, the effective interfacial conditions of the internal and external flow fields usually depend on the asymptotic matching of the stress at the outer edge of double-sided diffuse layers, rather than the simple difference of the electroosmotic slip velocities on both sides, which brings considerable challenges for approximate theoretical solutions and the acquisition of intuitive physical pictures. Moreover, to obtain the asymptotic matching conditions of the shear stress used for the connection of the internal and external flow fields, it is necessary to similarly solve for the electric potential distribution and ion transport in the double diffuse layer regions (referred to as the *inner layer* in the sense of perturbation expansion) that include the liquid-liquid interface, to obtain the inner layer shear stress balance equation. On one hand, the charging mechanism of conductive dielectric droplets is more complex, as it may include complex charging mechanisms such as spontaneous adsorption and partition effects at the interface, which may exhibit different ion distribution and transport behaviors under the induction of an external field [80,81], which brings challenges to the formulation of interfacial potential and component conditions under different charging mechanisms [50,82]. On the other hand, the coupling form between the interfacial ion transport and fluid flow of conductive dielectric droplets is more diverse, as there is not only the concentration polarization of adsorbed ions along the interface and the corresponding Marangoni stress and even interfacial rheological behavior, but also the concentration polarization across the interface mediated by adsorption kinetics or ion partition effects and the corresponding double-sided osmosis coupling effect, which brings prominent challenges to the interfacial ion and stress conditions and solutions under non-equilibrium conditions [49,80,81]. Table 7 compares the electrokinetic characteristics of relatively simple dielectric liquids and dielectric solids, which clearly shows the uniqueness of electrokinetic multiphase flow compared with solid-liquid interface electrokinetics. It should be noted that this paper will not cover the mechanism of action of ionic surfactants or other *macroscopic* impurities on interfacial rheology (such as the soluble Gibbs monolayer or insoluble Langmuir monolayer exhibiting low-dimensional viscoelasticity), and related content can be referred to in previous monographs and reviews [89,95,177].

Although there are essential differences in double-sided flow coupling and shear stress matching, considering the rich types of solid particle interfaces (such as dielectric solids, ionic gels, and solid metals),

Table 7
Comparison of electrokinetics at interfaces of liquid dielectrics and solid dielectrics.

Characteristics	Solid dielectrics	Liquid dielectrics
Surface structure	fixed distribution of adsorption sites	no fixed adsorption sites, ions merged within the solvent mixing layer
Electrification mechanism	adsorption, relatively well-established	adsorption / partition, still unclear
Normal charge distribution	usually single-side diffuse layer, image force and charge correlation are usually unimportant	double diffuse layer may exist, image force may be important
Interface configuration	elastic shear strain and interface deformation	interface tension and shear rate leading to interface deformation and motion
Inhomogeneous charging	require surface modification and external field	naturally induced by ion transport along finite-length mobile two-liquid interface
Ion concentration polarization	curved surface with large surface density	naturally induced by ion transport along finite-length mobile two-liquid interface

they may provide certain analogical references for understanding the physical pictures of conductive dielectric droplets in terms of interfacial polarizability and external field-induced effects, as shown in Table 8. For weakly conductive dielectric solutions, the charge transport behavior is somewhat similar to that of semiconductors, and related studies on electrokinetic flow near semiconductor interfaces may be referenced [4]. For highly conductive dielectric solutions, both sides of the interface are strong electrolyte solutions. On one hand, the spontaneous partition-induced charging mechanism is usually crucial, and related studies on electrokinetic flow of ionic gel layers represented by soft particles may be referred to [178–180]. On the other hand, the existence of partial non-polarizability of the interface and the coupling behavior of electrokinetic flow on both sides may refer to recent studies on low-dimensional conductive interfaces and electron-ion coupled electrokinetic flow [181,182]. In addition, hydrophobic dielectric solid walls are widely believed to have non-negligible hydrodynamic slip, and a slip boundary condition is generally used to capture the corresponding behavior [183], which can be analogized to a certain extent with the electrophoresis of dielectric droplets [184].

4.1.2. Compared with interface electrokinetics at metal and gas surfaces

For metallic droplets, two prominent characteristics are identified. On one hand, they typically have polarizable interfaces that are impermeable to ions. They can spontaneously get charged through specific adsorption or chemical reactions and can also be charged by an external electric field. However, under special circumstances outside the electrochemical window, they can also allow for normal current flow [11]. On the other hand, they cannot accommodate a static electric field since their internal conductivity is high. When subjected to an external electric field, the internal region forms a reverse induced electric field through the accumulation of free charges to cancel out the external electric field, thereby maintaining an equipotential droplet region. This simultaneously introduces a tangential concentration gradient of solute ions on the side of the electrolyte solution and triggers a diffusio-osmotic effect similar to Marangoni flow [11,12]. Unlike solid metals and conductive dielectrics, the internal Maxwell stress of metallic droplets is zero, which leads to significant differences in their electrokinetic behavior. To balance the viscous stress of the thin double layer outside the droplet, solid particles can achieve this through elastic deformation, conductive dielectrics can do so through non-zero internal Maxwell stress, possible Marangoni forces at the interface, and viscous shear stress, while metallic droplets can only balance external stresses through internal viscous shear stress. This results in the characteristic electrophoretic velocity of charged metallic droplets typically being higher in magnitude than that of solid particles and dielectric droplets. Moreover, their externally induced inhomogeneous charging effects give them an inherent strong nonlinearity, making them difficult to solve analytically [87]. It is worth noting that with the widespread application of liquid metals such as Ga, Ge, and Bi in recent years, their unique interfacial chemical reaction charging mechanisms and non-polarizable characteristics have also garnered significant attention [185]. However, research on their electrokinetic phenomena is still in the experimental exploration stage oriented towards applications [63]. Apart from Levich's early discussions on ion concentration polarization and limiting current effects [11], quantitative theoretical research is still lacking [186].

From the above discussions, it can be seen that compared with

metallic droplets, conductive dielectric droplets have a finite and non-zero electrostatic dielectric constant. Therefore, their interiors can accommodate electric fields and generate non-zero Maxwell stresses, leading to different behaviors in electrophoretic characteristic mobility. Moreover, due to the finite mobility of ions within the conductive dielectric medium, which is subject to viscous drag from the solvent molecular fluid background, both the droplet interface and interior allow for ion convection and diffusion. This implies that ion convection transport effects triggered by interfacial electroosmosis and diffusio-osmosis may be crucial. Consequently, more complex ion concentration polarization effects may occur at the liquid-liquid interface and within the droplet, leading to a richer electrokinetic flow behaviors under non-equilibrium transport conditions [12].

For gas bubbles, considering the polarizability of the interface and the negligible internal stress, their charging mechanisms and electrokinetic behaviors are simpler to model and solve compared with conductive dielectric droplets. For bubble electrophoresis, a stress-free condition is typically imposed at the gas-liquid interface, which intuitively indicates that bubble electrophoresis is not driven by electroosmotic slip velocity but by the effective shear stress contributed by the tangential osmotic pressure gradient within the double layer. This driving mechanism is very similar to that of droplet electrophoresis [88]. Specifically, since the tangential osmotic pressure gradient is closely related to ion concentration polarization and typically exhibits pronounced non-linear characteristics, the electrophoretic mobility of bubbles shows a non-linear relationship with the surface charge density even under the limit of a weak external electric field [38,88].

From a theoretical modeling perspective, the complexity of bubble electrophoresis compared with conductive dielectric droplets is mainly manifested in two aspects. On one hand, due to the significant density difference between gas and aqueous solution and the certain compressibility of gas, the effects of gravity and bubble volume changes are usually not negligible in experiments. On the other hand, the volume of bubbles used in experiments is typically large, which makes bubble deformation and ion relaxation and induced charging effects under strong external fields often non-negligible. These complexities usually result in a complex nonlinear relationship between the electrophoretic migration velocity of bubbles and the external electric field, which is difficult to explain with many existing linear theories [38,50]. Besides, many explanations still ignore the additional shear stress effect brought by electroosmosis [187,188]. Although existing theories have used matched asymptotic expansion methods to consider the ion relaxation effect under strong external fields and obtained approximate scaling laws ignoring gravity and bubble deformation [88], they still fail to match the existing experimental results of bubble electrophoresis under different conditions [189]. Moreover, theoretical research has shown that the ion concentration polarization effect under strong external fields cannot be ignored, yet there is currently no theory that fully considers the interfacial adsorption-induced charging kinetics behavior of potential-determining ions, thus making it difficult to capture the dynamic adsorption of ions under concentration polarization conditions and the resulting inhomogeneous charging and normal ion transport behaviors [88]. This further casts doubt on the accuracy of the existing measurement results of bubble surface charging [190,191].

Table 8

Analogy between liquid and solid phases adjacent to electrolyte solutions.

	PFD	PFC	HCD	WCD
Bulk conductivity	nearly insulated	very good	good	poor
Interface polarizability	thermodynamically polarizable	thermodynamically polarizable	partially polarizable	partially non-polarizable
Liquid phase	pure solvent	liquid metal / ionic liquid	SES that is not too dilute	WES / extremely dilute SES
Solid phase	pure solvent	solid metal	ionic gel / low-dimensional conductor	semi-conductors

4.2. Summary of transport mechanisms and dimensionless numbers

Electrokinetic multiphase flow problems generally exhibit the nonlinear characteristics of multiphysical field coupling, and the system geometry typically lacks high symmetry. This implies that selecting appropriate dimensionless governing parameters to grasp the main transport mechanisms is crucial. This section will follow the general analysis approach of electrokinetics, starting from three aspects: physicochemical charging mechanisms, physicochemical kinetic ion transport, and the coupling of physicochemical and electromechanical hydrodynamics. It will successively examine the interfacial physicochemical charging (iPC), interfacial ion transport (iIT), and interfacial fluid flow (iFF) at the liquid-liquid interface. Specifically, from the perspectives of qualitative mechanism description and semi-quantitative analysis with dimensionless numbers, this section will summarize and outline the typical transport mechanisms of spontaneous charging at the oil-water interface and electrokinetic multiphase flow. This approach will elucidate the potential novel phenomena in electrokinetic multiphase flow.

For the significant mechanisms in electrokinetic multiphase flow problems, we have summarized the dimensionless numbers as shown in Table 9. Some of these are referenced from previous theoretical modeling studies on electrokinetic multiphase flow systems, particularly distinguishing between descriptive parameters whose specific forms depend on the specific problem (marked with °) and governing parameters whose specific forms can be explicitly determined (marked with *), and combining this with the order-of-magnitude analysis of the corresponding governing equations and key parameters. Unless specifically stated otherwise, the term *interface* refers to the immiscible liquid-liquid interface. $X_{>} := \max_{\alpha} X_{\alpha}$ and $X_{<} := \min_{\alpha} X_{\alpha}$ represent the larger and smaller values between the quantity X 's on both sides of the interface in the macroscopic theoretical model, respectively, where the subscript $\alpha = 1, 2$ refers to either of the liquid phases, and $L_{n,\alpha}$ and L_s represent the characteristic lengths along the normal (pointing into phase α) and tangential directions across which the prescribed field X experiences a significant change.

It should be noted that some of the dimensionless numbers listed in the table are proposed for the first time (marked with **) or are systematically summarized for the first time (marked with °) in this paper. The following subsections will provide further detailed discussions on the specific phenomena and mechanism analyses involved. It should be clarified that the table only lists the dimensionless numbers that are closely related to the charging of liquid-liquid interfaces and electrokinetic multiphase flow phenomena involving charged solute ions and have been relatively widely studied. For the dimensionless numbers involved in general liquid-liquid two-phase physicochemical flows (such as Ca, We, Bo, Da, Ra, etc.), one can refer to previous review articles [95,118,198]. In addition, considering that typical electrokinetic multiphase flows are Stokes flows where the inertial term can be neglected, i.e., the Reynolds number generally satisfies $Re = UL/\nu \ll 1$, these are also not listed separately in the table here. Meanwhile, following the conventions in the field of electrohydrodynamics, some dimensionless parameters in the table have well-defined physical meanings, but their specific forms cannot be directly given and instead depend on the particular process [95,198], such as Du_{α} , $Du_{0,\alpha}$, \mathcal{F}_{ns} , \mathcal{F}_{nD} , \mathcal{X}_{η} , \mathcal{X}_e , and Ha_{α} .

The oil-water interface, characterized by fluidity, ion adsorbability, and non-polarizability, significantly influences the tangential and normal transport behaviors of adsorbed ions at the interface and ions within the diffuse layers. As shown in Table 9, $i_{b,\alpha}$ represents the current in the electrically neutral region of phase α , $i_{s,\alpha}$ represents the current near the interface within the diffuse layer on the side of phase α , i_{s0} denotes the tangential current of interfacially adsorbed ions, and i_{n0} denotes the normal current caused by interfacial chemical reactions or interphase ion transport.

Table 9
Characteristic mechanism and essential dimensionless parameters in EKmHD.

Type	Characteristic mechanism	Dimensionless parameter	Physical meaning	Literatures	
iPC	Interfacial solvent mixing	$\Delta_s = \frac{d_{pf}}{\lambda_{D,<}}$	thickness of solvent mixing layer **,°	Samec [30], Huang [82]	
	Disjoining pressure regulation	$\Pi_{\gamma} = \frac{\Pi}{\gamma/L_n}$	local inclination of aqueous film °	de Gennes [192], Tian [77]	
iIT	Effective surface conduction	$Du_{\alpha} = \frac{i_{s,\alpha}}{i_{b,\alpha}}$	relative intensity of surface conduction °	Dukhin [176], Pascall [12]	
		$Du_{0,\alpha} = \frac{i_{s0}}{i_{s,\alpha}}$	relative intensity of interfacial conduction °*	Baygents [49,50,151], Schnitzer [80]	
	$Z_{\alpha} = \frac{\zeta_{\alpha}}{V_T}$	two-liquid interfacial charging on α side *	Schnitzer [80,81]		
	$\delta_{\alpha} = \frac{\lambda_{D,\alpha}}{L_{n,\alpha}}$	thickness of equilibrium diffuse layer *	Pascall [12], Schnitzer [80]		
	$\mathcal{B}_X = \frac{\nabla_s X}{X_0/L_s}$	intensity of external non-equilibrium potential gradient *	Baygents [151], Yang [113]		
	$Pe_{\alpha} = \frac{u_s L_{n,\alpha}}{D_{\alpha}}$	intensity ratio of ion convection flux to diffusive flux *	Dukhin [193], Schnitzer [87,88]		
	Partial non-polarizability	$\mathcal{F}_{ns} = \frac{i_{n0}}{i_{s,>}}$	relative normal current compared with surface conduction °	Levich [11]	
relative normal conduction compared with diffusive current °			Rubinstein [194]		
iFF		double-sided stress matching	$\mathcal{X}_{\eta} = \frac{\eta_2/L_{n,2}}{\eta_1/L_{n,1}}$	double-sided ratio of viscous shear stresses °	Schnitzer [88], Huang [82]
			$\mathcal{X}_e = \frac{T_{nt,2}^e}{T_{nt,1}^e}$	double-sided ratio of Maxwell shear stresses °	Pascall [12], Schnitzer [80,87]
		$Ha_{\alpha} = \frac{T_{nt,\alpha}^e}{T_{nt,\alpha}^v}$	ratio of electric force to viscous force in streaming potential °	Cox [195], Yariv [196]	
		$\Xi_p = Z_{p,>}/Z_{\alpha}$	intensity ratio of partition-induced charging to adsorption-induced charging **,°	Verwey [25], Huang [82]	
		$\mathcal{E} = e \left \frac{q_{0\alpha}}{q_{0\beta}} \right $	double-sided variation of interfacial charging intensity **,°	Pascall [12], Huang [82]	
	Instability enhancement	$\mathcal{F}_M = \frac{L_n^2 \partial_c \gamma \partial_n c }{\eta D_{eff}}$	intensity of electro-Marangoni effect **,°	Krylov [177]	
	Multi-interface coupling	$\Xi_{s,\alpha} = \frac{Z_1^{(\alpha)} - Z_s^{(\alpha)}}{L_z/L_x}$	relative electroosmosis between two-liquid and solid-liquid interfaces **,°	Sherwood [197]	
		$\Pi_{\nabla} = \frac{\nabla_s \Pi}{\Pi/L_s}$	inhomogeneity of film disjoining pressure °	de Gennes [192], Anderson [86]	

4.2.1. Interface charging and ion transport

The oil-water interface (especially those between immiscible electrolyte solutions, i.e., ITIES) usually acts as a partially non-polarizable interface, with a certain concentration of ions typically distributed on both sides, an effect first pointed out by Verwey and Niessen [24]. If the interphase imbalanced partition dominates the charging mechanism, the relative importance of the double diffuse layers will also be highly sensitive to solvent properties (such as dielectric constants), solute properties (such as partition coefficients), and solution chemical environmental parameters (such as concentration, pH) [24,82]. The solvent diffusion across the oil-water interface will make the characteristic thickness of dielectric constant variation d_{pf} possibly comparable to the Debye length $\lambda_{D,<}$ of one liquid phase, thereby making the potential drop $\Delta\varphi_s$ caused by capacitive charging of the solvent mixing layer non-negligible. The significance of this potential drop $\Delta\varphi_s/\Delta\varphi_\infty$ as a governing parameter of the interfacial solvent mixing effect is closely related to the characteristic thickness of the interfacial mixing layer $\Delta_s = d_{pf}/\lambda_{D,<}$ and influences the subsequent degree of partition-induced charging $\Xi_{p,\alpha}$, which can be seen as the result of non-dimensionalizing the modified Poisson-Boltzmann equation using the phase-field interface thickness parameter (see Section 2.2). This effect was first pointed out by Gavach [199], systematically reviewed by Samec [30], and quantitatively characterized in electrokinetic multiphase flow by Huang et al. recently [82].

For nanoscale-thickness liquid films, the imbalanced partition-induced charging effect may influence the interaction between liquid-liquid and solid-liquid interfaces, thereby altering the disjoining pressure experienced by the liquid-liquid interface $\Pi = \sum_m \Pi_m$, which is composed of van der Waals interactions Π_{vdW} , electrostatic interactions of the electric double layer Π_{EDL} , and structural interactions such as steric effects Π_{str} [77,79]. This implies that local changes in ion concentration will affect the electrostatic interactions of the double layer and thus change the disjoining pressure by altering the charge at the liquid-liquid interface (and solid-liquid interface). The presence of a normal electric field at the interface will also change the surface tension through the *electrocapillarity effect*, thereby significantly affecting the equilibrium contact angle and the spreading behavior of the liquid film. Consequently, a dimensionless number Π_r can be constructed from the disjoining pressure Π and the pressure difference caused by local interfacial tension γ/L_n as a descriptive parameter to quantitatively capture the behavior of interfacial charging altering wettability. This can be seen as the non-dimensionalization result of the Young-Dupre equation or the thin liquid film approximation equation, reflecting the cosine value of the angle between the liquid film and the solid wall. For a general correlation between disjoining pressure and equilibrium wetting and wetting dynamics, one can refer to the systematic reviews by de Gennes and scholars in recent years [192,200].

The fluidity and ion adsorbability of the oil-water interface will further enhance the tangential transport of ions in the double diffuse layers $i_{sd,\alpha}$ [12] and the interfacial ion transport i_{s0} [49]. The transport of ions within the diffuse layer $i_{sd,\alpha}$, which is commonly considered as the *surface conduction* effect, can be quantitatively described using the celebrated Dukhin number Du_α in the field of solid-liquid electrokinetics as a governing parameter. This can be seen as the result of non-dimensionalizing the interfacial current conservation equation using the current in the bulk electrically neutral region. Specifically, if there are specifically adsorbed ions at the oil-water interface, they can also transfer along the interface through convection and electromigration. We refer to this as interfacial conduction i_{s0} , which was first pointed out by Baygents and Saville and has been systematically numerically studied [49,50,151] and studied recently by Hill [201]. This constitutes an inhomogeneous charging mechanism widely present at liquid-liquid interfaces but not typically found at traditional solid-liquid interfaces. While enhancing the effective surface conduction of ions, it will also further induce ion concentration polarization along the interface, which

is particularly important in cases of finite-length or finite-curvature liquid-liquid interfaces. A similar parameter $Du_{0,\alpha}$ can be defined as a governing parameter to describe the related effects. The following section further analyzes the main dominant factors of interfacial and surface conduction effects.

By analyzing the influencing factors of ion transport in the interfacial diffuse layer, it can be known that the specific magnitude of Du_α is usually closely related to the characteristic ζ potential (zeta potential) $Z_\alpha = \zeta_\alpha/V_T$, the equilibrium characteristic thickness of the diffuse layer δ_α , and the characteristic Maxwell shear stress at the liquid-liquid interface $Z_l^{(\alpha)} = \max\{Z_{p,\alpha}, Z_\alpha\}$ that determines the electroosmotic slip velocity. Here, $\zeta_\alpha = \varphi_{0,\alpha} - \varphi_{\infty,\alpha}$ is the ζ potential on the side of phase α , and $V_T = k_B T/e$ is the thermal potential. Therefore, the governing parameter Z_α can be seen as the result of non-dimensionalizing the interfacial potential matching condition using V_T . In particular, when the externally applied non-equilibrium potential \mathcal{B}_X or the ion convection transport intensity Pe_α is strong, it will induce a diffusive boundary layer under non-equilibrium conditions, further expanding the ion diffusion dominant region within the equilibrium diffuse layer to a larger spatial range [80,81,87,88,151]. Here, the external potential field X may be the electric potential φ , concentration c , temperature T , etc., and the corresponding characteristic potential difference X_0 is usually chosen as \bar{c}_∞ , \bar{T}_∞ for c , T , and as V_T for φ .

For partially non-polarizable oil-water interfaces, they also allow for the passage of normal ionic current across the interface through interfacial physicochemical kinetic behavior, where Du_α is also closely related to the interfacial normal current i_{n0} , which may significantly impact the interfacial stability and electrospreading behavior of strong electrolyte solution interfaces. Here, a dimensionless number \mathcal{F}_{ns} is introduced to describe the relative influence of normal current to tangential current at the interface, used to characterize the impact of the non-polarizability of liquid-liquid interfaces on their electrokinetic flow behavior, which was first noted by Levich. This can be seen as the result of non-dimensionalizing the interfacial charge conservation condition using the tangential current within the diffuse layer [11]. Moreover, for ion-selective permeable surfaces, the ion transport across the interface under the action of a normal electric field may trigger electroconvection near the interface and lead to instability phenomena or the formation of regular dissipative structures. Rubinstein has made outstanding contributions in the context of ion-selective surfaces. ITIES, as a typical ion-selective surface, its interfacial electroconvection effects have been widely observed in the traditional field of electrochemistry, but still lack a solid theoretical foundation based on fluid dynamics. To quantitatively describe the impact of induced ion concentration polarization on electroconvection instability, a dimensionless number \mathcal{F}_{nd} is introduced here as a descriptive parameter [194], where D_0 is the characteristic diffusion coefficient of the solute ions.

4.2.2. Interfacial fluid flow

For spontaneously charged oil-water interfaces, ions within the diffuse layers and possibly adsorbed ions at the interface can both drive the motion of the fluid near the interface under the influence of an external electric field or concentration gradient. The presence of adsorbed ions provides a new mechanism for the electrostatic force-driven motion at the liquid-liquid interface. For liquids with different viscosities and conductive dielectric properties, the matching of viscous stress and Maxwell stress on both sides of the interface significantly affects the characteristic magnitude of electrokinetic flow [12,87,88]. Consequently, the ratios of the viscous shear stress and Maxwell shear stress on both sides of the interface, \mathcal{X}_η and \mathcal{X}_e , can be defined respectively to capture the corresponding mechanisms. For pressure-driven streaming potential, the Hartmann number Ha_α should also be used to reflect the importance of the electro-viscous effect, defined as the ratio of the induced electrostatic force by the streaming potential to the viscous force on one side of the interface [195,196]. The following

section further analyzes the main influencing factors of the interfacial stress matching effect.

On one hand, the charging state of the liquid-liquid interface includes the net charge within the double diffuse layers and the adsorbed charge in the solvent mixing layer, where there is competition between the imbalanced partition and specific adsorption of solute ions. By analyzing the characteristic Maxwell shear stress in the momentum equation induced by partition- and adsorption-induced charging at the interface, corresponding dimensionless numbers can be defined [82] as $Z_{p,\alpha} = (\Delta\varphi_\infty/V_T)(C_\alpha/\sum_\alpha C_{\alpha,s})$ and $Z_a = (\Xi_{ll}/V_T)/\sum_\alpha C_{\alpha,s}$. As shown in Table 9, the dominance of partition- over adsorption-induced charging is defined as the governing parameter Ξ_p . Here, $\Delta\varphi_\infty$ is the interfacial distribution potential caused by imbalanced partition, Ξ_{ll} is the interfacial adsorption charge caused by specific adsorption, and $C_{\alpha,s} = \varepsilon_\alpha/\lambda_{D,\alpha}$ is the double layer capacitance of phase α . To describe the ratio of Maxwell shear stress on both sides of the interface under the same tangential electric field, a dimensionless parameter \mathcal{E} related to the ratio of the charge in the diffuse layers on both sides $q_{0,\alpha}/q_{0,\bar{\alpha}}$ can be used as a governing parameter for quantitative characterization [12]. When the difference in charges on both sides of the interface is significant, $\mathcal{E} \rightarrow 0$, indicating a weak coupling effect of double-sided concentration polarization; conversely, when the difference is minor, $\mathcal{E} \rightarrow 1$, indicating a strong coupling effect.

On the other hand, the partially polarizable characteristics of the oil-water interface are mainly manifested as the interfacial polarization effect induced by external fields or rebalanced through adsorption-partition of ions on both sides. This implies that the ion transport within the double diffuse layers will be mutually coupled through the effects of field-induced charging at ideally polarizable interfaces [12] or the rebalancing of charging at thermodynamically polarizable interfaces [82]. Here, the charged liquid-liquid interface under the action of an external tangential non-equilibrium potential field may lead to ion concentration polarization on both sides. The ion concentration polarization within the double diffuse layers not only may lead to diffusio-osmotic effects but also alter the interfacial potential difference across the phases, thereby providing negative feedback by inhibiting the further increase of the tangential concentration gradient. For example, the streaming potential effect near the two-phase interface will be simultaneously influenced by the coupling effects of double-sided concentration polarization \mathcal{E} and the matching of interfacial shear stresses \mathcal{R}_η and \mathcal{R}_e . Moreover, if there is field-induced polarization, a more complex space charge diffusion layer may form under non-equilibrium conditions, which will be more significantly affected by the external field-induced charging when the double-sided concentration polarization coupling coefficient \mathcal{E} is large [80,81].

The oil-water interface, as a multiphase soft interface, will also have a richer source of forces driving interfacial flow and factors triggering dynamic instability. In addition to the electroconvection induced by normal ion current through ion-selective surfaces mentioned above, specifically adsorbed ions at the oil-water interface can also lead to a reduction in liquid-liquid interfacial tension. Under inhomogeneous adsorption conditions, this can more easily trigger interfacial dynamic instability and emulsification, which is particularly significant in the case of ionic surfactants. Such inhomogeneous adsorption can be caused by external disturbances or formed by reasons such as convective transport accumulation at finite-length interfaces [12]. Krylov made foundational contributions in the study of electro-Marangoni instability systems, considering the Marangoni instability effect caused by the inhomogeneous adsorption of surfactant ions at the interface. Using linear stability analysis methods, he obtained the linear instability conditions for this charged interface system [177]. Consequently, \mathcal{F}_M can be introduced as a governing parameter to describe the characteristic intensity of the electro-Marangoni effect, where $D_{\text{eff}} = (z_+ - z_-)D_+D_-/(z_+D_+ - z_-D_-)$ is the effective diffusion coefficient of the solute cations and anions.

Furthermore, when there are solid wall constraints in the system, there may be hydrodynamic interface coupling behaviors between the electrokinetic flows at the charged liquid-liquid interface and the solid-liquid interface through the viscous transport between different interfacial electroosmotic slip velocities. Here, the characteristic electroosmotic slip velocity at the solid-liquid interface can be defined as $Z_s^{(\alpha)} = \zeta_s^{(\alpha)}/V_T$, and further, the characteristic scales of interfacial charge inhomogeneity L_Z and the inhomogeneity of the externally applied non-equilibrium potential L_X can be introduced for semi-quantitative description. Consequently, a governing parameter $\Xi_{s,\alpha}$ can be introduced to describe the relative electrokinetic flow between the liquid-liquid interface and the solid-liquid interface [197,202]. For the case of liquid films within the range of surface and interfacial interactions, their behavior will be affected by the aforementioned disjoining pressure, including the interaction of the electric double layer, thereby leading to significant impacts on the flow within the liquid film due to the interfacial charging regulation triggered by the external electric field or mediated by ion transport [57,77]. Thus, L_s can be defined as the characteristic length of the inhomogeneous distribution of charge regulation along the interface, and thus the degree of disjoining pressure inhomogeneity Π_∇ can be defined as a descriptive parameter, the value of which is closely related to \mathcal{B}_c and \mathcal{B}_E .

5. Analysis of key mechanisms in typical scenarios of EKmHD

Based on the classification of model systems in electrokinetic multiphase flow and the aforementioned transport mechanisms involved, the corresponding systems are categorized into three classes: droplet electrophoresis in free space, hydrodynamic interaction coupling multi-interface electrokinetic flow, nanoscale interaction coupling wetting dynamics. This section will organize the existing understanding based on the typical transport mechanisms and related dimensionless parameters of electrokinetic multiphase flow, using typical model systems as a guide. This will aid in a deeper understanding of the uniqueness of electrokinetic multiphase flow and outline its future development directions. It is worth noting that some of the typical scenarios discussed in this section (such as droplet electrophoresis, two-liquid parallel electroosmotic flow, and two-liquid streaming potential) are commonly used for measuring the charging property of liquid-liquid interfaces. Therefore, the analysis here will be helpful in understanding the advantages and limitations of electrokinetic measurement methods, where accurate measurement of interfacial charge is fundamental to the quantitative modeling and prediction of electrokinetic multiphase flows.

5.1. Droplet electrophoresis

Similar to how particle electrophoresis is commonly used to measure the spontaneous charge density at solid-liquid interfaces, droplet electrophoresis is an important method for obtaining the charging properties of liquid-liquid interfaces. From a historical perspective, the characteristic of liquid-liquid interfaces noted by early studies was their fluidity and ion mobility, which is also the most obvious difference compared with solid-liquid interfaces. Therefore, the interfacial viscous shear stress matching effect (\mathcal{R}_η) was one of the key focuses of early theories on droplet electrophoresis. In contrast, studies from different fields have shown significant differences in their understanding of ion distribution and transport behavior at liquid-liquid interfaces, which is a prominent case of the interdisciplinary characteristics of electrokinetic multiphase flow. These differences have also directly led to variations in the understanding of the interfacial Maxwell stress matching effect (\mathcal{R}_e), which is crucial for electrokinetic flow. It is worth noting that this key characteristic of droplet electrophoresis seems not to have received sufficient attention in research on measuring the charging of liquid-liquid interfaces based on droplet electrophoresis [5,203].

This section will review the development of the physical mechanisms

of droplet electrophoresis to illustrate the process by which various fields have progressively deepened their understanding of the transport mechanisms of electrokinetic multiphase flow through research on droplet electrophoresis, and will briefly describe the new developments and directions of droplet electrophoresis study in recent years. Specifically, we will focus on the historical debates of the *mobility scaling paradox* and the *droplet solidification effect*, which have had a profound impact on current research measuring the charging of liquid-liquid interfaces based on droplet electrophoresis.

5.1.1. Theories in early days and mobility scaling paradox

In fact, as mentioned in the historical review of interfacial charging and electrokinetic multiphase flow in Section 1, the interfacial physicochemical properties of mercury and oil-water interfaces, as well as the corresponding research fields and approaches, are very different. This has largely led to fundamental differences in the treatment of interfacial viscous and Maxwell shear stress matching (\mathcal{S}_η , \mathcal{S}_e) in droplet electrophoresis theories that originated from different fields focusing on different interfacial systems.

The Frumkin-Levich theory (hereinafter referred to as Levich's theory), which originated from the field of electrochemistry, primarily focuses on metallic droplets. The theoretical modeling highlights the influence of convective transport of ions within the interfacial layer (Du_α) and takes into account the polarizable characteristics of the liquid-liquid interface (\mathcal{E}) as well as the importance of the normal current at the interface (\mathcal{S}_{ns}) [11,37]. Specifically, it focuses on mercury droplets with a conductivity much higher than that of the electrolyte solution and an ideally polarizable interface (although it also examined the effect of the normal current at the interface later), assuming that the inhomogeneous distribution of induced polarization charges will lead to a gradient in interfacial tension, resulting in a jump in interfacial viscous shear stress. It also assumes that there is non-uniform convection along the interface leading to a normal current contribution from the ion flux to obtain the distribution of the induced electric field. Consequently, an expression for the electrophoretic mobility of metallic droplets was obtained, with a focus on the effects of the electrocapillary effect and surface conduction. In fact, Frumkin and Levich were among the first scholars to recognize the importance of interfacial polarization properties and surface convective conduction effects in electrokinetic flow behavior. This approach was later used by them to analyze various droplet electrokinetic phenomena and was included in Levich's monograph, such as the sedimentation current and potential caused by the gravitational sedimentation of metallic droplets, electrophoresis of metallic droplets with non-polarizable interfaces, and electrophoresis of conductive dielectric droplets with double-sided diffuse layers [11]. This perspective has been extended in recent years by Pascall and Squires to simple electrokinetic multiphase flow scenarios at the interface of highly conductive dielectrics [12].

The Booth-Jordan-Taylor theory (hereinafter referred to as Booth's theory), which originated from the field of colloid and interface science, focuses on oil droplets in emulsions. The theoretical modeling highlights the capture of the finite thickness property of the interfacial diffuse layer (δ_α) and assumes that both sides of the interface are conductive dielectrics [38,39]. Specifically, Booth and colleagues focused on liquid-liquid interfaces with double-sided conductive dielectrics and partially non-polarizable characteristics. They assumed that during electrophoresis, the diffuse layer maintains an equilibrium ion distribution. The induced polarization effect from the external electric field was linearly superimposed with the equilibrium double layer effect, and the induced polarization field was correlated with the conductivity ratio of the internal and external fluids. The theory specifically considered the ion partition effect and its influence on the distribution of ions within the droplet, as well as the velocity slip correction at the liquid-liquid interface due to the viscosity ratio of the internal and external fluids [38]. Around the same time, Jordan and Taylor used a similar approach to Booth's but primarily considered the case where the droplet was a

perfect dielectric with a relatively large dielectric constant and assumed the interface was polarizable. Thus, the induced polarization effect from the external electric field was related to the dielectric constant ratio of the internal and external fluids. By introducing a correction coefficient for electrophoretic mobility, they further estimated that the viscosity ratio correction for dielectric droplets could reach up to 12 %, and for cases where the background solution has poor conductivity, the influence of surface conduction effects needed to be further considered [11]. This would lead to a reduction in the correction ratio with increasing background solution conductivity and decreasing interfacial charge [39]. However, all those studies adopted the assumptions of Henry's theory used for solid particle electrophoresis [41], without considering the convective relaxation of double layer charges and the deformation of the EDL induced by the external field. The assumption of interface polarizability was also quite strong, and the applicability of the theory for droplets with different conductive dielectric properties remains open to discussion. This perspective was later extended by Baygents and Saville to cases allowing for tangential transport of specifically adsorbed ions at the interface ($Du_{0,\alpha}$) [49,50].

The significant differences in theoretical modeling and physical understanding led to what is referred to as the *scaling paradox* in droplet electrophoresis research, that is, why the predictions of Booth's theory and Levich's theory for metallic droplets show a scaling difference of $\mathcal{O}(\delta_w)$. Subsequently, Levine et al., Ohshima et al., and Pascall et al. conducted research from the perspective of the former theory [12,48,175]. Among them, Levine et al. and Ohshima et al. both focused on metallic droplets, and by introducing the induced polarization field corresponding to the relaxation effect into Booth's theory under the condition of a thin double layer, they obtained mobility results similar to Levich's theory. This suggests that the induced polarization effect of metallic droplets under an external field may be the key to those theoretical differences [175]. Pascall and Squires, under the assumptions of extremely weak external electric fields and thin double layers, examined the electroosmotic behavior of conductive liquid strips with different dielectric properties, pointing out the intrinsic reasons for the similar behaviors between highly conductive dielectrics and liquid metals. This is because the diffusio-osmotic effect triggered by the concentration gradient of highly conductive dielectrics cancels out the effect of Maxwell stress, thereby still leaving the mismatch of interfacial shear stress. Through discussions on the electrophoretic motion of metallic droplets and conductive dielectric droplets, the study further pointed out that the (electrocapillary effect similar to diffusio-osmosis and Marangoni flow) in Levich's theory and the electroosmotic effect in Booth's theory coexist, but the former is of a larger magnitude and thus the dominant mechanism [12]. However, the discussion on conductive dielectrics in this study strongly depends on the assumption that the internal induced electric field remains zero, and its conclusions are difficult to apply to cases where significant surface conduction occurs due to large induced charge density, which may lead to streaming potential and non-zero internal induced electric fields [12]. Besides, in the electrophoresis of conductive dielectric droplets, only the induced charging effect under the condition of a thin double layer was considered, making it difficult to apply to cases of spontaneous charging and double layer overlapping at the interface of liquid metals or conductive dielectric liquids, thus preventing the latter from being reduced to the results of perfect dielectrics under low ionic strength conditions. Corrections are also required when the metallic substrate is replaced by a dielectric one [88]. In fact, that work still finds it difficult to provide a sufficiently complete, self-consistent, and intuitive physical picture from the perspective of asymptotic matching of effective interfacial conditions of ion transport and stress [87], until the appearance of two important papers in recent years [80,81].

5.1.2. Mobile interface and droplet solidification effect

Since the 1980s, with the development of electrophoresis techniques, scholars have carried out extensive validations of the applicability of

early theories on dielectric droplet electrophoresis. Surprisingly, many scholars found that the electrophoretic mobility behavior of droplets is very similar to that of solid particles under many experimental conditions, leading to the gradual proposal of the so-called *droplet solidification effect*. Under this guidance, whether it is based on direct current electrophoresis or alternating current electroacoustics, research on the measurement of oil-water interface charging has almost directly applied the corresponding theories from solid particle electrophoresis in the conversion from oil droplet electrophoretic mobility to interfacial effective potential, usually without any detailed explanations [1,203,204]. Regarding the mechanism behind that simplified treatment, predecessors usually started from two aspects: hydrodynamic interface fluidity and charge redistribution at the liquid-liquid interface, proposing explanations based on purely theoretical hypotheses and a small amount of experimental evidence. In particular, apart from a few early measurement works that had preliminary discussions on the differences between droplet electrophoresis theory and solid particle electrophoresis, most scholars directly used those two hypotheses as the rationale for adopting the simplified treatment in experiments without verification.

In recent years, although there have been reviews critically discussing the differences between oil droplet electrophoresis and solid particle electrophoresis and the simplified treatment methods, there are still several shortcomings such as inaccurate fundamental concepts and unclear logic [78]. In response to this, we critically draw on the ideas of predecessors and combine the progress of modeling and simulation studies in recent years. We analyze the physical hypotheses and experimental evidence regarding the *impact of surface-active impurities on interfacial rheology* and the *immobile interface suppressing surface charge redistribution* to illustrate that changes in interfacial rheology are not the only key factor and that surface charge redistribution cannot be ignored.

Surface-active impurities impacting interface rheology. It is believed in some studies that only a trace amount of surface-active impurities adsorbed at the interface can suppress the internal circulation of droplets by increasing interfacial viscosity. Specifically, in terms of direct current electrophoresis, there is currently only direct observational evidence from early conference reports [205], and a few scholars have conducted electrophoretic measurements on particles/droplets with similar components but different phase states or the same components around the melting point. For example, Carruthers found that differences in end groups have more significant influence than phase states on electrophoretic mobility [206], and Anderson's measurements in surfactant solutions found that phase states have little impact on electrophoretic mobility [207]. For alternating current electrophoresis, the internal circulation of droplets should significantly affect the evolution of interfacial fluctuations, but some scholars claim that there is no relevant experimental evidence [203]. We point out that the importance of the influence of interfacial rheology on the electrophoretic mobility of droplets in direct current electrophoresis is still questionable [12]. On one hand, those limited experimental evidence still fails to illustrate the significance of the mechanism of internal circulation in pure two-liquid systems without surface-active substances and differences in end groups, and its effectiveness is largely limited by the large viscosity coefficients of the droplet materials used near the melting point and the inherent surfactant interference in the experimental system. On the other hand, even if surface-active impurities do change interfacial rheology, interfacial thermodynamic analysis shows that the change in interfacial rheological properties should be on the same order of magnitude as the change in interfacial tension [208], making it difficult to ignore the interfacial flow induced by the inhomogeneous distribution of surface-active impurities. In fact, the latter has been successfully used to explain the phenomenon that tiny bubbles rising in a liquid medium exhibit behavior similar to that of solid particles, without the need to introduce the hypothetical concept of interfacial viscosity [209]. Moreover, surface-active impurities often inevitably carry a net charge or alter the interfacial charging properties, and the differences should be

significant enough to observe in electrophoresis experiments. However, numerous electrophoresis experiments on various inert hydrophobic interfaces have shown similar curves of the dependence of interfacial effective ζ potential on chemical environments [210–212]. Therefore, although some researchers have proposed that oil-water interfaces are highly susceptible to adsorbing surface-active impurity ions, making their interfacial rheological behavior exhibit certain viscoelastic characteristics or even approach solidity [1,203], for non-polar oils commonly used in laboratories, after appropriate treatment, it can be considered that this effect is not dominant [78,110,208].

Immobile interface suppressing surface charge redistribution. Based on the physical assumption that charge redistribution at the interface induces a gradient in interfacial tension, some phenomena has been successfully explained through theoretical analysis similar to boundary layer theory, such as the direct current electrophoresis and sedimentation potential of liquid metals like mercury [11,37]. For dielectric droplets such as oil droplets, considering the impact of surface-active substances on interfacial rheological behavior that inhibits interfacial flow, their direct current electrophoretic behavior is believed to be similar to that of particles, while their alternating current electrophoretic behavior is related to the sensitivity of interfacial tension to ion adsorption. However, some scholars claim that there is no significant evidence for such effects [203]. We point out that due to the existence of multiple mechanisms of interfacial ion transport, including convection induced by interfacial hydrodynamic slip and diffusion-electromigration allowed by the mobility of the liquid, the significant impact of charge redistribution at the interface is actually hard to ignore. On one hand, even without internal circulation caused by interfacial hydrodynamic slip, the diffusion and electromigration of charges on the soft interface of the liquid-liquid interface can still lead to charge redistribution. A typical example is the polarizable metal droplet, which induces a large amount of inhomogeneously distributed interfacial charges near the liquid-liquid interface through electromigration under the action of an external electric field. Similarly, for the finite-length oil-water interface, there is also a spontaneous inhomogeneous charging effect where charges continuously accumulate downstream along the liquid-liquid interface, presenting an asymmetric charge transport behavior that is completely different from that of solid particles [81,141]. When the droplet viscosity is low and the interfacial tension is not high, it can also induce significant deformation of the droplet during its electrophoretic motion [150]. On the other hand, even if the mechanism that suppresses interfacial flow is absent, such as increased interfacial viscosity, the *droplet solidification* effect may still exist. That is, it may be caused by the reverse diffusio-osmosis under the conditions of a thin double layer and high interfacial charge density, which partially offsets the original electroosmosis. This interfacial reverse diffusio-osmosis phenomenon can actually be regarded as a kind of interfacial tension gradient in a certain sense [12,50,80,87].

In fact, around 1990, based on the regular perturbation theory under weak external field approximation and further numerical solutions, Ohshima et al. and Baygents & Saville had pointed out the limitations of the oversimplified assertions on droplet solidification [48,50,140]. Ohshima et al. indicated that for the electrophoresis of metallic droplets under weak external electric fields (the corresponding theory is also applicable to dielectric droplets with a relatively large dielectric constant), by considering the effects of interfacial hydrodynamic slip and induced polarization fields, both the electrophoretic mobility and sedimentation potential under the condition of a thin double layer are significantly greater than those of the corresponding metal particles. Besides, when the spontaneous surface charge density is not high, due to the enhanced surface conduction effect, the interfacial charging Z_a corresponding to the peak of electrophoretic mobility will shift to the lower values. When $Z_a \rightarrow \infty$, since the surface convective current is significantly compressed to the same order of magnitude as that of solid particles, the electrophoretic mobility of metallic droplets will be similar to that of solid particles, which is quite similar to Levich's findings in the

study of electrophoresis and sedimentation potential of metallic droplets [11,12,48]. Baygents & Saville indicated that for the electrophoresis of dielectric droplets under weak external electric fields, due to the inhomogeneous adsorption of ions caused by interfacial induced polarization, leading to the existence of an interfacial tension gradient, droplet electrophoresis may still be insensitive to the droplet's own viscosity, thus presenting behavior similar to particle electrophoresis. However, in more cases, they will still show significant differences, especially the occurrence of abnormal behaviors such as droplet reverse movement or weakened mobility. Moreover, the charge distribution within the droplet also has an important impact on the electrophoretic behavior of the droplet, which can be seen to some extent as an extension of Booth's early focus on the influence of the internal and surface charge distribution characteristics on the electrophoretic behavior of droplets [38]. This also indirectly illustrates that charge redistribution is important in more cases, and a complete, accurate, and quantitative understanding of it is crucial for characterizing the electrophoretic behavior of droplets.

The research methods of Ohshima et al. and Baygents et al. on droplet electrophoresis [48,50], as well as O'Brien et al. on solid particle electrophoresis [213], have profoundly influenced subsequent theoretical and numerical studies, such as the electrophoresis and deformation of metallic droplets and the electrophoresis of conductive dielectric droplets. Particularly, it has been pointed out that inert solid walls may exhibit effective slip boundaries due to hydrophobic effects, surface roughness, or gas cushion layers [183,214–216]. The influence of the effective slip length on the electroosmosis in microchannels and the electrophoretic behavior of colloidal particles has thus attracted widespread attention, which largely represents an extension of the research on the droplet solidification effect [184,217,218]. Khair et al. studied the effect of interfacial hydrodynamic slip on hydrophobic surfaces on particle electrophoretic behavior and found that it enhances both the convective effect within the double layer and surface conduction, leading to non-monotonic behavior of electrophoretic mobility with interfacial charge density when the effective slip length is large [217]. Ohshima et al. focused on the connection between droplet electrophoresis and the intrinsic hydrodynamic slip of hydrophobic solid-liquid interfaces from the perspective of interfacial slip effects, and paid attention to the electrophoretic behavior of droplets under different types of charge distribution and external alternating current electric field conditions, finding that droplet electrophoresis can be analogous to hydrophobic interfaces under conditions of weak external electric fields and low surface charge density [184]. In addition, Uematsu et al. allowed water droplets in the oil phase to be overall non-electrically neutral and examined their electrophoretic behavior under conditions of low surface charge density and weak external electric fields, particularly examining the influence of the charge distribution characteristics inside and on the surface of the droplets on the electrophoretic behavior. The study found that when the net charge is negligible, the electrophoretic mobility of the water droplet is in the opposite direction to the electric force felt by the surface charge density; however, this conclusion may stem from the inappropriate use of Henry's theory and requires further verification [219].

5.1.3. Novel development in recent years

In recent years, on the basis of the work by Frumkin-Levich [11,37], Baygents-Saville [50], and Pascall-Squires [12], studies on droplet electrophoresis (from the perspective of electrokinetic multiphase flow) has been successively extended to scenarios such as external field-induced polarization effects [73,80,81,87,88,151,154,220], droplet sedimentation potential or diffusio-phoresis effects [11,48,49,113,221], and inertial constraint effects [204].

With the vigorous development of the field of two-liquid electrohydrodynamics, the interface deformation of weakly conductive dielectric droplets under strong external fields \mathcal{E}_E and their anomalous electro-mechanical behaviors have attracted attention. Regarding the mechanism of droplet deformation, Baygents and Saville were the first

to study the applicability of the Taylor-Melcher leaky dielectric model from the perspective of ion interfacial transport inducing electrokinetic multiphase flow. They provided the matched asymptotic expansion form of the governing equations for spontaneously double-sided adsorbed charged droplets which shows the same form as leaky dielectric model, indicating that not explicitly including the extended space charge layer is not the fundamental reason why the leaky dielectric model fails to give consistent results with experiments. This work also for the first time pointed out the existence of the diffusive boundary layer under non-equilibrium conditions and provided the solution for the droplet's interface deformation field through the connection between the inner and outer regions [151]. Shortly thereafter, Zholkovskij, Masliyeh, and Czarnecki, based on the assumption of equilibrium partition-induced charging and using the magnitude of the external field as a regular perturbation condition, provided the normal stress matching conditions for externally induced charged dielectric droplets. Their deformation field solutions can reduce to the results of previous studies under the conditions of perfect dielectrics and leaky dielectrics [154]. For conductive dielectric droplets, Wang et al. expanded the research object to the deformation behavior of electrolyte solution droplets within a dielectric liquid under an external electric field and provided a numerical solution based on the Green function method [220]. Ma et al. further provided the upscaled coarse-grained effective boundary conditions for interfacial flow and ion transport using the matched asymptotic expansion method and provided a numerical solution for droplet deformation based on similar methods [73]. In addition, Schnitzer et al. extended the induced charge electrokinetic effect from solid metal particles with negligible spontaneous charging to the case of metal droplets, finding that due to the mismatch of Maxwell stress on both sides of the interface, the induced charge electroosmotic velocity is an order of magnitude larger than the solid case in the sense of $\mathcal{O}(\delta_w)$ [87]. In those studies, the modeling of weakly conductive dielectric droplets mainly corresponds to the case of extremely dilute strong electrolyte solutions. In contrast, Mori et al. examined the migration behavior of conductive dielectric droplets formed by weak electrolyte solutions under the action of an external electric field. This study focused on its correlation with the equilibrium of interfacial ion partition, which is similar to the treatment method summarized by Saville [47,81].

Through the examination of the applicability of the leaky dielectric model, Schnitzer et al. and Mori et al. focused on weakly conductive dielectric droplets and re-examined the *scaling paradox* between Booth's theory and Levich's theory from the perspective of electrokinetic multiphase hydrodynamics based on interfacial charging mechanisms and ion transport within the diffuse layer [80,81]. By considering the spontaneous interfacial charging mechanism and based on the assumption of a thin double layer, they used singular perturbation expansion to provide effective interfacial conditions for stress asymptotic matching (\mathcal{X}_η , \mathcal{X}_e) that include the effects of interfacial ion transport (Du_α , Pe_α), thereby successfully integrating the theoretical clues scattered across various fields by previous researchers [13]. Schnitzer et al. also extended the electrophoresis of colloidal particles under strong external fields from dielectric particles to metallic droplets and bubbles [173], studying the electrophoretic behavior of droplets and bubbles under moderate external field conditions that do not exceed the internal field within the spontaneously charged double layer [87,88]. These studies particularly focused on the impact of induced charge polarization effects on the ion distribution structure and colloidal particle electrophoretic mobility under non-equilibrium conditions. The moderate external field induces a new characteristic thickness and diffusive boundary layer beyond the equilibrium double layer thickness, causing significant ion exchange between the non-equilibrium diffuse layer and the electrically neutral region, which in turn has a notable impact on the interfacial Maxwell stress. This even induces a non-linear dependence of electrophoretic mobility on the external field and interfacial charge density, providing insights for the study of perfect dielectric and highly conductive dielectric droplets.

The theoretical study of the sedimentation potential of metallic droplets first appeared in Levich's monograph [11], which, based on the assumption of spontaneous adsorption-induced charging and the boundary condition of surface conduction, provided quantitative expressions for the dependence of sedimentation velocity and potential on droplet viscosity and surface conduction under low-speed conditions. This approximate solution was later verified by the semi-analytical and semi-numerical solutions given by Ohshima et al. under the assumption of a weak external field [48]. The theoretical study of the diffusiophoretic effect of droplets first appeared in the work of Baygents and Saville, focusing on a non-polarizable interface for conductive dielectric droplets with spontaneous double-sided adsorption-induced charging. They found that under the same conditions of interfacial charge density and colloid particle radius, the diffusiophoretic mobility of droplets can be several orders of magnitude higher than that of the corresponding solid particles [49]. Notably, as the earliest work to incorporate interfacial ion kinetics into the study of droplet electrokinetic multiphase flow, it also examined the contribution of the inhomogeneity of interfacial ion adsorption to the gradient of interfacial tension \mathcal{F}_M , finding that this contribution is almost negligible for simple inorganic ions. In recent years, there have been a series of semi-analytical and semi-numerical works on droplet diffusiophoresis, the theoretical models of which essentially inherit the analytical methods of Ohshima et al. and Baygents et al. It is particularly worth mentioning the work of Yang et al. Assuming a thin double layer, they used the matched asymptotic expansion method to provide a quantitative relationship between the diffusiophoretic mobility of droplets and the viscosity ratio of the inner and outer fluids as well as the interfacial charge density and achieved the quantitative experimental verification. Their results also indicate that the relative magnitude of the diffusiophoretic mobility of droplets compared with that of solid particles depends on the local direction of shear stress [113], which is consistent with our previous general analysis of the characteristics of electrokinetic multiphase flow [87,88].

Due to the significant density difference between gas bubbles and aqueous solutions, the rising of bubbles during electrophoresis poses considerable challenges to experimental operations and theoretical modeling. To address this, Kelsall et al. once balanced the buoyancy by applying a reverse electric field to suppress the upward motion of bubbles [222]. However, in actual experimental modeling, this study directly neglected the retarding effect brought about by interfacial electroosmosis, which makes the calculated interfacial charge density less convincing. Nevertheless, the electrophoretic mobility results obtained by controlling different variables such as external electric field strength, bubble radius, solution pH, and ionic strength provided valuable original data for subsequent research. In fact, the inhomogeneous normal pressure induced by buoyancy and the tangential Maxwell stress induced by the electric field force are difficult to linearly superimpose, thus making theoretical modeling extremely complex [88]. Sherwood proposed earlier that bubbles could be placed in a horizontally oriented rotating cylindrical cell, where inertia could be used as a constraint to balance the buoyancy of the bubbles [204]. The article provided correlation expressions between the interfacial charge density and electrophoretic mobility under different cylinder length limits. However, this study assumed that the bubble surface, due to the adsorption of surface-active impurities, was approximately in a no-slip condition, i.e., the bubble solidification assumption.

It should be noted that for the complex mechanisms revealed by theoretical studies, although there are currently several parametric simulation and experimental works, there is still a lack of sufficient numerical simulation studies to effectively verify them [150], and there are few electrokinetic experimental studies combined with charging mechanisms to provide sufficient evidence [39,40,110,113]. In particular, there are numerous theories on the electrophoresis of conductive dielectric droplets, many of which have unclear applicable ranges in assumptions regarding interfacial charging mechanisms and trans-interface ion transport, and there is still a lack of sufficient

mechanism comparisons between different theories [11,12,38,39,50,81]. The uncertainties at the mechanism level make it difficult to establish a universal closed-form correlation between electrophoretic mobility and interfacial charging properties, thus making it difficult to use for electrokinetic measurement of interfacial properties, and many results based on droplet electrophoresis for measuring the charging of liquid-liquid interfaces still face difficulties in quantitative interpretation [12,82]. In addition, regarding the complex spontaneous charging mechanisms of droplet electrophoresis (Z_a , Ξ_p , Δ_s), large interface deformation and instability (Ca, \mathcal{F}_{ns} , \mathcal{F}_{nd}), partial non-polarizability of the interface (\mathcal{F}_M), and the nonlinear electrokinetic flow behavior that may be caused by the coupling of ion concentration polarization on both sides (\mathcal{E}), the mechanisms behind are still not well-understood [80,81,88].

Here, we attempt to analyze the major difficulties that quantitative research on droplet electrophoresis may face. On one hand, there is still insufficient emphasis on understanding the strong coupling mechanism between the charging mechanisms at liquid-liquid interfaces and electrokinetic flow behavior [12,13,49], especially the integration with the understanding of charging mechanisms at interfaces in typical systems such as liquid metals, dielectric liquids with high or low permittivities in the fields of electrochemistry and interfacial physical chemistry. On the other hand, electrokinetics at liquid-liquid interfaces involve multiphase and multi-physical transport, leading to cross-scale coupling, thus posing technical challenges in experimental measurement and numerical simulation [81,203]. For example, the comparable thickness between the solvent mixing layer and the diffuse layer affects the accuracy of traditional sharp interface mechanical models, the dynamic evolution of multi-phase interfaces requires advanced meshing techniques such as adaptive refinement around the liquid-liquid solvent mixing layer, and there is a lack of reliable theoretical correlation formulas adapted to complex charging mechanisms.

5.2. Hydrodynamic interaction coupling

For electrokinetic multiphase flow systems involving charged solid-liquid interfaces, studies on their mechanisms has been significantly delayed compared with droplet electrophoresis, which may be arisen from the recent breakthrough developments in microfluidic technology around the turn of the 21st century. Due to the generally non-negligible influence of geometric constraints by solid walls, this not only leads to relative electroosmotic slip velocities between liquid-liquid and solid-liquid interfaces, thereby forming bulk shear stresses (Z_a , Ξ_p , $\Xi_{s,a}$), but also causes the ion concentration polarization effects and electroviscosity induced by effective interfacial-surface conduction to be related to the charging properties of both types of interfaces (Du_a , \mathcal{E} , Ha_a). Additionally, it modulates the triggering of interfacial electroconvection instabilities (\mathcal{F}_{nd} , \mathcal{F}_M). To a certain extent, those three typical characteristics can roughly correspond to scenarios such as two-liquid electroosmosis, two-liquid streaming potential, and two-liquid electroconvection, as shown in Fig. 9. Specifically, with different forms of geometric constraints, the characteristic scales and mechanisms of electrokinetic multiphase flows can also vary greatly. The geometries involved in this section include, but are not limited to, parallel liquid-liquid or gas-liquid interfaces in quasi-two-dimensional microchannels, bubbles or droplets in three-dimensional microchannels, liquid-infused surfaces or superhydrophobic surfaces with periodic microstructures, liquid films and liquid bridges between two-dimensional parallel plates, and droplets or capillary jets formed at the outlet of a needle.

5.2.1. Two-liquid parallel electrokinetics in quasi-two-dimensional microchannels

Two-liquid parallel electroosmosis was first used in the 1980s to measure the spontaneous charge of gas-liquid interfaces, a technique known as the plane interface technique [227]. Since the 21st century,

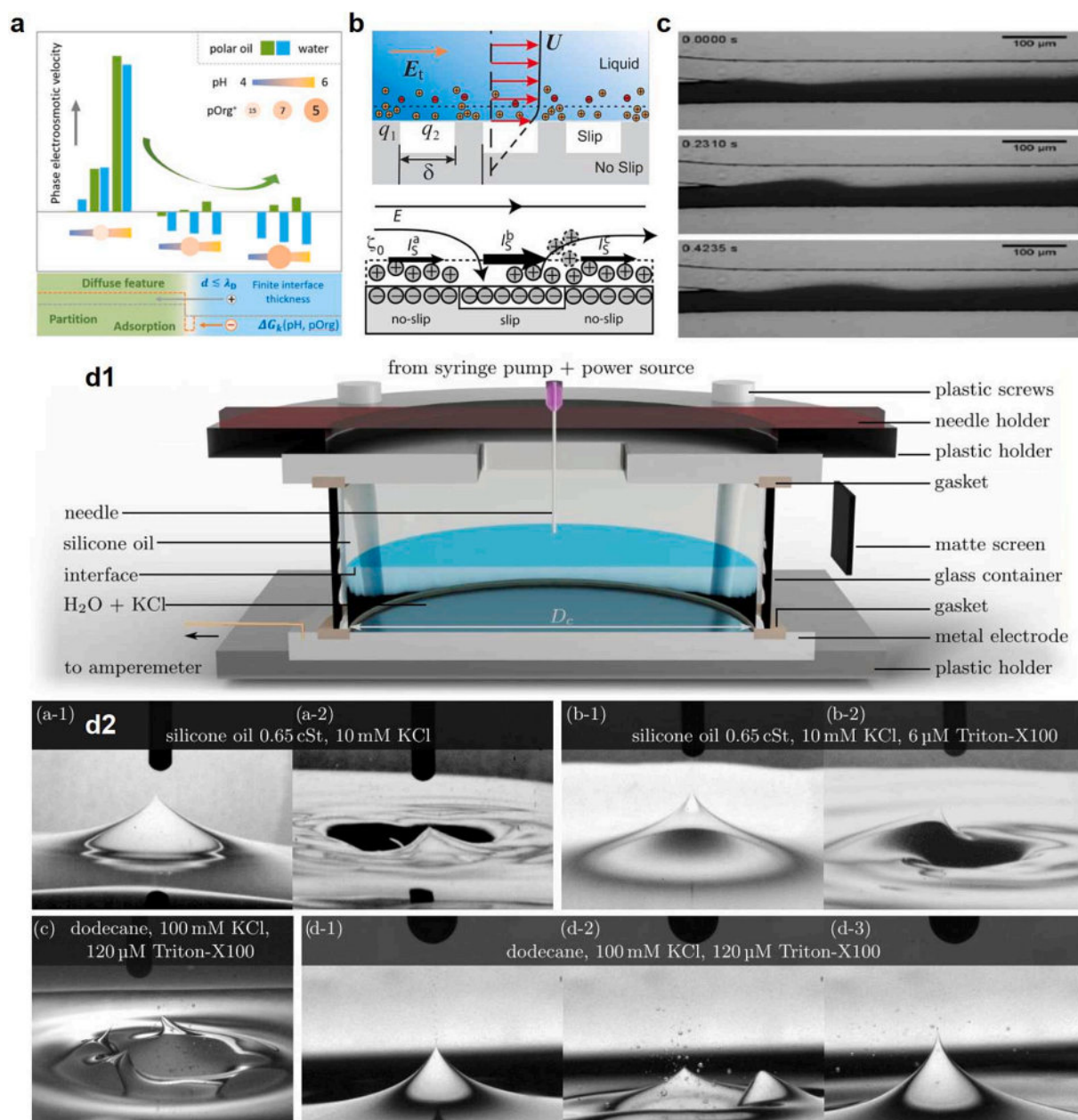


Fig. 9. Electrokinetic multiphase flow phenomena: hydrodynamic interaction coupling. (a) Non-monotonic behavior of two-liquid parallel electroosmosis dependent on the chemical environments including pH and impurity concentrations [82]. (b) Electroosmosis on superhydrophobic or liquid-infused surfaces, including possible surface conduction and induced charge effects [12,223,224]. (c) Interface flow instability at two-liquid interface of two-liquid parallel AC electroosmosis [225]. (d) Taylor cone and electro spray at oil-saline interface [226].

the phenomenon of two-liquid parallel electroosmosis has been introduced into microfluidic systems for applications such as driving poorly conductive dielectric liquids [228], regulating the flow rate ratio of two phases [229], and quantitative modeling studies of the EDL at gas-liquid interfaces [230]. Following the publication of experimental articles on the driving of two-liquid parallel electroosmotic flows, scholars have successively conducted theoretical modeling and analytical solutions for related systems, including steady-state or transient solutions for layered configurations [225,231], steady-state solutions for concentric configurations [232,233], and two-liquid systems coupled with other extra effects [234,235].

Among numerous theoretical modeling efforts, several milestone works merit attention. Choi et al. were the first to fully consider the possible spontaneous adsorption-induced and imbalanced partition-induced charging at the liquid-liquid interface, with their interfacial

conditions becoming the standard treatment in the majority of subsequent works [236]. Huang et al. noted the scale relationship between the thickness of the solvent mixing layer at the oil-water interface and the diffuse layer, and for the first time introduced the diffuse characteristics and finite-thickness effects of the liquid-liquid interface, as shown in Fig. 9(a) [82]. This study innovatively proposed a modified free energy scheme for the unified description of spontaneous partition- and adsorption-induced charging effects within the diffuse interface model, correlating the specific physicochemical properties of ions and solvents with their free energy behavior. It was found that when ion partition effects dominate, the interpolation functions of permittivity and dynamic viscosity need to be carefully selected, the sharp interface model needs to incorporate corrections for the potential jump within the solvent mixing layer, and the flow rate distribution relationship between the oil and water phases also exhibits a non-monotonic effect with

increasing pH value. Pascall and Squires, in order to study the electrophoretic behavior of conductive dielectric and metallic droplets with ideally polarizable interfaces under external electric field conditions, introduced a finite-length liquid strip immersed within a solid wall as a model system for analysis for the first time [12]. Based on the assumptions of an extremely weak external electric field and linear superposition, this study systematically discussed the electrokinetic slip effects of liquid strips with different conductive dielectric properties, focusing particularly on the impact of surface conduction effects on two-liquid electroosmotic flows. The study pointed out that the slip characteristics at the liquid-liquid interface can enhance the electroosmotic velocity and delay the inhibitory effects of high Du_w numbers on electroosmotic flow. However, the ion concentration polarization effects within the liquid strip under conditions of high surface conduction still require further investigation, which corresponds to the significance of Du_o on the streaming potential on the oil side.

The study of two-liquid parallel streaming potential can be traced back to the experimental research by Bull and Gortner on the jetting of electrolyte solutions into free spaces of air or oil phases, which demonstrated an excellent linear relationship between streaming potential and the pressure drop across the flow [23]. However, due to the immaturity of two-liquid electrokinetic theory at the time, the study adopted the streaming potential theory of solid-liquid interfaces with no-slip boundary characteristics, thus its quantitative results regarding the charging of gas-liquid or oil-water interfaces are questionable, with initial theoretical modeling studies mainly concentrated in the field of geology. In recent years, with the vigorous development of micro- and nanofluidic technologies, the two-liquid streaming potential has come back into focus. Ding et al. focused on the streaming potential of parallel two-liquid flows in a layered configuration within nanoscale channels. Based on Onsager's theory of irreversible thermodynamics, they systematically investigated the energy conversion efficiency from mechanical to electrical energy in this system, finding that the presence of a thin oil layer in the system could simultaneously increase the output power and the energy conversion efficiency [112]. Considering that the interfaces in two-liquid streaming potential systems are typically planar, theoretical modeling is greatly simplified compared with electrophoresis of droplets, also providing the possibility for its application in the measurement of charging properties at liquid-liquid interfaces. Alizadeh and Huang et al. constructed a relatively stable liquid-liquid interface by designing Y–Y shaped channels in microfluidic chips and successfully measured the streaming potential under different solution concentrations and pH conditions using a two-liquid streaming potential approach [237]. To further obtain the interfacial charge quantity, this study effectively reduced the charging at the solid-liquid interface through polymer coating treatment, thereby increasing the accuracy of the approximate correlation formula.

5.2.2. Three-dimensional micro-channel and liquid-infused surface

In the aforementioned two-liquid electroosmotic and streaming potential systems, the geometric configurations are low-dimensional parallel shear flows within quasi-two-dimensional microchannels. As will be mentioned later, with the increase in the length of the liquid-liquid interface, interfacial perturbations may gradually be amplified, thereby potentially facing various interfacial flow instability issues. Therefore, in practical applications, systems with special geometric constraints are typically employed to stabilize the liquid-liquid interface, among which the most representative are gas bubbles or droplets in three-dimensional microchannels and liquid-infused or superhydrophobic surfaces with periodic microstructures.

In three-dimensional microchannels, the simplest and most widely applied form is the capillary with a circular cross-section, while microchannels with rectangular cross-sections are commonly used in microfluidic systems. Takhistov et al. systematically investigated the electrophoretic motion of bubbles in capillaries, conducting microfluidic experiments and theoretical modeling based on Bretherton-type lubri-

cation analysis [238]. This study noted two inhibitory mechanisms of bubble propulsion within capillaries, including the high mobility of the bubble surface, and the fact that the electric field strength and liquid flow rate within the liquid film are both proportional to the film thickness; both factors make it difficult to establish sufficient pressure differences across the liquid film region and the front and rear edges of the bubble to drive bubble motion. Therefore, the study employed ionic surfactant-laden gas-liquid interfaces that carry charges opposite to those of the capillary solid walls and used appropriate supporting electrolyte concentrations to simultaneously regulate $\Xi_{s,w}$ and Du_w . In this way, the Marangoni effect was used to suppress the mobility of the bubble surface, and the increase in surface conductivity and the relative slip at the liquid-liquid and solid-liquid interfaces were used to suppress the electric field strength and net liquid flow rate within the liquid film, thereby achieving a significant increase in bubble mobility. Sherwood further studied the streaming potential effects formed by the motion of bubbles or droplets immersed in electrolyte solutions within capillaries under pressure-driven conditions [202]. He particularly focused on two limiting cases where the droplet radius is significantly smaller than the tube diameter and the droplet length is significantly longer than the tube diameter, finding that convection at the charged liquid-liquid interface can significantly increase the convective current, thereby enhancing the streaming potential effect. The non-linear relationship between the convective current and the pressure drop in the case of long droplets also leads to a non-linear dependence of the streaming potential on the latter. This study was later extended to droplets of arbitrary size and to microchannel bubble flows with corner flows [197,239], and has been used in recent years for qualitative detection of biochemical signals [240].

Liquid-infused surfaces represent a typical class of heterogeneous surfaces, constituted by periodically arranged lubricant-infused strips, which to a certain extent are equivalent to a liquid version of superhydrophobic surfaces. Since the discovery of the effective slip effect on hydrophobic surfaces, and given the comparable magnitude between the slip length and the Debye length, the electroosmotic slip velocity on such surfaces may be amplified. Squires was the first to focus on the electrokinetic flow phenomena that might arise from inhomogeneous slip interfaces, using the thin double layer assumption to provide a correlation between the effective electroosmotic slip velocity at the surface and the interfacial charge density, roughness, and Debye length, and discussed possible applications in electroosmotic pumps based on flow relations [224]. Particularly, this system also exhibits a significant surface conduction effect Du_w when the interfacial charge density is high, especially the convective transport of charges on finite-length charged liquid-liquid interfaces leading to their accumulation downstream and thus presenting an inhomogeneous distribution. This further causes inhomogeneous transport of ions in the diffuse layer and induces normal currents. Although this effect is relatively clear and intuitive at the level of the physical picture, and presents a richer double-sided coupling of ion concentration polarization in ITIES scenarios, it has so far received little attention [12]. In fact, most subsequent studies have shifted their focus to the impact of anisotropic strip orientation and inhomogeneous slip length on electrokinetic flow behavior, such as on superhydrophobic surfaces [223,241,242] or liquid-infused surfaces [243], as shown in Fig. 9(b). It is worth pointing out that some studies have experimentally verified those theoretical predictions, which also provides a potential approach for measuring the charging properties at liquid-liquid or gas-liquid interfaces, although the estimation methods for the slip length of the experimental system still require improvement [242,243].

5.2.3. Interface electroconvection and flow instability

The deformable and mobile characteristics of liquid-liquid interfaces make them susceptible to various interfacial flow instabilities when subjected to tangential or normal stresses [142]. For instance, in parallel shear flows, velocity perturbations near the interface may induce discontinuities in interfacial velocities, leading to the formation of

tangential vortices that make the stabilizing mechanism of viscous dissipation difficult to counteract, thereby giving rise to *Kelvin-Helmholtz instability*. If there is a viscosity discontinuity across the interface, velocity perturbations may induce a discontinuity in tangential vorticity at the interface, again overwhelming the stabilizing effect of viscous dissipation and leading to *Yih instability*. In the case of liquid film flows, an adsorbed surfactant concentration gradient at the interface may lead to strong convective shear at the interface, which can overcome the stabilizing effect of the surface tension gradient, resulting in *Marangoni instability*. For jets, radial interface shape perturbations that challenge the axial surface tension's stabilizing effect against the circumferential surface tension can lead to capillary-driven *Rayleigh-Plateau instability*. In density-stratified liquids under a gravitational field, if a denser fluid is positioned above a less dense fluid, shape perturbations at the interface can induce normal pressure jumps that overcome the stabilizing effect of surface tension, leading to *Rayleigh-Taylor instability*. In the case of two-phase displacement within a Hele-Shaw cell, if a low-viscosity fluid displaces a high-viscosity fluid, interface shape perturbations can similarly induce normal pressure jumps that defeat the stabilizing effect of surface tension, resulting in *Saffman-Taylor instability*.

For charged liquid-liquid interfaces, the presence of a net interfacial charge layer means that the action of an external non-equilibrium potential, represented by an applied electric field, will directly introduce additional Maxwell stress near the interface and bring about perturbations in tangential viscous stress or normal pressure differences. These act as sources of perturbation and can significantly affect the flow stability of the interface. In fact, in electrokinetic multiphase flows, there indeed exist electroconvection-induced interfacial flow instabilities corresponding to the three scenarios mentioned above, including *two-liquid parallel flow instability* corresponding to parallel shear flows, *jet and film instabilities* corresponding to film flows and jets, and *Faraday wave instability* and *electrokinetic displacement instability* corresponding to interfacial normal pressure differences. Additionally, in the field of electromechanical hydrodynamics, there are two classic types of electroconvection instability phenomena. One is the *Taylor cone* in electrohydrodynamics, where the interface of a dielectric liquid induces charges under the action of a strong normal external field, thereby producing a conical jet, also known as Frenkiel instability [45,135]. The other is *second-kind electroosmosis* in electrokinetics, where an electrolyte solution near ion-selective membranes, reactive electrodes, or polarizable metal surfaces induces a strong transient normal current under the action of a strong normal electric field, producing vortex convection similar to Rayleigh-Benard and further inducing a normal current exceeding the limiting current [194,244]. Experimental studies on electrokinetic multiphase flows have shown that bubbles or ITIES systems can also produce corresponding *electrospray and electrochemical instabilities* under the action of a strong normal electric field, which bear certain similarities to those two behaviors. However, due to the coupling of interfacial ion kinetic transport behavior, the above phenomena involve coupled component transport related to interfacial physicochemical kinetics and interfacial flow stability [245,246], and the related instability mechanisms are much richer. The current understanding of the mechanisms and theories of these phenomena is still in its infancy. Here, a brief introduction will be given to the interfacial instabilities involved in electrokinetic multiphase flow systems, providing clues for possible future follow-up research.

Electrokinetic multiphase flow systems such as two-liquid parallel electroosmosis and streaming potential, electrolyte solution jets, and film flows all involve quasi-planar interfaces of conductive dielectric liquids. The exploration of their mechanisms is a further in-depth study based on the existing research on interfacial flow stability in the classical field of electrohydrodynamics to some extent. The streaming potential in two-liquid parallel flows may primarily be due to the adsorption of solute ions, which brings about an interfacial tension gradient. This can lead to perturbations continuously accumulating at the downstream interface under finite-length conditions, resulting in periodic oscillatory

behavior or even instability of the interface. To a large extent, this is caused by the surface activity of solute ions rather than spontaneous adsorptive charging of the interface [247]. In contrast, the instability of two-liquid parallel electroosmotic flows is usually closely related to interfacial charging and does not depend on the surface activity of solute ions, thus it can widely exist in various ITIES systems [228,248]. In recent years, several experimental quantitative comparison studies have also emerged [225], as shown in Fig. 9(c). Study on jet instability typically focuses on cases without charging or assumes fluids to be perfect conductors. Lopez-Herrera et al. were among the first to apply the weakly conductive dielectric model to the study of jet instability. They successfully used a quasi-one-dimensional theoretical model to predict the size of droplets formed by the end instability and breakup of jets observed in experiments, and found that boundary charge conservation and bulk equipotential constraints can give almost consistent prediction results [144,249]. As one of the simplified cases of jets, the stability mechanism of the Armstrong liquid bridge between droplets loaded with electrodes has also attracted widespread attention from scholars. In recent years, it has been noted that its dynamic instability is closely related to the effective length between droplets, and its linear stability analysis based on charged jet flow matches well with experiments [250,251]. In addition, for the electrolyte solution film with surfactant-laden interfaces, the electroosmotic flow effect caused by interfacial charging also has an important impact on the interfacial stability under the action of electromagnetic fields [252,253].

Similar to the stratified fluid interfaces with density differences in a gravitational field, fluid interfaces with conductivity stratification may also induce interfacial instabilities under the action of an external electric field, and the interphase current across non-polarizable interfaces may significantly affect the stability of two-phase displacement within low-dimensional structures. Taylor and McEwan were the first to study the stability behavior of conductivity-stratified fluid interfaces under a normal direct current (DC) electric field [254], and Yih subsequently extended this to alternating current (AC) conditions [255]. It was not until recent years that systematic studies on the spatial structural characteristics and modulation methods of interfacial waves and electroconvective behavior in this system emerged [256–258]. This phenomenon was first observed by Faraday in a horizontal liquid interface system on a vibrated plate and is referred to as *Faraday waves*, hence its counterpart in electrokinetic flow scenarios is also known as *electro-Faraday waves* [256]. For scenarios commonly found in advanced manufacturing and life sciences, such as polymer electroforming and cell membrane electroporation, Gambhire and Thakkar were among the first to consider the effects of the conductivity and diffuse layer of electrolyte solutions on interfacial stability [259]. A series of studies represented by Kumaran focused on the electric field-induced interfacial instability effects when an elastic film is present at the liquid-liquid interface [260–262]. It is worth noting that in Hele-Shaw structures, normal electric fields and interphase currents can also become an effective means of enhancing the stability of two-phase displacement. Mirzadeh and Bazant, based on the assumption of a non-polarizable liquid-liquid interface, used linear stability analysis to study the effect of interfacial normal electric fields on the stability of electrokinetic displacement, as shown in Fig. 10(a). The study found that the normal electric field across a non-polarizable interface can shift the critical wavelength for instability when the viscosity ratio of the fluid at the front and rear of the interface is less than 1 (an unfavorable viscosity ratio), and the intensity of the interphase current and the electroosmotic mobility on either side of the interface jointly affect the stability conditions of the interface [263]. This line of research was later extended to studies on the viscous fingering of leaky dielectric liquid interfaces under an externally applied electric field [264].

In scenarios such as the preparation of microdroplets via electro-spraying, voltammetric characteristic testing of ITIES, and hydrogen production through the electrolysis of alkaline solutions, there is often a strong externally applied electric field applied normally across the

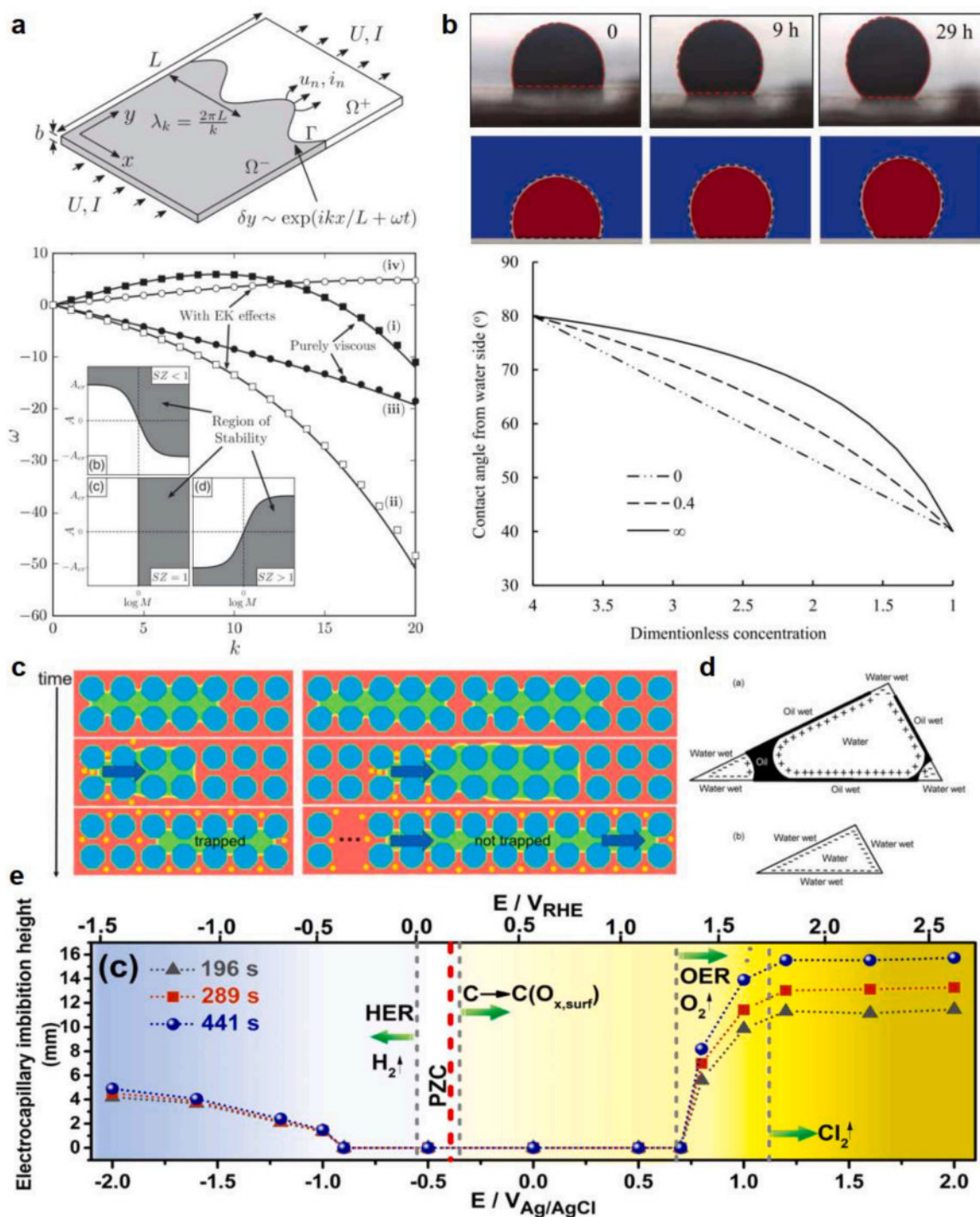


Fig. 10. Electrokinetic multiphase flow phenomena: nanoscale interaction coupling. (a) Injecting currents to suppress viscous fingering instability [263]. (b) Ion-tuned wettability model and droplet wetting dynamics [147]. (c) Ganglia mobility regulated by dynamic wettability [148]. (d) Two phase streaming potential for different two-phase configuration at cross section of throats [276,277]. (e) Hydrophobic nanoporous carbon scaffolds reveal the origin of polarity-dependent electrocapillary imbibition [75].

interface of electrolyte solutions. Experimental studies have observed that in these scenarios, various interfacial flow instabilities similar to phenomena that have been widely studied in different fields as mentioned earlier, such as the Taylor cone, electroconvection, and interfacial turbulence, are produced. Dehe et al. arranged electrodes on both sides of the oil-water interface, focusing on the interfacial instability behavior induced by the normal electric field applied by the needle-like electrode on the electrolyte solution interface, including the

formation of Taylor cones, electro spraying, and reverse deflection, among other complex interfacial evolution behaviors, as shown in Fig. 9 (d) [226]. The study pointed out that the disruption of the oil-water interface and the ejection of microdroplets into the oil phase have a significant impact on the interfacial evolution. Through numerical simulations, the study systematically investigated the interaction between interfacial hydrodynamic stress and Maxwell stress on the interfacial evolution process. It was found that the charge density of the

microdroplets formed by electrospraying shows a certain dependence on the viscosity of the oil phase. Furthermore, the behavior of microdroplets impacting the needle-like electrode and weakening the electric field was taken into account, providing a quantitative explanation for the reverse deflection behavior.

Considering that the liquid-liquid interface in ITIES systems is a soft interface with ion-selective permeability, theoretically, there may exist similar effects to electroconvection and interfacial turbulence. The former mainly refers to strong-field-induced electroconvection, thereby presenting transport exceeding the limiting current, while the latter refers to Marangoni flow and interfacial vortex turbulence induced by interphase mass transfer, promoting interfacial mixing and emulsification. In fact, those behaviors have been widely observed in voltammetric characteristic tests of ITIES conducted in the field of electrochemistry, but they exhibit many novel behaviors. For example, under the limit of a strong normal electric field, different ITIES systems show different behaviors such as enhanced or weakened interphase mass transfer [265]. Furthermore, for ITIES interface systems with adsorbed surfactants, the aqueous phase potential and pH value will accompany periodic oscillation characteristics on the baseline during the voltammetric scan process [266–268]. It should be noted that although those phenomena of interfacial electrochemical instability have been widely observed, there is still a lack of solid theoretical support from the perspective of electrokinetic multiphase hydrodynamics to date. The preliminary work already carried out includes Aogaki et al.'s research on abnormal limiting current induced by interphase mass transfer [60], as well as research groups such as Kakiuchi and Krylov studying interfacial electrochemical instability [269,270] and interfacial turbulence [177,271] induced by inhomogeneous electrowetting effects.

Eckert et al. and Lohse et al. have been deeply involved in the field of physicochemical two-phase hydrodynamic mechanisms of hydrogen production through microelectrode electrolysis for many years, successively conducting in-depth research on the solute and temperature Marangoni interfacial convection of electrogenerated hydrogen bubbles [272], the evolution and coalescence dynamics phase diagram of hydrogen bubbles under different electrolysis voltages [273,313], and the impact mechanism of interfacial force balance relationships on the novel dynamics behaviors of hydrogen bubbles [187]. In recent years, Bashkatov et al. unexpectedly discovered in experiments that the rise and growth of hydrogen bubbles are accompanied by the migration of microdroplets within the bubble [274]. Through experimental observation, data processing, and numerical simulation, this study indicates that the Worthington jet, formed during the coalescence process of satellite and main bubbles, is the main mechanism leading to the electrospray of electrolyte solution and the formation of microdroplets within the bubble. The significance of this study lies in the fact that microdroplets can significantly affect the desorption dynamics process from the electrode surface through subsequent merging effects with rising bubbles, and they may also serve as an important means for studying the spontaneous adsorption-induced charging and in-situ characterization of Marangoni flow at the interface of electrogenerated hydrogen bubbles. It is worth noting that existing studies have all adopted the assumption of uniform charge for the spontaneous adsorption-induced charging of hydrogen bubbles in electrolyte solutions, indicating that the effects of externally induced interfacial charging, as well as the coupling mechanisms of Marangoni convection and surface conduction on the evolution dynamics of hydrogen bubbles, still require further evaluation.

5.3. Nanoscale interaction coupling

The presence of a three-phase contact line and a liquid film of nanoscale thickness is a significant characteristic that distinguishes electrokinetic multiphase flows from traditional single-phase electrokinetic flows near solid-liquid boundaries. In this case, the charged solid-liquid interface and the charged liquid-liquid interface within the elec-

trolyte solution will be coupled through complex surface and interfacial interactions, thereby affecting the equilibrium contact angle and the dynamic behavior of the contact line (including the nanoscale liquid film). For such scenarios, the equilibrium contact angle and the dynamic behavior of the contact line are closely related to the distribution of disjoining pressure of the liquid film and the interfacial tension [111,192]. The former describes the additional local effective pressure on the liquid-liquid interface due to nanoscale interactions with the solid-liquid interface, while the latter correlates the pressure difference across the liquid-liquid interface with the local shape of the interface. Based on the capillary number commonly used in multiphase interfacial deformation flows, $Ca_g = \eta u A_g / \gamma$ (where A_g is the shape factor related to the geometric shape of the interface), the effects of interfacial interaction regulation and the inhomogeneity of liquid film disjoining pressure associated with the charged liquid-liquid interface can be described using Π_γ and Π_∇ as shown in Table 9.

This section will focus on the mechanism of electrokinetic multiphase flow involving the nanoscale interaction coupling between charged liquid-liquid interfaces and solid walls, as shown in Fig. 10. The sources of electrokinetic transport include not only ion transport and the dynamic changes or inhomogeneous distribution of interfacial tension and wettability induced by the heterogeneity of solid walls, thereby coupling two-phase flow, that is, ions altering interfacial properties and inhomogeneous wettability coupling two-phase electrokinetic displacement [275]; but also the changes in interfacial tension and contact angle induced by the external electric field, thereby coupling two-phase electrokinetic displacement, that is, the coupling of electro-wetting and electroosmotic flow with two-phase electrokinetic displacement. The following will classify the relevant electrokinetic multiphase flow systems into three categories from the perspectives of system geometric configuration and interfacial evolution behavior: droplet mobilization or liquid film spreading dynamics, electrokinetic two-phase displacement in microchannels or porous media, and electrokinetic transport in unsaturated porous media with quasi-static interfaces. A brief introduction will be given to the existing research on their transport mechanisms in sequence.

As the foundation for ion-tuned wettability coupling with droplet wetting dynamics, studies on how solution ion composition variation affects film disjoining pressure and equilibrium contact angles have been of interest since the latter half of the last century. This interest primarily stems from the petroleum industry's practical need to understand the mechanisms of ion-tuned wettability for the recovery of residual oil films, such as oil film stability [278,279] and wettability regulation [149,280]. It is noteworthy that during the mobilization of residual oil droplets, ion transport induces dynamic changes and inhomogeneous distribution of wettability on solid surfaces. Although there have been numerous studies on contact line dynamics under conditions of inhomogeneous wettability [281,282], research coupling ion transport with droplet wetting dynamics has only gradually gained attention in recent years, such as in the detachment of residual oil droplets [147] and film stability [283], as shown in Fig. 10(b). However, the current understanding of the relaxation times and effects of inhomogeneous distribution induced by ion transport on wettability changes is still limited, and further studies are required.

Compared with ion-tuned wettability, the electrocapillary effect induced by an external normal electric field has a more significant impact on the equilibrium contact angle. This phenomenon, known as *electrowetting*, involves complex multiscale physical processes near the three-phase contact line [57]. There are important differences between the electrowetting of strong electrolyte solutions and that under traditional dielectric or leaky dielectric liquid environments, such as charge-induced polarization effects [141], interfacial charge regulation effects [284], and electroconvection and diffusive boundary layer phenomena under strong non-equilibrium conditions [267]. It is worth noting that the current understanding of electrowetting for conductive dielectric droplets composed of electrolyte solutions is still limited, and some

numerical simulation studies still use the classical treatment methods of electrohydrodynamics [285,286], thus failing to fully consider the important impact of the interfacial double layer [185,287,288]. For ITIES systems, the non-polarizable characteristics of the interface also mean that it allows interphase current to pass through, which may further affect the non-equilibrium transport behavior of the interface. The ion selectivity of the interface will lead to possible symmetry breaking in the direction of the applied electric field. Therefore, the rich interfacial physicochemical kinetic behavior of ITIES provides new approaches for the active regulation of electrowetting behavior and transpiration-driven power generation.

In addition to droplet wetting and liquid film spreading dynamics near solid walls, two-phase flow within microchannels or porous media often involves displacement behavior. This two-phase electrokinetic displacement can be similarly divided into two cases: ion transport-mediated and external field-driven, where the geometric constraints of microchannels or porous media often couple with interfacial effects to influence multiphase flow behavior. In fact, the regulation of two-phase displacement behavior within microchannels traditionally often employs amphiphilic molecules or nanoparticle systems with surface activity, based on dynamic changes in interfacial tension, regulation in interfacial rheological behavior, dynamic changes in wettability, or combinations of those factors [275]. The presence of solute ions provides the extra possibility for active control by external electric fields, such as the stability control of two-phase displacement in straight channels coupled with electrowetting and electroosmotic effects [263,289], and electrochemical reactions coupled with electroosmotic imbibition in conductive nanoporous media [75], as shown in Fig. 10(e). Research on the mechanism of coupling between ion transport and wetting dynamics largely stems from new developments in the geological field in recent years, namely the mechanisms possibly related to the effectiveness of low-salinity waterflooding, such as capillary filling regulation, recovery of residual mobile oil films, and mobilization of trapped oil ganglia [148,290], as shown in Fig. 10(c).

In fact, low-salinity waterflooding, as a low-cost and environmentally friendly enhanced oil recovery method, has received increasing attention and importance in the geological field in contemporary society advocating low-carbon and green development [79,291]. Among these, the mechanism of ion-tuned wettability is believed to play an important role [292,293], and the ion partition effect brought by highly polar oils may provide a new mechanism for wettability change [294,295], although there is still a lack of sufficient research on the latter. Considering that the role of wettability in displacement behavior usually strongly depends on the system's geometric size (see the definitions of Ca_g and Π_v), the pore size and its heterogeneity of porous media may have an important impact on pore events such as cooperative filling, Haines jump, and film flow in two-phase displacement, which may lead to a non-monotonic dependence of the long-term behavior of two-phase displacement in porous structures with preferential flow paths on wettability [296–298]. Moreover, since ion-tuned wettability depends on both nanoscale interfacial interactions and ion transport processes, the heterogeneity of porous media will lead to dynamic changes and inhomogeneous distribution of wettability in different pores, thereby making the behavior of two-phase displacement exhibit more complex non-monotonic characteristics.

The *self-potential* method commonly used in the geological field for measurement also falls under the category of electrokinetic multiphase flow phenomena in porous media, primarily utilizing the streaming potential effect of quasi-steady two-phase flow at the liquid-liquid interface within unsaturated porous media [299]. As previously mentioned, the streaming potential in systems such as two-phase parallel flow, droplets in three-dimensional channels, and liquid-infused surfaces is significantly higher than that of single-phase flow. In fact, theoretical modeling of similar phenomena appeared successively around the 1990s [300–302], and has influenced research to this day [303,304]. In addition, Jackson and Vinogradov focused on the impact

of wettability on the streaming potential of two-phase flow in porous media [277], as shown in Fig. 10(d). It is worth noting that Wurmstich and Morgan [305], and Revil et al. [276,302] were among the first to introduce Onsager's reciprocal principle into multiphysical transport modeling in porous media [72], which to some extent inspired the subsequent development of two-phase conductivity methods used in geological exploration [306].

6. Summary and perspectives

6.1. Concluding remarks

This review synthesizes emerging integrative perspectives that bridge microscopic interfacial charging mechanisms with macroscopic electrokinetic transport, unifying diffuse and sharp interface paradigms. The polarization of electric double layers (EDLs) emerges as a cornerstone phenomenon governing interfacial electrohydrodynamics. A coherent framework must interconnect three cross-scale critical elements: (1) unified descriptions of ion partitioning/adsorption mechanisms, (2) thermodynamic and kinetic constraints on interface polarizability, and (3) upscaled models coupling equilibrium interfacial charging with non-equilibrium electrokinetic transport. Our analysis reveals that ion partitioning and adsorption represent complementary limiting behaviors at charged liquid-liquid interfaces, while the summarized polarizability-based classification system establishes a unified foundation for predicting electrokinetic responses across diverse systems [82].

By integrating multiphase electromechanical hydrodynamics with interfacial mass transfer principles, we systematically deconstruct assumptions inherent to classical macroscopic theories. The dimensionless parameters proposed in this work—serving as symmetry-breaking indicators for EDL polarization—enable mechanistic discrimination of transport regimes in two-liquid systems. Through case studies spanning free droplet electrophoresis to multi-interface coupled flows, we demonstrate the universal applicability of these parameters in resolving long-standing paradoxes, particularly those involving scale disparity between nanoscopic screening layers and macroscopic flow features. This approach provides a transferable methodology for analyzing broader classes of charged soft matter systems.

6.2. Some perspectives

6.2.1. Interfacial charge-mass coupling in soft membranes

While conventional ion-selective membranes rely on static solid frameworks [72], their liquid-liquid analogs represented by ITIES systems exhibit dynamic ion-selective interfaces where polarization couples with interfacial evolution (deformation, rupture, coalescence). The bilateral coupling of diffuse layers across these mobile interfaces remains underexplored [12], particularly regarding how interfacial restructuring modulates trans-membrane ion transfer. This system serves as an ideal platform for mimicking biological membrane functionality, offering new avenues to decode neural ion transport mechanisms [307] while addressing unresolved challenges in quantifying interface permselectivity under flow conditions.

6.2.2. Nanoconfined electrohydrodynamic correlations

Building upon classical electrolyte theories by Arrhenius, Debye, and Onsager [308,309], we identify three critical knowledge gaps, i.e., many-body electrostatic correlations (overscreening) versus steric exclusion in subnanometer interfacial zones, ion-modulated solvent phase distribution within Bjerrum-length-scale mixing layers [82], and electrorheological feedback on interfacial mechanics through Marangoni-diffusioosmotic coupling [50,203]. These mechanisms underpin emerging phenomena such as droplet solidification effects and nonlinear bubble electrophoresis [88,222], challenging the validity of conventional leaky dielectric models [13,81] at extreme ion

concentrations.

6.2.3. Electrokinetic control of multiphase flows

Extending Levich's physicochemical hydrodynamics framework [310,311], we emphasize electrokinetic regulation as a paradigm-shifting strategy surpassing traditional surface tension-based control. The inherent field responsiveness of charged interfaces enables precision manipulation through three key mechanisms, i.e., electroconvective instabilities for enhanced mixing [257], Faradaic electropatterning or electrospinning for interfacial architecture design [312], and electro-spray-assisted phase manipulation in energy applications [187,313]. Emerging applications span digital microfluidics to hydrogen geo-storage, requiring fundamental advances in understanding wettability dynamics under coupled electro-chemo-mechanical stimuli [118,263].

6.2.4. Integration of experiments, theories, and simulations

Resolving the coupled charge transport and hydrodynamic physics across nanoscale solvent mixing/diffuse layers and micron-scale viscous transport demands coordinated advances across two domains. One is *in situ experimental characterization*. While molecular dynamics simulations combined with X-ray spectrometry elucidate quasi-static interfacial structures [5], dynamic measurements of evolving interfaces (e.g., during droplet electrophoresis) remain technically challenging. Current macroscale observables like droplet electrophoretic mobility lack direct connections to interfacial kinetic processes, while simplified geometric configuration in microfluidic platforms that isolate liquid-liquid interfaces from solid boundaries may help [237]. The other is *multiscale modeling and cross-validation protocols*. Effective frameworks must hierarchically integrate particle-level statistics (equilibrium charging), diffuse interface descriptions (non-equilibrium transport), and matched asymptotic expansions (coarse-grained description), bridging nanoscopic interfacial layers to macroscopic flows. Recent phase-field models incorporating solvent mixing and adsorption-partition coupling demonstrate promising progress [82], achieving quantitative reconciliation between sharp/diffuse interface paradigms. Besides, establishing causality between interfacial molecular rearrangements and macroscopic transport requires correlative approaches combining operando spectroscopy, high-fidelity simulations, and machine learning-assisted inverse analysis.

CRedit authorship contribution statement

Yunfan Huang: Writing – original draft, Investigation, Data curation. **Moran Wang:** Writing – review & editing, Supervision, Conceptualization.

Declaration of competing interest

The authors declare that they have no known competing financial interests or personal relationships that could have appeared to influence the work reported in this paper.

Acknowledgments

The authors would like to thank the anonymous referee who provided useful and detailed comments on the manuscript. This work was financially supported by the National Natural Science Foundation of China (No. 12272207, 12432013) and the National Key Research and Development Program of China (No. 2019YFA0708704).

Data availability

No data was used for the research described in the article.

References

- [1] Hunter RJ, Ottewill RH, Rowell RL. Zeta potential in colloid science. Principles and applications. Academic Press; 1981.
- [2] Lyklema J. Fundamentals of interface and colloid science II: solid-liquid interfaces. Academic Press; 1995.
- [3] Jacob SB, Masliyah H. Electrokinetic and colloid transport phenomena. New Jersey: John Wiley & Sons, Inc.; 2006.
- [4] Bockris JO, Reddy AKN, Gamboa-Aldeco M. Modern electrochemistry 2A: fundamentals of electrochemistry. New York: Springer; 2000.
- [5] Uematsu Y. Electrification of water interface. *J Phys Condens Matter* 2021;33(42):423001.
- [6] Saville D. Electrokinetic effects with small particles. *Annu Rev Fluid Mech* 1977;9(1):321–37.
- [7] Kirby BJ, Hasselbrink Jr EF. Zeta potential of microfluidic substrates: 1. Theory, experimental techniques, and effects on separations. *Electrophoresis* 2004;25(2):187–202.
- [8] Ghosal S. Electrokinetic flow and dispersion in capillary electrophoresis. *Annu Rev Fluid Mech* 2006;38(1):309–38.
- [9] Lyklema J. Principles of the stability of lyophobic colloidal dispersions in non-aqueous media. *Adv Colloid Interface Sci* 1968;2(2):67–114.
- [10] Markin VS, Volkov AG. The gibbs free energy of ion transfer between two immiscible liquids. *Electrochim Acta* 1989;34(2):93–107.
- [11] Levich V. Physicochemical hydrodynamics. Russia: Fizmatgiz Moscow; 1959.
- [12] Pascall AJ, Squires TM. Electrokinetics at liquid/liquid interfaces. *J Fluid Mech* 2011;684:163–91.
- [13] Bazant MZ. Electrokinetics meets electrohydrodynamics. *J Fluid Mech* 2015;782:1–4.
- [14] Lippmann G. Relations entre les phénomènes électriques et capillaires. *Ann Chim Phys* 1875;5(11):494–549.
- [15] Chapman DL, Li A. A contribution to the theory of electrocapillarity. *Lond Edinb Dubl Philos Mag* 1913;25(148):475–81.
- [16] Gouy M. Sur la constitution de la charge électrique à la surface d'un électrolyte. *J Phys Theor Appl* 1910;9(1):457–68.
- [17] Grahame DC. The electrical double layer and the theory of electrocapillarity. *Chem Rev* 1947;41(3):441–501.
- [18] Senter G. General and physical chemistry. *Ann Rep Prog Chem* 1912;9(0):1–35.
- [19] Ellis R. A neutral oil emulsion as a model of a suspension colloid. *Trans Faraday Soc* 1913;9:14–25.
- [20] Lewis W. Note on the electric charge on an oil droplet in an emulsion. *Trans Faraday Soc* 1932;28:597–607.
- [21] Dean R. Potentials at oil-water interfaces. *Nature* 1939;144(3635):32.
- [22] McTaggart H, XLV. Electrification at liquid gas-surfaces. *Lond Edinb Dubl Philos Mag* 1914;28(165):367–78.
- [23] Bull HB, Gortner RA. Studies on electrokinetic potentials: IX. The electrical field of force at liquid-liquid interfaces. *Proc Natl Acad Sci* 1931;17(5):288–94.
- [24] Verwey EJW, Niessen KF, XL. The electrical double layer at the interface of two liquids. *Lond Edinb Dubl Philos Mag* 1939;28(189):435–46.
- [25] Verwey E. Theory of the electric double layer of stabilized emulsion. *Proc Konink Nederland Akad Wetenschap* 1950;53:375.
- [26] Donnan F. The osmotic pressure of colloidal salts. *Nature* 1911;87(2176):45.
- [27] Vanýsek P. Electrochemistry on liquid-liquid interfaces. Berlin, Heidelberg: Springer; 1985.
- [28] Ohshima H, Ohki S. Donnan potential and surface potential of a charged membrane. *Biophys J* 1985;47(5):673–8.
- [29] Markin VS, Volkov AG. The phase boundary potentials at the interface between two immiscible electrolyte solutions. *Russ Chem Rev* 1988;57(12):1124–41.
- [30] Samec Z. Electrical double layer at the interface between two immiscible electrolyte solutions. *Chem Rev* 1988;88(4):617–32.
- [31] Koryta J, Vanýsek P, Březina M. Electrolysis with an electrolyte dropping electrode. *J Electroanal Chem Interfacial Electrochem* 1976;67(2):263–6.
- [32] Laforge FO, Carpino J, Rotenberg SA, Mirkin MV. Electrochemical attosyringe. *Proc Natl Acad Sci* 2007;104(29):11895–900.
- [33] Liu S, Li Q, Shao Y. Electrochemistry at micro- and nanoscopic liquid/liquid interfaces. *Chem Soc Rev* 2011;40(5):2236–53.
- [34] Chen C-C, Cang C, Fenske S, Butz E, Chao Y-K, Biel M, et al. Patch-clamp technique to characterize ion channels in enlarged individual endolysosomes. *Nat Protoc* 2017;12(8):1639–58.
- [35] Quincke G. Ueber die fortführung materieller theilchen durch strömende elektricität. *Ann Phys* 1861;189(8):513–98.
- [36] Mooney M. Variations in the cataphoretic mobilities of oil drops in water. *Phys Rev* 1924;23(3):396–411.
- [37] Frumkin A. New electrocapillary phenomena. *J Colloid Sci* 1946;1(3):277–91.
- [38] Booth F. The cataphoresis of spherical fluid droplets in electrolytes. *J Chem Phys* 1951;19(11):1331–6.
- [39] Jordan D, Taylor AJ. The electrophoretic mobilities of hydrocarbon droplets in water and dilute solutions of ethyl alcohol. *Trans Faraday Soc* 1952;48:346–55.
- [40] Taylor AJ, Wood FW. The electrophoresis of hydrocarbon droplets in dilute solutions of electrolytes. *Trans Faraday Soc* 1957;53:523–9.
- [41] D. Henry, The cataphoresis of suspended particles. Part I.—The equation of cataphoresis, *Proceedings of the Royal Society of London. Series A, Containing Papers of a Mathematical and Physical Character* 133 (821) (1931) 106–129.
- [42] Millikan RA. The isolation of an ion, a precision measurement of its charge, and the correction of stokes's law. *Phys Rev* 1911;32(4):349–97.
- [43] Gill EWB, Alfrey GF. Electrification of liquid drops. *Nature* 1949;164(4180):1003.

- [44] Allan RS, Mason SG, Marion LE. Particle behaviour in shear and electric fields I. Deformation and burst of fluid drops. *Proc R Soc Lond A* 1962;267(1328):45–61.
- [45] Taylor GI. Disintegration of water drops in an electric field. *Proc R Soc Lond A* 1964;280(1382):383–97.
- [46] Melcher JR, Taylor GI. Electrohydrodynamics: a review of the role of interfacial shear stresses. *Annu Rev Fluid Mech* 1969;1(1):111–46.
- [47] Saville DA. Electrohydrodynamics: the Taylor-Melcher leaky dielectric model. *Annu Rev Fluid Mech* 1997;29(1):27–64.
- [48] Ohshima H, Healy TW, White LR. Electrokinetic phenomena in a dilute suspension of charged mercury drops. *J Chem Soc* 1984;80(12):1643–67.
- [49] Baygents J, Saville D. The migration of charged drops and bubbles in electrolyte gradients: diffusiophoresis. *Phys Chem Hydrodyn* 1988;10:543–60.
- [50] Baygents JC, Saville D. Electrophoresis of drops and bubbles. *J Chem Soc Faraday Trans* 1991;87(12):1883–98.
- [51] Dukhin SS, Deryagin BV. The thermodynamics of irreversible processes, as applied to the theory of capillary osmosis and diffusiophoresis. In: *Doklady Akademii Nauk*. vol. 159. Russian Academy of Sciences; 1964. p. 401–4.
- [52] Nadim A, Borhan A. Effects of surfactants on the motion and deformation of a droplet in thermocapillary migration. *Physicochem Hydrodyn* 1989;11(5–6):753–64.
- [53] Schlüter M, Herres-Pawlus S, Niekem U, Tuttlies U, Bothe D. Small-scale phenomena in reactive bubbly flows: experiments, numerical modeling, and applications. *Ann Rev Chem Biomol Eng* 2021;12(1):625–43.
- [54] Dwivedi P, Pillai D, Mangal R. Self-propelled swimming droplets. *Curr Opin Colloid Interface Sci* 2022;61:101614.
- [55] Choi K, Ng AHC, Fobel R, Wheeler AR. Digital microfluidics. *Annu Rev Anal Chem* 2012;5(1):413–40.
- [56] Mugele F, Baret J-C. Electrowetting: from basics to applications. *J Phys Condens Matter* 2005;17(28):R705–74.
- [57] Mugele F, Heikenfeld J. Electrowetting: fundamental principles and practical applications. John Wiley & Sons; 2019.
- [58] Vlahovska PM. Electrohydrodynamics of drops and vesicles. *Annu Rev Fluid Mech* 2019;51(1):305–30.
- [59] Papageorgiou DT. Film flows in the presence of electric fields. *Annu Rev Fluid Mech* 2019;51(1):155–87.
- [60] Aogaki R, Kitazawa K, Fueki K, Mukaibo T. Theory of polarographic maximum current-I. Conditions for the onset of hydrodynamic instability in a liquid metal electrode system. *Electrochim Acta* 1978;23(9):867–74.
- [61] Aogaki R, Kitazawa K, Fueki K, Mukaibo T. Theory of polarographic maximum current-II. Growth or decay rate of the electrochemical and hydrodynamic instability. *Electrochim Acta* 1978;23(9):875–80.
- [62] Xiang W, Lu Y, Wang H, Sun X, Chen S, He Z, et al. Liquid-metal-based magnetic fluids. *Nat Rev Mater* 2024;9(6):433–49.
- [63] Mutschke G, Weier T. Directed transfer of liquid metal droplets between electrodes. *Nat Chem Eng* 2024;1(4):275–6.
- [64] Qiu Z, Texter J. Ionic liquids in microemulsions. *Curr Opin Colloid Interface Sci* 2008;13(4):252–62.
- [65] Santos CS, Baldelli S. Gas-liquid interface of room-temperature ionic liquids. *Chem Soc Rev* 2010;39(6):2136–45.
- [66] Rotenberg B, Pagonabarraga I. Electrokinetics: insights from simulation on the microscopic scale. *Mol Phys* 2013;111(7):827–42.
- [67] Lu Y, Xia Y, Luo G. Phase separation of parallel laminar flow for aqueous two phase systems in branched microchannel. *Microfluid Nanofluid* 2011;10(5):1079–86.
- [68] Hardt S, Hahn T. Microfluidics with aqueous two-phase systems. *Lab Chip* 2012;12(3):434–42.
- [69] Chao Y, Shum HC. Emerging aqueous two-phase systems: from fundamentals of interfaces to biomedical applications. *Chem Soc Rev* 2020;49(1):114–42.
- [70] Chao Y, Ramirez-Soto O, Bahr C, Karpitschka S. How liquid-liquid phase separation induces active spreading. *Proc Natl Acad Sci* 2022;119(30):e2203510119.
- [71] Hester EW, Carney S, Shah V, Arnheim A, Patel B, Di Carlo D, et al. Fluid dynamics alters liquid-liquid phase separation in confined aqueous two-phase systems. *Proc Natl Acad Sci* 2023;120(49):e2306467120.
- [72] Marbach S, Bocquet L. Osmosis, from molecular insights to large-scale applications. *Chem Soc Rev* 2019;48(11):3102–44.
- [73] Ma M, Booty MR, Siegel M. A model for the electric field-driven flow and deformation of a drop or vesicle in strong electrolyte solutions. *J Fluid Mech* 2022;943:A47.
- [74] Pratt LR, Pohorille A. Hydrophobic effects and modeling of biophysical aqueous solution interfaces. *Chem Rev* 2002;102(8):2671–92.
- [75] Pan B, Valappil MO, Rateick R, Clarkson CR, Tong X, Debuhr C, et al. Hydrophobic nanoporous carbon scaffolds reveal the origin of polarity-dependent electrocapillary imbibition. *Chem Sci* 2023;14(6):1372–85.
- [76] Volkov AG, Markin VS. Chapter 4 electric properties of oil/water interfacesvol. 4. Elsevier; 2004. p. 91–182.
- [77] Tian H, Wang M. Electrokinetic mechanism of wettability alternation at oil-water-rock interface. *Surf Sci Rep* 2017;72(6):369–91.
- [78] Rashidi M, Zargartalebi M, Benneker AM. Mechanistic studies of droplet electrophoresis: a review. *Electrophoresis* 2021;42(7–8):869–80.
- [79] Liu F, Wang M. Review of low salinity waterflooding mechanisms: wettability alteration and its impact on oil recovery. *Fuel* 2020;267:117112.
- [80] Schnitzer O, Yariv E. The Taylor-Melcher leaky dielectric model as a macroscale electrokinetic description. *J Fluid Mech* 2015;773:1–33.
- [81] Mori Y, Young YN. From electrodiffusion theory to the electrohydrodynamics of leaky dielectrics through the weak electrolyte limit. *J Fluid Mech* 2018;855:67–130.
- [82] Huang Y, Wang M. Solvent mixing and ion partitioning effects in spontaneous charging and electrokinetic flow of immiscible liquid-liquid interface. *Phys Rev Fluids* 2024;9(10):103701.
- [83] Berg HC. Chemotaxis in bacteria. *Annu Rev Biophys Bioeng* 1975;4(1):119–36.
- [84] Snyderman R, Goetzl EJ. Molecular and cellular mechanisms of leukocyte chemotaxis. *Science* 1981;213(4510):830–7.
- [85] Roussos ET, Condeelis JS, Patsialou A. Chemotaxis in cancer. *Nat Rev Cancer* 2011;11(8):573–87.
- [86] Anderson JL. Colloid transport by interfacial forces. *Annu Rev Fluid Mech* 1989;21(1):61–99.
- [87] Schnitzer O, Frankel I, Yariv E. Electrokinetic flows about conducting drops. *J Fluid Mech* 2013;722:394–423.
- [88] Schnitzer O, Frankel I, Yariv E. Electrophoresis of bubbles. *J Fluid Mech* 2014;753:49–79.
- [89] Lyklema J. Fundamentals of interface and colloid science III: liquid-liquid interfaces. Academic Press; 2000.
- [90] Van Der Hoeven PC, Lyklema J. Electrostatic stabilization in non-aqueous media. *Adv Colloid Interface Sci* 1992;42:205–77.
- [91] Morrison ID. Electrical charges in nonaqueous media. *Colloids Surf A Physicochem Eng Asp* 1993;71(1):1–37.
- [92] Dukhin A, Parlia S. Ion-pair conductivity theory fitting measured data for various alcohol-toluene mixtures across entire concentration range. *J Electrochem Soc* 2015;162(4):H256.
- [93] Chang C-H, Franses EI. Adsorption dynamics of surfactants at the air/water interface: a critical review of mathematical models, data, and mechanisms. *Colloids Surf A Physicochem Eng Asp* 1995;100:1–45.
- [94] He Y, Yazhgur P, Salonen A, Langevin D. Adsorption-desorption kinetics of surfactants at liquid surfaces. *Adv Colloid Interface Sci* 2015;222:377–84.
- [95] Manikantan H, Squires TM. Surfactant dynamics: hidden variables controlling liquid flows. *J Fluid Mech* 2020;892:P1.
- [96] Onuki A. Ginzburg-landau theory of solvation in polar fluids: ion distribution around an interface. *Phys Rev E* 2006;73(2):021506.
- [97] Onuki A. Nonionic and ionic surfactants at an interface. *Europhys Lett* 2008;82(5):58002.
- [98] Onuki A, Okamoto R, Araki T. Phase transitions in soft matter induced by selective solvation. *Bull Chem Soc Jpn* 2011;84(6):569–87.
- [99] Luo G, Malkova S, Yoon J, Schultz David G, Lin B, Meron M, et al. Ion distributions near a liquid-liquid interface. *Science* 2006;311(5758):216–8.
- [100] V. S. Markin, A. G. Volkov, Potentials at the interface between two immiscible electrolyte solutions, *Adv Colloid Interface Sci* 31 (1–2) (1990) 111–152.
- [101] Bard AJ, Faulkner LR, White HS. Electrochemical methods: fundamentals and applications. John Wiley & Sons; 2022.
- [102] Mareček V, Samec Z, Koryta J. Charge transfer across the interface of two immiscible electrolyte solutions. *Adv Colloid Interface Sci* 1988;29(1):1–78.
- [103] Dryfe RAW. The electrified liquid-liquid interface. *Adv Chem Phys* 2009;141:153–215.
- [104] Dukhin SS, Kretschmar G, Miller R. Dynamics of adsorption at liquid interfaces: theory, experiment, application. Elsevier; 1995.
- [105] Onsager L, Samaras NNT. The surface tension of Debye-Hückel electrolytes. *J Chem Phys* 1934;2(8):528–36.
- [106] Kakiuchi T, Senda M. Thermodynamics of the electrocapillarity of oil-water interfaces. *Bull Chem Soc Jpn* 1983;56(10):2912–8.
- [107] Markin VS, Volkov AG. Electrocapillary phenomena at the interface between two immiscible liquids. *Prog Surf Sci* 1989;30(3–4):233–356.
- [108] Volkov AG, Deamer DW, Tanelian DL, Markin VS. Electrical double layers at the oil/water interface. *Prog Surf Sci* 1996;53(1):1–134.
- [109] Shao Y. Electrochemistry at liquid-liquid interfaces. Amsterdam: Elsevier; 2007. p. 785–809.
- [110] Marinova KG, Alargova RG, Denkov ND, Velev OD, Petsev DN, Ivanov IB, et al. Charging of oil-water interfaces due to spontaneous adsorption of hydroxyl ions. *Langmuir* 1996;12:2045–51.
- [111] Israelachvili JN. Intermolecular and surface forces. 3rd ed. San Diego: Academic Press; 2011.
- [112] Ding Z, Jian Y, Tan W. Electrokinetic energy conversion of two-layer fluids through nanofluidic channels. *J Fluid Mech* 2019;863:1062–90.
- [113] Yang F, Shin S, Stone HA. Diffusiophoresis of a charged drop. *J Fluid Mech* 2018;852:37–59.
- [114] de Vos WM, Lindhoud S. Overcharging and charge inversion: finding the correct explanation(s). *Adv Colloid Interface Sci* 2019;274:102040.
- [115] Koopal L, Tan W, Avena M. Equilibrium mono- and multicomponent adsorption models: from homogeneous ideal to heterogeneous non-ideal binding. *Adv Colloid Interface Sci* 2020;280:102138.
- [116] Rotenberg B, Pagonabarraga I, Frenkel D. Coarse-grained simulations of charge, current and flow in heterogeneous media. *Faraday Discuss* 2010;144(0):223–43.
- [117] Probst RF. Physicochemical hydrodynamics. New York: John Wiley & Sons; 1994.
- [118] Lohse D, Zhang X. Physicochemical hydrodynamics of droplets out of equilibrium. *Nat Rev Phys* 2020;2(8):426–43.
- [119] Levich VG. Theory of the macroscopic kinetics of heterogeneous and homogeneous-heterogeneous systems. *Russ Chem Rev* 1965;34(10):792.
- [120] Krishna R, Wesselingh JA. The Maxwell-Stefan approach to mass transfer. *Chem Eng Sci* 1997;52(6):861–911.

- [121] Anderson DM, McFadden GB, Wheeler AA. Diffuse-interface methods in fluid mechanics. *Annu Rev Fluid Mech* 1998;30(1):139–65.
- [122] Schrage RW. A theoretical study of interphase mass transfer. New York: Columbia University Press; 1953.
- [123] Krylov VS. Problems of the theory of transport processes in systems with intensive mass exchange. *Russ Chem Rev* 1980;49(1):59.
- [124] Giustini A, Drenckhan W, Poulard C. Interfacial tension of reactive, liquid interfaces and its consequences. *Adv Colloid Interface Sci* 2017;247:185–97.
- [125] Zhang L, McNeece CJ, Hesse MA, Wang M. Reactive transport of protons in electro-osmotic displacements with electrolyte concentration difference in a microcapillary. *Anal Chem* 2018;90(20):11802–11.
- [126] Koryta J. Electrochemical polarization phenomena at the interface of two immiscible electrolyte solutions—III. Progress since 1983. *Electrochim Acta* 1988;33(2):189–97.
- [127] Bird R, Stewart W, Lightfoot E. Transport phenomena. Wiley; 2006.
- [128] Melcher JR. Continuum electromechanics. MA: MIT Press Cambridge; 1981.
- [129] Marcus Y. Electrostriction in electrolyte solutions. *Chem Rev* 2011;111(4):2761–83.
- [130] Eringen AC, Maugin GA. Electrohydrodynamics. New York, New York, NY: Springer; 1990. p. 551–73.
- [131] Huang Y, Wang M. Nonnegative magnetoresistance in hydrodynamic regime of electron fluid transport in two-dimensional materials. *Phys Rev B* 2021;104(15):155408.
- [132] Bazant MZ, Storey BD, Kornyshev AA. Double layer in ionic liquids: overscreening versus crowding. *Phys Rev Lett* 2011;106(4):046102.
- [133] Davidson SM, Andersen MB, Mani A. Chaotic induced-charge electro-osmosis. *Phys Rev Lett* 2014;112(12):128302.
- [134] Zhakin AI. Electrohydrodynamics of charged surfaces. *Physics-Uspexhi* 2013;56(2):141–63.
- [135] Fernández de la Mora J. The fluid dynamics of Taylor cones. *Annu Rev Fluid Mech* 2006;39(1):217–43.
- [136] Castellanos A. Electrohydrodynamics 380. Springer Science & Business Media; 1998.
- [137] Ramos A. Electrokinetics and electrohydrodynamics in microsystems vol. 530. Springer Science & Business Media; 2011.
- [138] Hua J, Lim LK, Wang C-H. Numerical simulation of deformation/motion of a drop suspended in viscous liquids under influence of steady electric fields. *Phys Fluids* 2008;20(11):113302.
- [139] Li Z-T, Li G-J, Huang H-B, Lu X-Y. Lattice Boltzmann study of electrohydrodynamic drop deformation with large density ratio. *Int J Modern Phys C* 2011;22(07):729–44.
- [140] Ohshima H. A simple expression for the electrophoretic mobility of charged mercury drops. *J Colloid Interface Sci* 1997;189(2):376–8.
- [141] Li M, Li D. Redistribution of mobile surface charges of an oil droplet in water in applied electric field. *Adv Colloid Interface Sci* 2016;236:142–51.
- [142] Leal LG. Advanced transport phenomena: fluid mechanics and convective transport processes vol. 7. Cambridge University Press; 2007.
- [143] Tomar G, Gerlach D, Biswas G, Alleborn N, Sharma A, Durst F, et al. Two-phase electrohydrodynamic simulations using a volume-of-fluid approach. *J Comput Phys* 2007;227(2):1267–85.
- [144] López-Herrera JM, Popinet S, Herrada MA. A charge-conservative approach for simulating electrohydrodynamic two-phase flows using volume-of-fluid. *J Comput Phys* 2011;230(5):1939–55.
- [145] Luo K, Wu J, Yi H-L, Tan H-P. Numerical analysis of two-phase electrohydrodynamic flows in the presence of surface charge convection. *Phys Fluids* 2020;32(12):123606.
- [146] Aziz R, Joekar-Niasar V, Martínez-Ferrer PJ, Godínez-Brizuela OE, Theodoropoulos C, Mahani H. Novel insights into pore-scale dynamics of wettability alteration during low salinity waterflooding. *Sci Rep* 2019;9(1):9257.
- [147] An S, Zhan Y, Mahani H, Niasar V. Kinetics of wettability alteration and droplet detachment from a solid surface by low-salinity: a lattice-Boltzmann method. *Fuel* 2022;329:125294.
- [148] Liu F, Wang M. Wettability effects on mobilization of ganglia during displacement. *Int J Mech Sci* 2022;215:106933.
- [149] Liu F, Wang M. Electrokinetic mechanisms and synergistic effect on ion-tuned wettability in oil-brine-rock systems. *Trans Porous Media* 2021;140(1):7–26.
- [150] Rivas N, Frijters S, Pagonabarraga I, Harting J. Mesoscopic electrohydrodynamic simulations of binary colloidal suspensions. *J Chem Phys* 2018;148(14):144101.
- [151] Baygents JC, Saville DA. The circulation produced in a drop by an electric field: a high field strength electrokinetic model. *AIP Conf Proc* 1990;197(1):7–17.
- [152] Arrigan DWM, Herzog G. Theory of electrochemistry at miniaturised interfaces between two immiscible electrolyte solutions. *Curr Opin Electrochem* 2017;1(1):66–72.
- [153] Gschwend GC, Olaya A, Peljo P, Girault HH. Structure and reactivity of the polarised liquid-liquid interface: what we know and what we do not. *Curr Opin Electrochem* 2020;19:137–43.
- [154] Zholkovskij EK, Masliyah JH, Czarnecki JAN. An electrokinetic model of drop deformation in an electric field. *J Fluid Mech* 2002;472:1–27.
- [155] Kupershtokh AL, Medvedev DA. Lattice Boltzmann equation method in electrohydrodynamic problems. *J Electrostat* 2006;64(7):581–5.
- [156] Sherwood JD. Breakup of fluid droplets in electric and magnetic fields. *J Fluid Mech* 1988;188:133–46.
- [157] Feng JQ, Scott TC. A computational analysis of electrohydrodynamics of a leaky dielectric drop in an electric field. *J Fluid Mech* 1996;311:289–326.
- [158] Krüger T, Kusumaatmaja H, Kuzmin A, Shardt O, Silva G, Viggen EM. The lattice Boltzmann method: principles and practice. Springer; 2017.
- [159] Landau LD, Lifshitz E. Statistical physics, part I vol. 5. Elsevier; 1980.
- [160] Petsev DN, van Swol F, Frink LJD. Molecular theory of electric double layers. IOP Publishing; 2021.
- [161] Sweeney JB, Scriven LE, Davis HT. Gradient theory of the electric double layer at hydrocarbon-water interfaces. *J Chem Phys* 1987;87(10):6120–7.
- [162] Riaud A, Zhao S, Wang K, Cheng Y, Luo G. Lattice-Boltzmann method for the simulation of multiphase mass transfer and reaction of dilute species. *Phys Rev E* 2014;89(5):053308.
- [163] van der Sman RGM, van der Graaf S. Diffuse interface model of surfactant adsorption onto flat and droplet interfaces. *Rheol Acta* 2006;46(1):3–11.
- [164] Li Q, Luo KH, Kang QJ, He YL, Chen Q, Liu Q. Lattice Boltzmann methods for multiphase flow and phase-change heat transfer. *Prog Energy Combust Sci* 2016;52:62–105.
- [165] Schoeler AM, Josephides DN, Sajjadi S, Lorenz CD, Mesquida P. Charge of water droplets in non-polar oils. *J Appl Phys* 2013;114(14):144903.
- [166] Yang SH, Im DJ. Electrostatic origins of the positive and negative charging difference in the contact charge electrophoresis of a water droplet. *Langmuir* 2017;33(48):13740–8.
- [167] Lu Y, Jiang L, Yu Y, Wang D, Sun W, Liu Y, et al. Liquid-liquid triboelectric nanogenerator based on the immiscible interface of an aqueous two-phase system. *Nat Commun* 2022;13(1):5316.
- [168] Akai T, Blunt MJ, Bijeljic B. Pore-scale numerical simulation of low salinity water flooding using the lattice Boltzmann method. *J Colloid Interface Sci* 2020;566:444–53.
- [169] Aziz R, Niasar V, Erfani H, Martínez-Ferrer PJ. Impact of pore morphology on two-phase flow dynamics under wettability alteration. *Fuel* 2020;268:117315.
- [170] Mahani H, Berg S, Ilic D, Bartels WBB, Joekar-Niasar V. Kinetics of low-salinity-flooding effect. *SPE J* 2014;20(01):8–20.
- [171] O'Brien R. The solution of the electrokinetic equations for colloidal particles with thin double layers. *J Colloid Interface Sci* 1983;92(1):204–16.
- [172] Yariv E. Migration of ion-exchange particles driven by a uniform electric field. *J Fluid Mech* 2010;655:105–21.
- [173] Schnitzer O, Yariv E. Strong-field electrophoresis. *J Fluid Mech* 2012;701:333–51.
- [174] Schnitzer O, Yariv E. Nonlinear electrophoresis at arbitrary field strengths: small-Debye-length analysis. *Phys Fluids* 2014;26(12):122002.
- [175] Levine S, O'Brien RN. A theory of electrophoresis of charged mercury drops in aqueous electrolyte solution. *J Colloid Interface Sci* 1973;43(3):616–29.
- [176] Dukhin SS. Non-equilibrium electric surface phenomena. *Adv Colloid Interface Sci* 1993;44:1–134.
- [177] Krylov VS. Hydrodynamics and mass exchange at the phase boundaries with regular dissipative structures. Berlin, Heidelberg: Springer Berlin Heidelberg; 1987. p. 47–75.
- [178] Lyklema J. The structure of the electrical double layer on porous surfaces. *J Electroanal Chem Interfacial Electrochem* 1968;18(4):341–8.
- [179] Ohshima H. Electrophoresis of soft particles. *Adv Colloid Interface Sci* 1995;62(2):189–235.
- [180] Dukhin SS, Zimmermann R, Werner C. Electrokinetic fingerprinting of grafted polyelectrolyte layers—a theoretical approach. *Adv Colloid Interface Sci* 2006;122(1):93–105.
- [181] Lizée M, Marcotte A, Coquinot B, Kavokine N, Sobnath K, Barraud C, et al. Strong electronic winds blowing under liquid flows on carbon surfaces. *Phys Rev X* 2023;13(1):011020.
- [182] Robert A, Berthoumieux H, Bocquet M-L. Coupled interactions at the ionic graphene-water interface. *Phys Rev Lett* 2023;130(7):076201.
- [183] Lauga E, Stone HA. Effective slip in pressure-driven Stokes flow. *J Fluid Mech* 2003;489:55–77.
- [184] Gopmandal PP, Bhattacharyya S, Ohshima H. On the similarity between the electrophoresis of a liquid drop and a spherical hydrophobic particle. *Colloid Polym Sci* 2017;295(10):2077–82.
- [185] Karimi-Sibaki E, Vakhrushev A, Kadylnykova A, Wu M, Ludwig A, Bohacek J, et al. A multiphase model for exploring electrochemical marangoni flow. *Electrochem Commun* 2023;155:107567.
- [186] Zhang X-D, Sun Y, Chen S, Liu J. Unconventional hydrodynamics of hybrid liquid made of liquid metals and aqueous solution under applied fields. *Front Energy* 2018;12(2):276–96.
- [187] Bashkatov A, Hossain SS, Yang X, Mutschke G, Eckert K. Oscillating hydrogen bubbles at Pt microelectrodes. *Phys Rev Lett* 2019;123(21):214503.
- [188] Bashkatov A, Babich A, Hossain SS, Yang X, Mutschke G, Eckert K. H₂ bubble motion reversals during water electrolysis. *J Fluid Mech* 2023;958:A43.
- [189] Takahashi M. ζ potential of microbubbles in aqueous solutions: electrical properties of the gas-water interface. *J Phys Chem B* 2005;109(46):21858–64.
- [190] Yang C, Dabros T, Li D, Czarnecki J, Masliyah JH. Measurement of the zeta potential of gas bubbles in aqueous solutions by microelectrophoresis method. *J Colloid Interface Sci* 2001;243(1):128–35.
- [191] Najafi AS, Drelich J, Yeung A, Xu Z, Masliyah J. A novel method of measuring electrophoretic mobility of gas bubbles. *J Colloid Interface Sci* 2007;308(2):344–50.
- [192] de Gennes PG. Wetting: statics and dynamics. *Rev Mod Phys* 1985;57(3):827–63.
- [193] Mishchuk NA, Dukhin SS. Electrophoresis of solid particles at large Peclet numbers. *Electrophoresis* 2002;23(13):2012–22.
- [194] Rubinstein I, Shtilman L. Voltage against current curves of cation exchange membranes. *J Chem Soc Faraday Trans* 1979;75(0):231–46.
- [195] Cox R. Electroviscous forces on a charged particle suspended in a flowing liquid. *J Fluid Mech* 1997;338:1–34.
- [196] Yariv E, Schnitzer O, Frankel I. Streaming-potential phenomena in the thin-Debye-layer limit. Part 1. General theory. *J Fluid Mech* 2011;685:306–34.

- [197] Sherwood JD, Xie Y, van den Berg A, Eijkel JCT. Theoretical aspects of electrical power generation from two-phase flow streaming potentials. *Microfluid Nanofluid* 2013;15(3):347–59.
- [198] Squires TM, Quake SR. Microfluidics: fluid physics at the nanoliter scale. *Rev Mod Phys* 2005;77(3):977–1026.
- [199] Gavach C, Seta P, D'Epenoux B. The double layer and ion adsorption at the interface between two non miscible solutions: part I. Interfacial tension measurements for the water-nitrobenzene tetraalkylammonium bromide systems. *J Electroanal Chem Interfac Electrochem* 1977;83(2):225–35.
- [200] Bonn D, Eggers J, Indekeu J, Meunier J, Rolley E. Wetting and spreading. *Rev Mod Phys* 2009;81(2):739–805.
- [201] Hill RJ. Roles of interfacial-exchange kinetics and interfacial-charge mobility on fluid-sphere electrophoresis. *J Fluid Mech* 2025;1005:A1.
- [202] Sherwood J. Streaming potential generated by a long viscous drop in a capillary. *Langmuir* 2008;24(18):10011–8.
- [203] Hunter RJ. Recent developments in the electroacoustic characterisation of colloidal suspensions and emulsions. *Colloids Surf A Physicochem Eng Asp* 1998;141(1):37–66.
- [204] Sherwood JD. Electrophoresis of gas bubbles in a rotating fluid. *J Fluid Mech* 1986;162:129–37.
- [205] Linton M, Sutherland K. Dynamic surface forces, drop circulation, and liquid-liquid mass transfer (April 8–13, 1957). 1957.
- [206] Carruthers JC. The electrophoresis of certain hydrocarbons and their simple derivatives as a function of pH. *Trans Faraday Soc* 1938;34:300.
- [207] Anderson PJ. The relation of the electrokinetic potential to adsorption at the oil/water interface. *Trans Faraday Soc* 1959;55(0):1421–9.
- [208] Lyklema J. 4 - Gibbs monolayersvol. 3. Academic Press; 2000. p. 4.1–4.101.
- [209] V. Levich, *Motions of drops and bubbles in fluid media*, Fizmatgiz Moscow, Russia, 1959, book section VIII, pp. 472–531.
- [210] Kirby BJ, Hasselbrink EF. Zeta potential of microfluidic substrates: 2. Data for polymers. *Electrophoresis* 2004;25(2):203–13.
- [211] Creux P, Lachaise J, Graciaa A, Beattie JK, Djerdjev AM. Strong specific hydroxide ion binding at the pristine oil/water and air/water interfaces. *J Phys Chem B* 2009;113(43):14146–50.
- [212] Agmon N, Bakker HJ, Campen RK, Henchman RH, Pohl P, Roke S, et al. Protons and hydroxide ions in aqueous systems. *Chem Rev* 2016;116(13):7642–72.
- [213] O'Brien RW, White LR. Electrophoretic mobility of a spherical colloidal particle. *J Chem Soc Faraday Trans* 1978;74(0):1607–26.
- [214] Huang DM, Cottin-Bizonne C, Ybert C, Bocquet L. Ion-specific anomalous electrokinetic effects in hydrophobic nanochannels. *Phys Rev Lett* 2007;98(17):177801.
- [215] Tandon V, Kirby BJ. Zeta potential and electroosmotic mobility in microfluidic devices fabricated from hydrophobic polymers: 2. Slip and interfacial water structure. *Electrophoresis* 2008;29(5):1102–14.
- [216] Maduar SR, Belyaev AV, Lobaskin V, Vinogradova OI. Electrohydrodynamics near hydrophobic surfaces. *Phys Rev Lett* 2015;114(11):118301.
- [217] Khair AS, Squires TM. The influence of hydrodynamic slip on the electrophoretic mobility of a spherical colloidal particle. *Phys Fluids* 2009;21(4):042001.
- [218] Ohshima H. Electrokinetic phenomena in a dilute suspension of spherical solid colloidal particles with a hydrodynamically slipping surface in an aqueous electrolyte solution. *Adv Colloid Interface Sci* 2019;272:101996.
- [219] Uematsu Y, Ohshima H. Electrophoretic mobility of a water-in-oil droplet separately affected by the net charge and surface charge density. *Langmuir* 2022;38(14):4213–21.
- [220] Wang Q, Ma M, Siegel M. Deformation and stability of a viscous electrolyte drop in a uniform electric field. *Phys Rev Fluids* 2019;4(5):053702.
- [221] Lou J, Lee E. Diffusiophoresis of concentrated suspensions of liquid drops. *J Phys Chem C* 2008;112(32):12455–62.
- [222] Kelsall GH, Tang S, Yurdakul S, Smith AL. Electrophoretic behaviour of bubbles in aqueous electrolytes. *J Chem Soc Faraday Trans* 1996;92(20):3887–93.
- [223] Belyaev AV, Vinogradova OI. Electro-osmosis on anisotropic superhydrophobic surfaces. *Phys Rev Lett* 2011;107(9):098301.
- [224] Squires TM. Electrokinetic flows over inhomogeneously slipping surfaces. *Phys Fluids* 2008;20(9):092105.
- [225] Demekhin EA, Ganchenko GS, Navarkar A, Amiroudine S. The stability of two layer dielectric-electrolyte micro-flow subjected to an external electric field. *Phys Fluids* 2016;28(9):092003.
- [226] Dehe S, Hardt S. Deformation modes of an oil-water interface under a local electric field: from Taylor cones to surface dimples. *Phys Rev Fluids* 2021;6(12):123702.
- [227] Usui S, Imamura Y, Sasaki H. Measurement of zeta potential at aqueous solution surface by means of plane interface technique. *J Colloid Interface Sci* 1987;118(2):335–42.
- [228] Brask A, Goranović G, Jensen MJ, Bruus H. A novel electro-osmotic pump design for nonconducting liquids: theoretical analysis of flow rate-pressure characteristics and stability. *J Micromech Microeng* 2005;15(4):883.
- [229] Gao Y, Wang C, Wong TN, Yang C, Nguyen N-T, Ooi KT. Electro-osmotic control of the interface position of two-liquid flow through a microchannel. *J Micromech Microeng* 2007;17(2):358.
- [230] Lee JSH, Li D. Electroosmotic flow at a liquid-air interface. *Microfluid Nanofluid* 2006;2(4):361–5.
- [231] Choi W, Sharma A, Qian S, Lim G, Joo SW. Is free surface free in micro-scale electrokinetic flows? *J Colloid Interface Sci* 2010;347(1):153–5.
- [232] Liu M, Liu Y, Guo Q, Yang J. Modeling of electroosmotic pumping of nonconducting liquids and biofluids by a two-phase flow method. *J Electroanal Chem* 2009;636(1):86–92.
- [233] Movahed S, Khani S, Wen JZ, Li D. Electroosmotic flow in a water column surrounded by an immiscible liquid. *J Colloid Interface Sci* 2012;372(1):207–11.
- [234] Shit GC, Mondal A, Sinha A, Kundu PK. Two-layer electro-osmotic flow and heat transfer in a hydrophobic micro-channel with fluid-solid interfacial slip and zeta potential difference. *Colloids Surf A Physicochem Eng Asp* 2016;506:535–49.
- [235] Zheng J, Jian Y. Rotating electroosmotic flow of two-layer fluids through a microparallel channel. *Int J Mech Sci* 2018;136:293–302.
- [236] Choi W, Sharma A, Qian S, Lim G, Joo SW. On steady two-fluid electroosmotic flow with full interfacial electrostatics. *J Colloid Interface Sci* 2011;357(2):521–6.
- [237] Alizadeh A, Huang Y, Liu F, Daiguji H, Wang M. A streaming-potential-based microfluidic measurement of surface charge at immiscible liquid-liquid interface. *Int J Mech Sci* 2023;247:108200.
- [238] Takhistov P, Indeikina A, Chang H-C. Electrokinetic displacement of air bubbles in microchannels. *Phys Fluids* 2002;14(1):1–14.
- [239] Lac E, Sherwood JD. Streaming potential generated by a drop moving along the centreline of a capillary. *J Fluid Mech* 2009;640:55–77.
- [240] Ma Y, Sun M, Duan X, van den Berg A, Eijkel JCT, Xie Y. Dimension-reconfigurable bubble film nanochannel for wetting based sensing. *Nat Commun* 2020;11(1):814.
- [241] Bahga SS, Vinogradova OI, Bazant MZ. Anisotropic electro-osmotic flow over super-hydrophobic surfaces. *J Fluid Mech* 2010;644:245–55.
- [242] Dehe S, Rofman B, Bercovici M, Hardt S. Electro-osmotic flow enhancement over superhydrophobic surfaces. *Phys Rev Fluids* 2020;5(5):053701.
- [243] Fan B, Bhattacharya A, Bandaru PR. Enhanced voltage generation through electrolyte flow on liquid-filled surfaces. *Nat Commun* 2018;9(1):4050.
- [244] Bazant MZ, Squires TM. Induced-charge electrokinetic phenomena: theory and microfluidic applications. *Phys Rev Lett* 2004;92(6):066101.
- [245] Gao P, Lu X-Y. Instability of an oscillatory liquid layer with insoluble surfactants. *J Fluid Mech* 2008;595:461–90.
- [246] Li S, Chen Y-Z, Cheng Z, Peng J. The role of soluble surfactant in the linear instability of a film coating inside a tube. *J Fluid Mech* 2023;973:A46.
- [247] Kaneelil PR, Pahlavan AA, Herrada MA, LeRoy K, Stengel K, Warner S, et al. Symmetry breaking of a parallel two-phase flow in a finite length channel. *Phys Rev Fluids* 2022;7(3):033904.
- [248] Mandal S, Ghosh U, Bandopadhyay A, Chakraborty S. Electro-osmosis of superimposed fluids in the presence of modulated charged surfaces in narrow confinements. *J Fluid Mech* 2015;776:390–429.
- [249] López-Herrera JM, Gañán-Calvo AM. A note on charged capillary jet breakup of conducting liquids: experimental validation of a viscous one-dimensional model. *J Fluid Mech* 2004;501:303–26.
- [250] Pan X, Hu M, Xu B, Wang F, Huo P, Chen F, et al. Armstrong liquid bridge: formation, evolution and breakup. *Phys Rev Fluids* 2021;6(9):093901.
- [251] Sun M, Xie Y. Micro liquid bridge in periodic electric pulses: the impact of frequency. *Phys Rev Fluids* 2024;9(12):123701.
- [252] Bonhomme O, Liot O, Biance A-L, Bocquet L. Soft nanofluidic transport in a soap film. *Phys Rev Lett* 2013;110(5):054502.
- [253] Pototsky A, Suslov SA. Electromagnetically driven flow in unsupported electrolyte layers: lubrication theory and linear stability of annular flow. *J Fluid Mech* 2024;984:A75.
- [254] Taylor GI, McEwan AD. The stability of a horizontal fluid interface in a vertical electric field. *J Fluid Mech* 1965;22(1):1–15.
- [255] Yih C-S. Stability of a horizontal fluid interface in a periodic vertical electric field. *Phys Fluids* 1968;11(7):1447–9.
- [256] Dehe S, Hartmann M, Bandopadhyay A, Hardt S. The spatial structure of electrostatically forced faraday waves. *J Fluid Mech* 2022;939:A6.
- [257] Dehe S, Hartmann M, Bandopadhyay A, Hardt S. Controlling the electrostatic faraday instability using superposed electric fields. *Phys Rev Fluids* 2022;7(8):L082002.
- [258] Liu Q, Du Z, Wu J. Electrohydrodynamic conduction induced convection in a film with interface charge. *Int J Heat Fluid Flow* 2022;98:109063.
- [259] Gambhire P, Thaokar R. Electrokinetic model for electric-field-induced interfacial instabilities. *Phys Rev E* 2014;89(3):032409.
- [260] Kumaran V. Instabilities due to charge-density-curvature coupling in charged membranes. *Phys Rev Lett* 2000;85(23):4996–9.
- [261] Ziebert F, Bazant MZ, Lacoste D. Effective zero-thickness model for a conductive membrane driven by an electric field. *Phys Rev E* 2010;81(3):031912.
- [262] McClure JE, Li Z. Capturing membrane structure and function in lattice Boltzmann models. *Phys Rev E* 2023;107(2):024408.
- [263] Mirzadeh M, Bazant MZ. Electrokinetic control of viscous fingering. *Phys Rev Lett* 2017;119(17):174501.
- [264] Zhao J, Wang Z, Gu Y, Sauret E. Electrohydrodynamic viscous fingering of leaky dielectric fluids in a channel. *Phys Fluids* 2023;35(3):034105.
- [265] Austin LJ, Banczyk L, Sawistowski H. Effect of electric field on mass transfer across a plane interface. *Chem Eng Sci* 1971;26(12):2120–1.
- [266] Yoshikawa K, Matsubara Y. Spontaneous oscillation of pH and electrical potential in an oil-water system. *J Am Chem Soc* 1983;105(19):5967–9.
- [267] Trojánek A, Mareček V, Samec Z. Visualization of the interfacial turbulence associated with remarkable faradaic current amplification at a polarized water/1,2-dichloroethane interface. *Electrochem Commun* 2017;80:1–4.
- [268] Trojánek A, Mareček V, Samec Z. Mixed electrolyte effect on the stability of the interface between two immiscible electrolyte solutions. *Electrochim Acta* 2021;399:139405.
- [269] Kakiuchi T. Electrochemical instability at liquid/liquid interfaces. Springer; 2005. p. 155–70.

- [270] Kitazumi Y, Kakiuchi T. A model of the electrochemical instability at the liquid-liquid interface based on the potential-dependent adsorption and Gouy's double layer theory. *J Electroanal Chem* 2010;648(1):8–14.
- [271] Kovalchuk NM, Vollhardt D. Marangoni instability and spontaneous non-linear oscillations produced at liquid interfaces by surfactant transfer. *Adv Colloid Interface Sci* 2006;120(1):1–31.
- [272] Yang X, Baczymalski D, Cierpka C, Mutschke G, Eckert K. Marangoni convection at electrogenerated hydrogen bubbles. *Phys Chem Chem Phys* 2018;20(17):11542–8.
- [273] Bashkatov A, Hossain SS, Mutschke G, Yang X, Rox H, Weidinger IM, et al. On the growth regimes of hydrogen bubbles at microelectrodes. *Phys Chem Chem Phys* 2022;24(43):26738–52.
- [274] Bashkatov A, Bürkle F, Demirkir C, Ding W, Sanjay V, Babich A, et al. Electrolyte spraying within H₂ bubbles during water electrolysis. *arXiv [physics.flu-dyn]* 2024. arXiv:2409.00515.
- [275] Lei W, Lu X, Wang M. Multiphase displacement manipulated by micro/nanoparticle suspensions in porous media via microfluidic experiments: from interface science to multiphase flow patterns. *Adv Colloid Interface Sci* 2023;311:102826.
- [276] Revil A, Cerepi A. Streaming potentials in two-phase flow conditions. *Geophys Res Lett* 2004;31(11).
- [277] Jackson MD, Vinogradov J. Impact of wettability on laboratory measurements of streaming potential in carbonates. *Colloids Surf A Physicochem Eng Asp* 2012;393:86–95.
- [278] Ruckenstein E, Manciu M. Specific ion effects via ion hydration: II. Double layer interaction. *Adv Colloid Interface Sci* 2003;105(1):177–200.
- [279] Lima ERA, Horinek D, Netz RR, Biscaia EC, Tavares FW, Kunz W, et al. Specific ion adsorption and surface forces in colloid science. *J Phys Chem B* 2008;112(6):1580–5.
- [280] Morrow NR. Interfacial phenomena in petroleum recovery, Vol. 36 of Surfactant Science Series. New York and Basel: Marcel Dekker; 1990.
- [281] Wasan DT, Nikolov AD. Spreading of nanofluids on solids. *Nature* 2003;423(6936):156–9.
- [282] Zhang Z, Xu X. Effective boundary conditions for dynamic contact angle hysteresis on chemically inhomogeneous surfaces. *J Fluid Mech* 2022;935:A34.
- [283] Norouziadeh M, Leroy P, Soulaire C. A lubrication model with slope-dependent disjoining pressure for modeling wettability alteration. *Comput Phys Commun* 2024;298:109114.
- [284] M. Bazant, R. Bennewitz, L. Bocquet, N. Brilliantov, R. Dey, C. Drummond, R. Dryfe, H. Girault, K. Hatzell, K. Kornev, A. A. Kornyshev, I. Kratochvilova, A. Kucernak, M. Kulkarni, S. Kumar, A. Lee, S. Lemay, H. Medhi, A. Mount, F. Mugele, S. Perkin, M. Rutland, G. Schatz, D. Schiffrin, E. Smela, E. Smirnov, M. Urbakh, A. Yaroshchuk, Electrotunable wetting, and micro- and nanofluidics: general discussion, *Faraday Discuss* 199 (0) (2017) 195–237.
- [285] Sinn N, Schür MT, Hardt S. No-contact electrostatic manipulation of droplets on liquid-infused surfaces: experiments and numerical simulations. *Appl Phys Lett* 2019;114(21):213704.
- [286] Dwivedi RK, Muralidhar K. Contact line dynamics of a water drop spreading over a textured surface in the electrowetting-on-dielectric configuration. *Phys Rev E* 2022;106(4):045111.
- [287] Monroe CW, Daikhin LI, Urbakh M, Kornyshev AA. Electrowetting with electrolytes. *Phys Rev Lett* 2006;97(13):136102.
- [288] Liu J, Wang M, Chen S, Robbins MO. Uncovering molecular mechanisms of electrowetting and saturation with simulations. *Phys Rev Lett* 2012;108(21):216101.
- [289] Siddiqui MAQ, Sadeghinezhad E, Regenauer-Lieb K, Roshan H. Electrolytic flow in partially saturated charged micro-channels: electrocapillarity vs electro-osmosis. *Phys Fluids* 2022;34(11):112001.
- [290] Abu-Al-Saud MO, Esmailzadeh S, Riaz A, Tchepeli HA. Pore-scale study of water salinity effect on thin-film stability for a moving oil droplet. *J Colloid Interface Sci* 2020;569:366–77.
- [291] Shehata AM, Alotaibi MB, Nasr-El-Din HA. Waterflooding in carbonate reservoirs: does the salinity matter? *Spe Reserv Eval Eng* 2014;17(3):304–13.
- [292] Liu J, Wani OB, Alhassan SM, Pantelides ST. Wettability alteration and enhanced oil recovery induced by proximal adsorption of Na⁺, Cl⁻, Ca²⁺, Mg²⁺, and SO₄²⁻ ions on calcite. *Phys Rev Appl* 2018;10(3):034064.
- [293] Molnar IL, Gerhard JI, Willson CS, O'Carroll DM. Wettability effects on primary drainage mechanisms and NAPL distribution: a pore-scale study. *Water Resour Res* 2020;56(1):e2019WR025381.
- [294] Gravelleau M, Soulaire C, Tchepeli HA. Pore-scale simulation of interphase multicomponent mass transfer for subsurface flow. *Transp Porous Media* 2017;120(2):287–308.
- [295] Golmohammadi M, Mohammadi S, Mahani H, Ayatollahi S. The non-linear effect of oil polarity on the efficiency of low salinity waterflooding: a pore-level investigation. *J Mol Liq* 2022;346.
- [296] Lei W, Lu X, Liu F, Wang M. Non-monotonic wettability effects on displacement in heterogeneous porous media. *J Fluid Mech* 2022;942:R5.
- [297] Liu F, Wang M. Trapping patterns during capillary displacements in disordered media. *J Fluid Mech* 2022;933:A52.
- [298] Liu F, Wang M. Phase diagram for preferential flow in dual permeable media. *J Fluid Mech* 2022;948:A19.
- [299] Revil A, Jardani A. The self-potential method: theory and applications in environmental geosciences. Cambridge: Cambridge University Press; 2013 (pp. iii–iii).
- [300] Morgan F, Williams E, Madden T. Streaming potential properties of westerly granite with applications. *J Geophys Res Solid Earth* 1989;94(B9):12449–61.
- [301] Sprunt ES, Mercer TB, Djabbarah NF. Streaming potential from multiphase flow. *Geophysics* 1994;59(5):707–11.
- [302] Revil A, Schwaeger H, Cathles III L, Manhardt P. Streaming potential in porous media – 2. Theory and application to geothermal system. *J Geophys Res* 1999;104(9):20033–48.
- [303] Revil A, Linde N, Cerepi A, Jougnot D, Matthäi S, Finsterle S. Electrokinetic coupling in unsaturated porous media. *J Colloid Interface Sci* 2007;313(1):315–27.
- [304] Jackson MD. Multiphase electrokinetic coupling: insights into the impact of fluid and charge distribution at the pore scale from a bundle of capillary tubes model. *J Geophys Res Solid Earth* 2010;115(B7).
- [305] Wurmstich B, Morgan FD. Modeling of streaming potential responses caused by oil well pumping. *Geophysics* 1994;59(1):46–56.
- [306] Qiang S, Shi X, Revil A, Kang X, Liu Y, Wu J. Residual NAPL morphology effects on electrical resistivity: insights from micromodel displacement experiments and pore network simulations. *Water Resour Res* 2022;58(12):e2022WR033233.
- [307] Li P, Liu J, Yuan J-H, Guo Y, Wang S, Zhang P, et al. Artificial funnel nanochannel device emulates synaptic behavior. *Nano Lett* 2024;24(20):6192.
- [308] Bazant MZ, Kilic MS, Storey BD, Ajdari A. Towards an understanding of induced-charge electrokinetics at large applied voltages in concentrated solutions. *Adv Colloid Interface Sci* 2009;152(1):48–88.
- [309] Bazant MZ, Squires TM. Induced-charge electrokinetic phenomena. *Curr Opin Colloid Interface Sci* 2010;15(3):203–13.
- [310] Levich V, Krylov V. Surface-tension-driven phenomena. *Annu Rev Fluid Mech* 1969;1(1):293–316.
- [311] Stone HA, Stroock AD, Ajdari A. Engineering flows in small devices: microfluidics toward a lab-on-a-chip. *Annu Rev Fluid Mech* 2004;36(1):381–411.
- [312] Soares RMD, Siqueira NM, Prabhakaram MP, Ramakrishna S. Electrospinning and electrospray of bio-based and natural polymers for biomaterials development. *Mater Sci Eng C* 2018;92:969–82.
- [313] Demirkir Ç, Yang R, Yang R, Bashkatov A, Sanjay V, Lohse D, Krug D. To jump or not to jump: Adhesion and viscous dissipation dictate the detachment of coalescing wall-attached bubbles. *arXiv* 2025.